© DelphineCastel / ONLYLYON Tourisme & Congrès

# International Tissue Elasticity Conference™

## *October 21-23, 2024*

## Lyon, France

LabTAU - Unité de recherche U1032

LABTAU
LABORATOIRE THÉRAPIE ET APPLICATIONS ULTRASONORES

Inserm

CENTRE LÉON BÉRARD

Lyon 1

PROCEEDINGS of the Eighteenth International Tissue Elasticity Conference.
Contains the detailed program, and full abstracts with all authors, references, and figures

# Contents

# About

## Foreword

Dear Conference Delegate: It is a great pleasure to have been asked to write this foreword and to welcome you to the **Eighteenth International Tissue Elasticity Conference™** (ITEC™) in Lyon, Auvergne-Rhône-Alpes, France. After the long delay since our Seventeenth conference was held virtually, when the COVID-19 pandemic was still sweeping the world, I am delighted that our colleagues at the Inserm Laboratoire Thérapie et Applications Ultrasonores (LabTAU) in Lyon, have enabled us to resume ITEC™ with this first conference in a new series under a new organising team. Being back in-person is so important for the essential exchange of information and enjoying each other's company with the time and opportunity for the friendly discussions and networking, for which ITEC is so well known. Credit is especially due to Stefan Catheline, Rémi Souchon, Bruno Giammarinaro, Jorge Torres and Sandrine Iochem who, through their hard work and dedication, have taken over the organization from Cheryl Taylor and me. Please join me in thanking the team in Lyon for make the conference a success.

When the late Jonathan Ophir and Kevin Parker conceived this conference series they expressed the purpose as "to advance the field of measurement and imaging of the elastic attributes of soft tissues through tutorials and scientific presentations of the state of the art in the field, within a unique and unified forum that would bring together researchers from several countries and ultimately contribute to the rapid development and clinical introduction of this new medical imaging technology". Twenty-two years on, there is now wide medical acceptance of the first generation of clinical elastography systems with a long history of scientific discovery and technical innovation, and the field is poised for introduction of new generations of routine clinical and preclinical biomechanical property imaging and measurement methods. In the past, ITEC tended to emphasise ultrasound as the underlying imaging modality for extracting biomechanical information. In 2020 we began a trend to change ITEC to reflect the reality that tissue elasticity measurement and imaging is a truly multimodal field that spans resolutions from subcellular to the macroscopic, with applications that include fundamental mechanobiology, preclinical research and clinical applications. This year, thanks to all of you who have submitted abstracts, we are delighted to be able to run the conference with an exciting programme that truly reflects this, and indeed extends the trend, making ITEC an exceptional opportunity for cross-disciplinary exchange of ideas and knowledge across the resolution scales and between ultrasound, magnetic resonance and optical imaging modalities.

It takes substantial effort to prepare an ITEC tutorial. We are particularly grateful for the tutorials to be given by Mathias Fink ("Shear wave elastography - an historical perspective"), Richard Ehmann ("Magnetic resonance elastography: basic principles and applications"), Ivan Pelivanov ("Guided-wave optical coherence elastography (OCE) to quantify macroscopic elasticity in the cornea"), and Elisa Konofagou (opening lecture: "May the force be with you - elasticity imaging in informing cardiovascular disease and cancer treatment"). Finally, huge thanks are due to all helpers, reviewers, session chairs, award judges and contributors, without whom the conference could not maintain

the high standards for which it is known.

ITEC must evolve if it is to serve the needs of researchers and practitioners of elastometry and elastography. We would be hugely grateful if you would complete the feedback forms distributed at the conferece or, if you prefer, speak directly to any of the organising panel. May your research be inspired by the presentations and discussions during the Eighteenth ITEC, and may you make new friends, establish productive collaborations and renew old acquaintances. I hope also that you will have the time to avail yourselves of the rich 2000-year historical and cultural heritage that Lyon, France's third largest metropolitan region, has to offer, and to explore this extremely beautiful part of France.

Jeffrey Bamber, past and retiring General Conference Organizer, ITEC Conferences, from 2013.

## Organizing committee

Stefan Catheline  Rémi Souchon  Bruno Giammarinaro  Jorge Torres

Sandrine Iochem  Cheryl Taylor  Jeff Bamber

# Detailed program

The name of the chairpersons might change.

USM I (Ultrasound Methods), Chairpersons: Stefan Catheline & Gabrielle Laloy-Borgna

USM II (Ultrasound Methods) + FIP (Forward and Inverse Problems), Chairpersons: Jeff Bamber & Jean-Luc Gennisson

GWA (Guided Waves Applications), Chairpersons: Jorge Torres & Bharat Tripathi

PMT (Properties and Models of Tissues), Chairpersons: Rémi Souchon & Guillermo Rus

MRM (Magnetic Resonance Methods), Chairpersons: Olivier Rouviere & Simon Chatelin

MEL (Microelastography), Chairpersons: Gabriel Regnault & Gabrielle Laloy-Borgna

CAP (Clinical Applications), Chairpersons: Inas Faris & Noé Jiménez

USM III (Ultrasound Methods), Chairpersons: Marie Muller & Philippe Garteiser

OPM (Optical Methods), Chairpersons: Thomas Dehoux & Rémi Souchon

CRN (Correlation and Natural Noise), Chairpersons: Agathe Marmin & Thomas Payen

BGNL (Bubble, granular and nonlinear physics), Chairpersons: Thomas Gallot & Bruno Giammarinaro

AAP (Animal Applications), Chairpersons: Gwenaël Pagé & Elisa Konofagou

## Monday, October 21st

| | | | |
|---|---|---|---|
| 8:15–9:00 | **Registration** | | |
| 9:00–9:15 | | WELCOME SESSION | |
| 9:15–10:00 | USM I | **Mathias Fink**<br>Tutorial | SHEAR WAVE ELASTOGRAPHY – AN HISTORICAL PERSPECTIVE |
| 10:00–10:15 | USM I | **Tom Meyer**<br>Charité - Universitätsmedizin, Germany | FUNCTIONAL TIME HARMONIC ELASTOGRAPHY OF THE LIVER: EXPLORING HEPATIC STIFFNESS PULSATION AS A DIAGNOSTIC MARKER |
| 10:15–10:30 | USM I | **Noé Jimenez**<br>Instituto de Instrumentación para Imagen Molecular, Spain | ACOUSTIC VORTICES AND PHASE GRADIENT TECHNIQUES FOR ULTRASOUND ELASTOGRAPHY |
| 10:30–11:00 | **Coffee break** | | |
| 11:00–11:15 | USM II | **Ren Koda**<br>Gunma University, Japan | EVALUATION OF SHEAR WAVE AMPLITUDE PROPAGATING THROUGH THE CHEST WALL USING C-SWE FOR ASSESMENT OF FLUID ACCUMULATION IN INFLAMED LUNGS. |
| 11:15–11:30 | USM II | **Axel Nierding**<br>Université Paris Saclay - CNRS, France | ULTRASOUND SHEAR WAVE ELASTOGRAPHY FOR MONITORING DIAPHRAGM FUNCTION IN HUMAN. |
| 11:30–11:45 | USM II | **John Civale**<br>The Institute of Cancer Research, UK | PRECLINICAL VIBRATIONAL SHEAR WAVE ELASTOGRAPHY: A REPEATABILITY STUDY |
| 11:45–12:00 | USM II | **Naoki Tano**<br>Tokyo Institute of Technology, Japan | ADAPTIVE FILTER FOR REMOVAL OF SUBORDINAL SHEAR WAVES IN CONTINUOUS SHEAR WAVE ELASTOGRAPHY FOR LIVER IMAGING |
| 12:00–12:15 | FIP | **Yousef Almashakbeh**<br>The Hashemite University, Jordan | AN EXPERIMENTAL STUDY ON THE DIAGNOSIS OF SKIN LESIONS USING TORSIONAL WAVE PROPAGATION AND RECONSTRUCTION ALGORITHMS. |
| 12:15–12:30 | FIP | **Samuel Croquette**<br>Institut Langevin, France | EXPLORING THE LIMITS TO QUANTITATIVE ELASTOGRAPHY: SUPERSONIC SHEAR IMAGING IN STRETCHED SOFT STRIPS. |
| 12:30–13:45 | **Lunch** | | |
| 13:45–14:00 | GWA | **Guillermo Rus**<br>University of Granada, Spain | NON-INVASIVE SKIN PATHOLOGY DIAGNOSIS USING TORSIONAL WAVE ELASTOGRAPHY BIOMARKERS |
| 14:00–14:15 | GWA | **Naoki Tano**<br>Tokyo Institute of Technology, Japan | HIGH-RESOLUTIONAL SHEAR WAVE PHASE ESTIMATION WITHIN SMALL ROI AND ITS APPLICATION IN MULTI-LAYERED ELASTIC STRUCTURES EVALUATION. |
| 14:15–14:30 | GWA | **Inas H Faris Al Azzawi**<br>University of Granada, Spain | EVALUATING CORNEAL ELASTICITY: A NONLINEAR APPROACH USING TORSIONAL WAVE TECHNOLOGY. |
| 14:30–14:45 | GWA | **Agathe Marmin**<br>University of Washington, USA | TOWARDS A CLINICAL USE OF ROBOTIZED TRANSIENT OPTICAL COHERENCE ELASTOGRAPHY IN HUMAN SKIN |

| | | | |
|---|---|---|---|
| 14:45–15:00 | GWA | **Jerome Baranger**<br>Physics For Medecine, France | NON-LINEAR ELASTICITY OF THE BRACHIAL ARTERY IN KOROTKOFF SOUNDS GENERATION |
| 15:00–15:15 | GWA | **Jiayuan Zhu**<br>LabTAU, France | EXPERIMENTAL CHARACTERIZATION OF YOUNG'S MODULUS USING OPTICAL ELASTOGRAPHY IN A SOFT ELASTIC STRING. |
| 15:15–15:30 | GWA | **Sibylle Gregoire**<br>LabTAU, France | FLEXURAL PULSE WAVE VELOCITY IN BLOOD VESSELS |
| 15:30–15:45 | **Group photo** | | |
| 15:45–16:15 | **Coffee break / Poster session** | | |
| 16:15-16:30 | PMT | **Iyad Chaoui**<br>Université de Tours, France | EXPLORING BIOMECHANICAL PROPERTIES OF THE ANTERIOR BLADDER WALL: PRELIMINARY STUDY ON SHEAR WAVE ELASTICITY IMAGING FOR BLADDER CANCER TUMOR GRADE ASSESSMENT. |
| 16:30-16:45 | PMT | **Ricardo Andrade**<br>Nantes Université, France | DIRECT IN VIVO CHARACTERIZATION OF TENSILE ANISOTROPY AND SHEAR ANISOTROPY OF SKELETAL MUSCLE BY ULTRASOUND SHEAR WAVE ELASTOGRAPHY |
| 16:45-17:00 | PMT | **Can Deniz Bezek**<br>Uppsala University, Sweden | SPEED-OF-SOUND AS A NOVEL TISSUE CHARACTERIZATION METHOD |
| 17:00-17:15 | PMT | **Sapna Bisht**<br>Indian Institute of Technology Gandhinagar, India | ELUCIDATING THE EFFECT OF FLUID CONTENT ON MODEL-FREE ELASTOGRAPHY ESTIMATES USING VISCOELASTIC PHANTOMS |
| 17:15-17:30 | PMT | **Ricardo Andrade**<br>Nantes Université, France | IN VIVO ASSESSMENT OF SHEAR MODULUS ALONG THE FIBERS OF PENNATE MUSCLE DURING PASSIVE LENGTHENING AND CONTRACTION USING STEERED ULTRASOUND PUSH BEAMS |
| 17:30-17:45 | PMT | **Marius Burman Ingeberg**<br>UMC Utrecht, The Netherlands | EXPLORING THE RELATIONSHIP BETWEEN CARDIAC-INDUCED BRAIN STRAIN AND BOTH GLOBAL BOUNDARY CONDITIONS AND LOCAL MICROSTRUCTURERE |
| 17:45-18:00 | PMT | **Noah Jaitner**<br>Charité - Universitätsmedizin, Germany | NONE-INVASIVE QUANTIFICATION OF PORTAL PRESSURE BY COMBINED 3D MRI DEFORMATION MAPPING AND MR ELASTOGRAPHY |
| 18:15–20:00 | **Welcome reception** | | |

## Tuesday, October 22nd

| | | | |
|---|---|---|---|
| 8:45–9:30 | MRM | **Richard Ehmann**<br>Tutorial | MAGNETIC RESONANCE ELASTOGRAPHY: BASIC PRINCIPLES AND APPLICATIONS |
| 9:30–9:45 | MRM | **Amirhosein Baradaran Najar**<br>University of Montreal Hospital Research Center, Canada | MULTIFREQUENCY MR ELASTOGRAPHY FOR GRADING LIVER INFLAMMATION IN VOLUNTEERS AND PATIENTS WITH METABOLIC DYSFUNCTION-ASSOCIATED FATTY LIVER DISEASE: A PILOT STUDY |
| 9:45–10:00 | MRM | **Gwenaël Pagé**<br>CEA, France | QUANTIFICATION OF BRAIN TUMORS STIFFNESS BY MAGNETIC RESONANCE PASSIVE ELASTOGRAPHY: FROM SEISMOLOGY TO MEDICAL DIAGNOSIS. |
| 10:00–10:15 | MRM | **Sabine Bensamoun**<br>Université de technologie de Compiègne, France | MAGNETIC RESONANCE ELASTOGRAPHY (MRE) LUNG STIFFNESS: APPLICATION TO LONG-COVID PATIENTS. |
| 10:15–10:30 | MRM | **Rémi Souchon**<br>LabTAU, France | OBSERVATION OF POROELASTIC WAVES USING MR ELASTOGRAPHY. |
| 10:30–11:00 | **Coffee break** | | |
| 11:00–11:15 | MEL | **Sajad Ghazavi**<br>University of Montreal Hospital Research Center, Canada | MAPPING MICROSCALE VISCOELASTICITY: CHARACTERIZATION THROUGH A 2D BOUNDARY-CONDITION-FREE NONLINEAR INVERSION TECHNIQUE |
| 11:15–11:30 | MEL | **Thomas Dehoux**<br>Institut Lumière Matière, France | BRILLOUIN LIGHT SCATTERING REVEALS SUB-NANOMETRIC PORE MECHANICS IN CELLS. |
| 11:30–11:45 | MEL | **Hari S Nair**<br>University of Montreal Hospital Research Center, Canada | DEEP NEURAL NETWORK FOR SHEAR MODULUS RECONSTRUCTION OF ELASTIC MATERIALS IN MICROELASTOGRAPHY |
| 11:45–12:00 | MEL | **Sibylle Gregoire**<br>LabTAU, France | MICRO-ELASTOGRAPHY OF BIOPSY TISSUE, APPLICATION TO ENDOMETRIOSIS |
| 12:00–12:15 | CAP | **Laurent Sandrin**<br>Echosens | FibroScan® : 23 Years at the Forefront of Liver Health |
| 12:15–13:30 | **Lunch** | | |
| 13:30–13:45 | CAP | **Arnaud Héroux**<br>University of Montreal Hospital Research Center, Canada | QUANTIFYING SHEAR WAVE SPEED AND ATTENUATION AT THE COMMON EXTENSOR TENDON OF THE ELBOW: A FIRST STEP IN DIFFERENTIATING FIBROMYALGIA FROM PSORIATIC ARTHRITIS |
| 13:45–14:00 | CAP | **David Bradway**<br>Duke University, USA | COMPARING SHEARWAVE SPEED MEASUREMENT YIELD USING FUNDAMENTAL AND HARMONIC TRACKING IN SKELETAL MUSCLE. |
| 14:00–14:15 | CAP | **Simon Chatelin**<br>ICube, University of Strasbourg, France | ULTRASOUND ELASTOGRAPHY TO PREVENT AGEING AND RUPTURE IN THE BREAST IMPLANTS. |

| | | | |
|---|---|---|---|
| 14:15–14:30 | CAP | **Mercedes David**<br>University of Montreal Hospital Research Center, Canada | ULTRASOUND ELASTOGRAPHY OF BACK MUSCLE BIOMECHANICAL PROPERTIES: A SYSTEMATIC REVIEW AND META-ANALYSIS OF CURRENT METHODS. |
| 14:30–14:45 | CAP | **David Bradway**<br>Duke University, USA | 3D ROTATIONAL SWEI IN MUSCLE AND ANISOTROPIC PHANTOMS. |
| 14:45–15:00 | CAP | **Iman Rafati**<br>University of Montreal Hospital Research Center, Canada | ULTRASOUND SHEAR WAVE SPEED AND ATTENUATION ASSESSMENTS OF LIVER CANCERS: PRELIMINARY RESULTS |
| 15:00–15:15 | CAP | **Philippe Garteiser**<br>Laboratory of Imaging Biomarkers, Center for Research on Inflammation, Inserm, France | QUANTIFICATION OF VISCOELASTIC PARAMETERS WITH MRE IN A COHORT OF DIABETIC PATIENTS WITH NON-ALCOHOLIC STEATOHEPATITIS |
| 15:15–15:45 | CAP | **Elisa Konofagou**<br>Plenary session | MAY THE FORCE BE WITH YOU – ELASTICITY IMAGING IN INFORMING CARDIOVASCULAR DISEASE AND CANCER TREATMENT |
| 15:45–16:15 | **Coffee break / Poster session** | | |
| 16:15-16:30 | USM III | **Christina Proestaki**<br>Columbia University in the city of New York, USA | SPARSE EWI: TOWARDS AN AUTOMATED AND REAL TIME ARRHYTHMIA MAPPING TECHNIQUE |
| 16:30-16:45 | USM III | **Marie Muller**<br>North Carolina State University, USA | ULTRASOUND STIMULATION OF ULTRA-LOW CROSSLINKED HYDROGELS TO ENHANCE WOUND HEALING |
| 16:45-17:00 | USM III | **Adrien Besson**<br>E-Scopics SAS, France | ON FRUGAL ELASTOGRAPHIES FOR ULTRAPORTABLE ULTRASOUND |
| 17:00-17:15 | USM III | **Toûka Meki**<br>Physics For Medecine, France | In-vivo 3D ELASTIC AND BACKSCATTER TENSOR IMAGING USING A 128 ELEMENTS MATRIX TRANSDUCER. |
| 17:15-17:30 | USM III | **Utsav Ratna Tuladhar**<br>Rochester Institute of Technology, USA | FAST ULTRASOUND ELASTIC MODULUS RECONSTRUCTION USING DEEP NEURAL NETWORK. |
| 17:30-17:45 | USM III | **Tom Meyer**<br>Charité - Universitätsmedizin, Germany | POINT OF CARE CARDIAC TIME HARMONIC ULTRASOUND ELASTOGRAPHY USING PORTABLE VIBRATION PILLOWS |
| 17:45–19:30 | **Free time and travel to Gala dinner** | | |
| 19:30–21:30 | **Gala dinner** | | |

## Wednesday, October 23rd

| | | | |
|---|---|---|---|
| 8:30–9:15 | OPM | **Ivan Pelivanov**<br>Tutorial | GUIDED-WAVE OPTICAL COHERENCE ELASTOGRAPHY (OCE) TO QUANTIFY MACROSCOPIC ELASTICITY IN THE CORNEA |
| 9:15–9:30 | OPM | **Jakob Jordan**<br>Charité - Universitätsmedizin, Germany | OPTICAL TIME HARMONIC ELASTOGRAPHY |
| 9:30–9:45 | OPM | **Maud Legrand**<br>ICube, University of Strasbourg, France | PASSIVE ELASTOGRAPHY USING SPECKLE CONTRAST IMAGING |
| 9:45–10:00 | OPM | **Gabriel Regnault**<br>LabTAU, France | RECONSTRUCTION OF ANISOTROPIC SHEAR MODULI USING NON-CONTACT OPTICAL COHERENCE ELASTOGRAPHY |
| 10:00–10:15 | OPM | **Ginger Schmidt**<br>Massachusetts Institute of Technology, USA | ASYNCHRONOUS, SEMI-REVERBERANT ELASTOGRAPHY |
| 10:15–10:45 | **Coffee break** | | |
| 10:45–11:00 | CRN | **Hannah Schleifer**<br>Columbia University in the city of New York, USA | EVALUATION OF MYOCARDIAL INFARCTION RECOVERY WITH ELECTROMECHANICAL ACTIVATION AND TIME TO PEAK PRINCIPAL STRAIN |
| 11:00–11:15 | CRN | **Thomas Gallot**<br>Universidad de la República, Uruguay | PASSIVE AND ACTIVE ELASTOGRAPHY BY WAVE EQUATION INVERSION |
| 11:15–11:30 | CRN | **Janie Hanrard**<br>Physics For Medecine, France | IN VIVO AND IN VITRO 3D QUANTIFICATION OF NATURAL WAVE VELOCITY IN THE HUMAN HEART |
| 11:30–11:45 | CRN | **Bruno Giammarinaro**<br>LabTAU, France | HOW TO EXTRACT SHEAR WAVE SPEED AND ATTENUATION FROM A DIFFUSE WAVE FIELD? |
| 11:45–12:00 | CRN | **Nina Dufour**<br>ICube, University of Strasbourg, France | NOISE CORRELATION INSPIRED METHOD : AN APPROACH FOR MULTIMODAL IMAGING ELASTOGRAPHY |
| 12:00–13:15 | **Lunch** | | |
| 13:15–13:30 | BGNL | **Gabrielle Laloy-Borgna**<br>LabTAU, France | BUBBLE-INDUCED SHEAR WAVE IN A SINGLE CELL |
| 13:30–13:45 | BGNL | **Yuzhe Fan**<br>University of Magdeburg, Germany | AN OPTICAL RHEOMETRY USING SHEAR WAVE EXCITATION THROUGH NON-SPHERICAL BUBBLE COLLAPSE |
| 13:45–14:00 | BGNL | **Adrien Rohfritsch**<br>LabTAU, France | IN VIVO STUDY OF THE IMPACT OF ULTRASONIC INERTIAL CAVITATION ON THE STIFFNESS OF PANCREATIC TUMORS IN MURINE MODEL |
| 14:00–14:15 | BGNL | **Bharat Tripathi**<br>University of Galway, Ireland | NONLINEAR ELASTIC PARAMETER RESPONSIBLE FOR SHEAR SHOCK FORMATION IN BRAIN |
| 14:15–14:30 | BGNL | **Gwenaël Pagé**<br>CEA, France | NON LINEAR STORAGE MODULUS QUANTIFICATION WITH MR ELASTOGRAPHY: FROM IN VITRO TO IN VIVO |
| 14:30–15:00 | **Coffee break** | | |

| | | | |
|---|---|---|---|
| 15:00–15:15 | AAP | **Jean-Luc Gennisson**<br>Université Paris Saclay - CNRS, France | DEVELOPMENT OF HIGH FREQUENCY ULTRASOUND SHEAR WAVE ELASTOGRAPHY FOR PRECLINICAL LIVER INVESTIGATION: A PILOT STUDY ON OGT MODEL. |
| 15:15-15:30 | AAP | **Aude Loumeaud**<br>ICube, University of Strasbourg, France | AN ORIGINAL PIEZOELECTRIC ACTUATOR DESIGN WITH DEDICATED SEQUENCES FOR MOUSE MULTI-ORGAN MAGNETIC RESONANCE ELASTOGRAPHY (MRE) AT 7T |
| 15:30-15:45 | AAP | **Hari S Nair**<br>University of Montreal Hospital Research Center, Canada | HIGH-FREQUENCY ELASTIC WAVE STIMULATION AND IMAGING OF DISPLACEMENTS IN MOUSE MACROPHAGES |
| 15:45-16:00 | AAP | **Guillaume Flé**<br>University Hospital Erlangen, Germany | IMAGING THE ELECTROMECHANICAL PROPERTIES OF THE MOUSE BRAIN DURING TRANSCRANIAL ELECTRICAL STIMULATION: NUMERICAL SIMULATIONS |
| 16:00-16:15 | AAP | **Tiffany, Bakir Ageron**<br>Creatis, France | FREE-BREATHING IN VIVO MAGNETIC RESONANCE ELASTOGRAPHY OF MOUSE LIVER: PROSPECTIVE VS RETROSPECTIVE SYNCHRONIZATION. |
| 16:15–17:00 | **Student Awards and Closing Session** | | |

# List of Abstracts – Talks

**October 21st**

## SHEAR WAVE ELASTOGRAPHY – AN HISTORICAL PERSPECTIVE

*Mathias Fink*

Langevin Institute, ESPCI Paris, PSL Research University, CNRS, 1 rue Jussieu, 75005, Paris, France

In the last 20 years, Shear Wave Elastography became a very successful technique that is now widely used in medical diagnosis and is now commercialized by several companies. It is based on a multi-wave approach combining ultrasound and low frequency shear waves. We will give a historical perspective on all this field and we will show how these ideas has emerged in the ultrasound community. We will describe the different approaches that were proposed and the limitations of each of them. We will show why some techniques have disappeared and we will discussed future perspectives of this field.

# EVALUATION OF SHEAR WAVE AMPLITUDE PROPAGATING THROUGH THE CHEST WALL USING C-SWE FOR ASSESMENT OF FLUID ACCUMULATION IN INFLAMED LUNGS.

*Ren Koda*[1,*], *Hayato Taniguchi*[2], *Yasuyuki Shiraishi*[3], *Kazumasa Osawa*[1], *Kento Shimizu*[4], *Marie Tabaru*[4], *Yoshiki Yamakoshi*[1,4]

[1]Gunma University, Kiryu, Gunma, JAPAN; [2]Yokohama City University Medical Center Advanced Critical Care Center, Yokohama, Kanagawa, JAPAN; [3]Aging and Cancer PreClinical Research Center, Tohoku University, Sendai, Miyagi, JAPAN; [4]Tokyo Institute of Technology, Yokohama, Kanagawa, JAPAN.

**Background:** Continuous Shear Wave Elastography (C-SWE) [1] is a technique for visualizing the elasticity of internal tissues in living organs. Recently, C-SWE has been applied to measure the shear wave velocity propagating through the lung parenchyma by determining the phase difference of the shear wave between B-lines from the Doppler signal through B-lines [2]. However, B-lines are not always observed stably with a number and intensity suitable for shear wave velocity measurement. Although lung ultrasound surface wave elastography [3] measures the surface wave velocity in lung tissue, surface wave velocity is thought to be affected by local density changes due to fluid accumulation on the inflamed lung.
**Aims:** It is hypothesized that in inflamed lungs, shear waves propagating through the chest wall are attenuated by energy leakage onto the localized fluid-filled lung surface. In this paper, we obtain the amplitude of shear waves propagating through the chest wall using C-SWE, and evaluate the attenuation of shear wave amplitude for the assessment of fluid accumulation in inflamed lungs.
**Methods:** For point-of-care lung ultrasound, measurements were performed in a goat pulmonary fibrosis model using tablet echo-based C-SWE. The model was prepared by intratracheal nebulization of bleomycin only in the left lung of goats. The experimental setup is shown in Figure (a). The position of the ultrasound probe and the actuator tip was placed between the ribs. The shear wave frequency was set to 78.1Hz.
**Results:** Figure (b) shows the results of the shear wave propagation map and shear wave amplitude map of the normal and inflamed lung in the goat experiment. As shown in Figure (b-4), the shear wave amplitude measurement shows high values in the right part of the image, i.e., near the vibration point, and decreases along the chest wall. Figure (c) shows the normalized shear wave amplitude distribution in the horizontal direction at the chest wall center depth. When the attenuation per unit length was evaluated, the inflamed lung model showed higher attenuation than the normal lung model, and the attenuation tended to increase especially in cases where inflammation progressed.
**Conclusions:** To evaluate fluid accumulation due to inflammation, we assessed the attenuation of shear waves propagating through the chest wall in the direction of propagation. In a goat inflammatory lung model, attenuation tended to increase, especially in cases where disease progression was prominent.
**Acknowledgements:** Part of this study was based on JKA and its promotion funds from KEIRIN RACE.

**References:**

[1] Yamakoshi Y, et al. IEEE Trans Ultrason Ferroelectr Freq Control. 64, 340-348 (2017).
[2] Koda R, et al. Ultrason Imaging. 45, 30-41 (2023).
[3] Zhang X, et al. IEEE TUFFC, 64, 1298-1304 (2017).

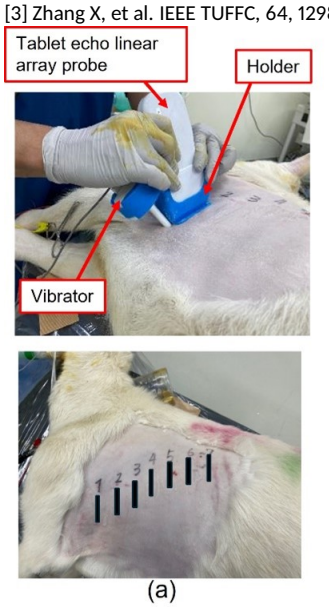


(a) Experimental setup for goat lung elastography

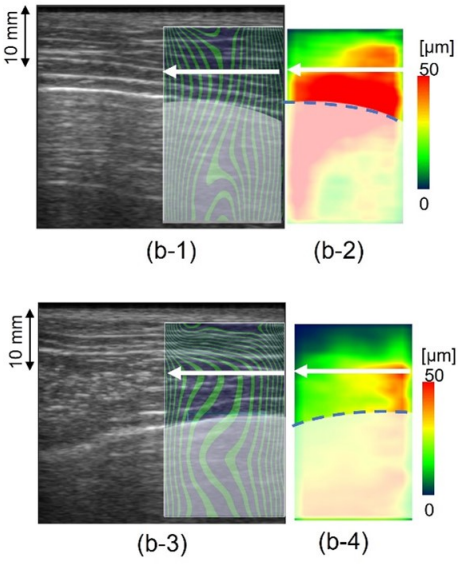


(b) Shear wave propagation and amplitude map of normal (b-1)(b-2) and inflamed lungs (b-3)(b-4).

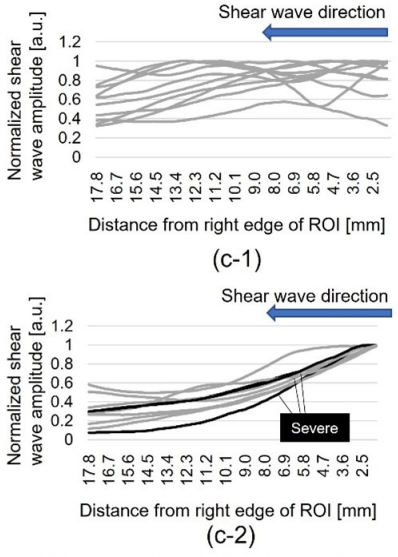


(c) Normalized shear wave amplitude in horizontal direction obtained with normal (c-1) and inflamed lung models (c-2).

# ULTRASOUND SHEAR WAVE ELASTOGRAPHY FOR MONITORING DIAPHRAGM FUNCTION IN HUMAN

*Axel Nierding*[1,2,*], *Thomas Poulard*[2,3], *Corentin Cornu*[2], *Quentin Fossé*[4], *Martin Dres*[1,4], *Marie-Cécile Nierat*[1], *Thomas Similowski*[1,4], *Damien Bachasson*[1,3], *Jean-Luc Gennisson*[2]

[1]Sorbonne Université, INSERM, UMRS1158 Neurophysiologie Respiratoire Expérimentale et Clinique, Paris, France ; [2] Université Paris-Saclay, Inserm, CNRS, CEA, BioMaps, Orsay, France ; [3] Institute of Myology, Neuromuscular Investigation Center, Paris, France ; [4]Groupe Hospitalier Universitaire APHP-Sorbonne Université, hôpital Pitié-Salpêtrière, R3S, Paris, France.

**Background:** The diaphragm is the main respiratory muscle. Assessing its function is of primary importance in various clinical settings such as the intensive care unit (ICU) where it is prone to dysfunction [1]. Reference methods rely on the measurements of esophageal and gastric pressure using invasive probes to monitor transdiaphragmatic pressure (Pdi). Alternatively, the diaphragm function can be noninvasively explored by conventional ultrasound. Some indexes such as diaphragm thickening fraction or excursion suffer from a lack of specificity and sensitivity and are highly operator dependent. Previous works demonstrates that shear wave elastography (SWE) may be used to estimate active muscle mechanics [2]. Whether diaphragm shear modulus (SMdi) may serve as a measurement of diaphragm function remains to be clarified. Given the diaphragm's relatively small thickness (about 2mm) and highly specific architecture, shear waves are likely to be guided and must be optimized to obtain more precise SWE values.
**Aims:**This work aimed at investigating the ability of SWE to monitor SMdi during ventilation and to optimize SWE by adding viscosity properties in analysis.
**Methods:** 13 Healthy participants and 25 patients under mechanical ventilation were studied. By using a dedicated ultrasound sequence, diaphragm SWE was assessed by an ultrafast ultrasound device (Aixplorer, Supersonic Imagine, France) driven a linear transducer array (SL10-2) on the zone of apposition of the right costal hemidiaphragm (Fig. A). In healthy participants SWE was assessed during isovolumetric inspiratory effort and inspiratory loading. In mechanically ventilated patients, change in pressure support level and measurement during spontaneous ventilation trial during weaning. Average diaphragm shear modulus (SMdi) was extracted from shear modulus map. Additionally, as the thickness of the diaphragm changes during breathing cycles, problem of guided shear wave can occur. To better understand this point, the experiment was modeled by a three-layer phantom of different thickness and compared with a SimSonic numerical simulation. Behavior of the mechanical properties of the diaphragm were then studied as a function of its thickness along the breathing cycle *in vivo*.
**Results:** In healthy participants, SMdi was strongly correlated with Pdi (R=0.70, 95% CIs (0.66, 0.73), P<0.001) (Fig. B) [3]. In mechanically ventilated patients, SMdi was also strongly correlated with Pdi (n = 17, r=0.55–0.86, all p<0.05), except in those with a high breathing rate (n = 8, r=-0.43-0.52, all p>0.06) [2] explained by the limited sampling rate of SWE. Regarding guidance of shear waves, good agreement was found between numerical model simulations, three-layers phantom models, and in vivo measurements (Fig. C) [5].
**Conclusions:** Our results support previous findings regarding the guidance of shear waves in confined tissues and highlight the potential of SWE for the in vivo assessment of diaphragm viscoelasticity.
**Acknowledgments:** These works are supported by the "Fondation EDF", "AFM", and ANR under grant number: ANR-21-CE19-0052-02.

**Acknowledgments:**

[1] Demoule et al. Am J Respir Crit Care Med 2013
[2] Hug et al. Exerc Sport Sci Rev 2015; [3] Bachasson et al. J Appl Physiol 2019
[4] Fossé et al. Crit Care 2020; [5] Poulard et al. IEEE-IUS 2020.

A

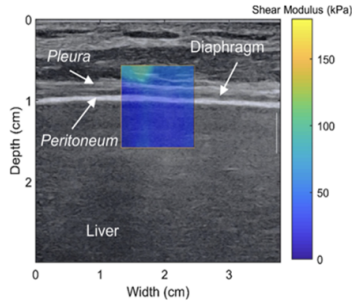


B

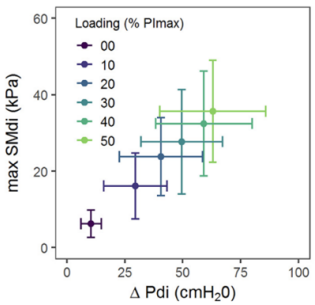


C

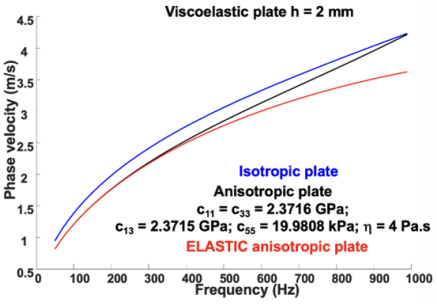

# FUNCTIONAL TIME HARMONIC ELASTOGRAPHY OF THE LIVER: EXPLORING HEPATIC STIFFNESS PULSATION AS A DIAGNOSTIC MARKER

*Tom Meyer*[1,*], *Paul Spiesecke*[1], *Brunhilde Wellge*[1], *Caroline Zöllner*[1], *Hans-Peter Müller*[1], *Thomas Fischer*[1], *Marvin Doyley*[2], *Heiko Tzschätzsch*[1], *Ingolf Sack*[1]

[1]Charité – Universitätsmedizin Berlin, Berlin, GERMANY; [2]University of Rochester, Rochester, New York, USA

**Background:** Ultrasound elastography is clinically established for quantification of hepatic stiffness and liver fibrosis detection. Doppler ultrasound measures blood velocity and can reveal functional information such as pulsatility of hepatic vessels. As the relationship between blood perfusion and hepatic stiffness varies across liver diseases including fibrosis and portal hypertension, assessment of blood flow driven stiffness changes could provide important diagnostic information about liver function[1]. Ultrafast and parallel acquisitions of time-resolved Doppler flow and time harmonic elastography (THE)[2] showed that hepatic stiffness varies in synchrony with pulsations of portal venous blood flow in healthy controls[3].
**Aims:** Exploring the potential of hepatic stiffness pulsatility as a novel diagnostic marker for hepatic function in patients with liver fibrosis and healthy controls.
**Methods:** 15 healthy volunteers (7 women; age range: 25-55) and 12 patients with a fibrosis degree 2 to 4 (7 women, age range: 19-93) were investigated using time resolved THE. Multifrequency harmonic vibrations (30, 40, 50 Hz) were induced using a custom-designed vibration bed (GAMPT, Merseburg, Germany). Data were acquired using a Verasonics Vantage 64 system (Washington, USA) equipped with a 2.75 MHz convex transducer. Time-resolved shear wave speed (SWS) maps as surrogate for stiffness were obtained using k-MDEV inversion[4]. To account for potential spatial heterogeneity in the temporal variation of hepatic stiffness, SWS maps of the liver were clustered using correlation based hierarchical clustering of spatially resolved SWS time curves. The spatially averaged SWS time curves of each cluster were analyzed for minimum and maximum SWS values within a cardiac cycle as a metric of pulsatility.

**Results:** In healthy controls, the spatially dominant SWS pattern corresponded to portal venous blood flow (mean SWS = 1.39 ± 0.13 m/s; ΔSWS = 0.06 ± 0.02 m/s). Patients with fibrosis showed a reduced pulsatility (mean SWS = 2.24 ± 0.26 m/s; ΔSWS = 0.03 ± 0.02 m/s; $p < 0.05$). For increased heterogeneity no dominant cluster could be determined. No correlation between SWS and pulsatility was found, suggesting no direct coupling of tissue compliance and stiffness. Notably, 2 patients with hepatic arterial buffer response showed an increased arterial blood flow to which stiffness changes were synchronized unlike the typical portal venous blood flow-stiffness correlation patterns.

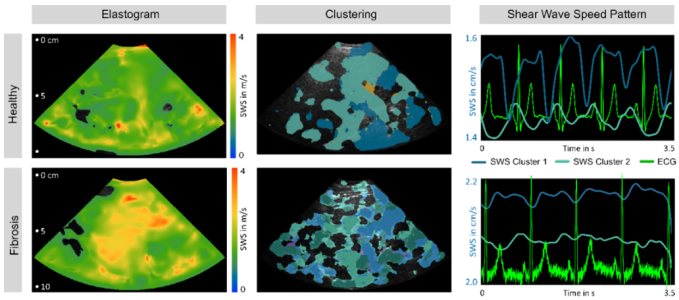


*Figure 1: Representative stiffness maps, with corresponding spatial clustering and temporal variation with ECG as reference for the cardiac cycle.*

**Conclusions:** Taken together, our results demonstrate the potential value of stiffness pulsation as a diagnostic marker to distinguish between congestive liver disease and matrix-remodeling associated fibrosis. The observed difference between arterialized and normally perfused livers is currently investigated in more patients in our institution.
**Acknowledgments:** German Research Foundation (FOR5628, CRC1340 and GRK2260) and Pfizer (WP2487656).

**References:**

[1] Baikpour, M., et al., Portal Venous Pulsatility Index: A Novel Biomarker for Diagnosis of High-Risk Nonalcoholic Fatty Liver Disease. AJR Am J Roentgenol, 2020. 214(4): p. 786-791.
[2] Tzschatzsch, H., et al., Two-Dimensional Time-Harmonic Elastography of the Human Liver and Spleen. Ultrasound Med Biol, 2016. 42(11): p. 2562-2571.
[3] Tom Meyer, B.W., Thomas Fischer, Marvin Doyley, Heiko Tzschätzsch, Ingolf Sack, Functional Time Harmonic Elastography of the Liver: Stiffness Pulsatility as a Novel Marker of Tissue Compliance, in IEEE IUS 2022. Venice, Italy.
[4] Tzschatzsch, H., et al., Tomoelastography by multifrequency wave number recovery from time-harmonic propagating shear waves. Medical Image Analysis, 2016. 30: p. 1-10.

# ACOUSTIC VORTICES AND PHASE GRADIENT TECHNIQUES FOR ULTRASOUND ELASTOGRAPHY

*Enrique González-Mateo*[1], *Francisco Camarena*[1], *Noé Jiménez*[1,*]

[1] Instituto de Instrumentación para Imagen Molecular, Universitat Politècnica de València - CSIC, Camino de Vera S/N, 46022, Valencia, SPAIN

**Background**: During the last decades ultrasound elastography has been developed as a reliable technique for medical diagnosis. Commonly, tissues are deformed under the action of the acoustic radiation force by using a pushing acoustic beam. However, using focused beams the acoustic radiation force can only push the tissue in the direction of the propagation of the beam and the degree of freedom to displace the tissue in other directions is limited. In addition, using spectral methods the computational costs associated with calculating the wavenumber of the propagating waves using spatiotemporal Fourier transforms can be remarkably high.
**Aims:**We present an efficient method for ultrasound elastography based on acoustic vortices to transfer to tissues, in addition to linear, angular momentum. By twisting the tissue in alternating angles, efficient shear wave generation is achieved. Then, to generate the image, we propose a real-time method for shear wave velocity mapping combining spatial filtering and phase gradient techniques.
**Methods**: A focused vortex beam is generated by a 1.1-MHz piezoelectric source and a helicoidal phase-plate lens that allows the selection of the topological charge of the vortex. The vortex beam was focused into a CIRS-049 phantom and ex-vivo liver-tissue phantoms, and displacements were measured by a 5-MHz probe using a 2-kHz-PRF US and a Vantage system (Verasonics, USA). Then, the angular spectrum of tissue shear-wave displacements is filtered in a directional and bandpass manner. Next, the gradient of the harmonic displacement phase map is calculated to locally estimate the wavenumber. Finally, the phase velocity map at the selected frequency is obtained. Results were compared with a spectral wavenumber estimator for local phase velocity imaging using a pushing beam [1]. Computational times were calculated for different map sizes. **Results:** When the vortex is focused on the tissue phantom, displacement data shows that the angular momentum is transferred to the medium at the focal spot. Under time modulation, this results in a point source of torsional shear waves that quasi-omnidirectionally propagates away from the focus. Then, retrieved elasticity maps show a strong similarity with those obtained by state-of-the-art spectral techniques, but maps are generated in real-time. Experimental results show that the values of 2.50±0.03 m/s and 4.23±0.07 m/s for the background and inclusion, respectively, prove a good agreement with the manufacturer's values of 2.45 m/s and 4.50 m/s, with relative errors ranging from 2-5%. Using this approach images are generated two orders of magnitude faster than other spectral techniques [1], therefore, it may be suitable for real-time elastography applications.
**Conclusions:** First, the use of acoustic vortices to twist the tissue results in a robust excitation of shear waves with quasi-omnidirectional radiation pattern and arbitrary waveform, which have a great impact in imaging quality for elastography. In addition, the combination of the spatial filtering and phase gradient results in a very efficient strategy to compute the viscoelastic maps, suitable for spectral real-time applications.
**Acknowledgements:** This research has been supported by grants RYC2021-034920-I, CNS2023-145707. PID2022-142719OB-C21 funded by MCIN/AEI/10.13039/501100011033.

**References:**

[1] P. Kijanka, M. W. Urban, IEEE Transactions on Ultrasonics, Ferroelectrics, and Frequency Control 67 (3) (2020) 526–537

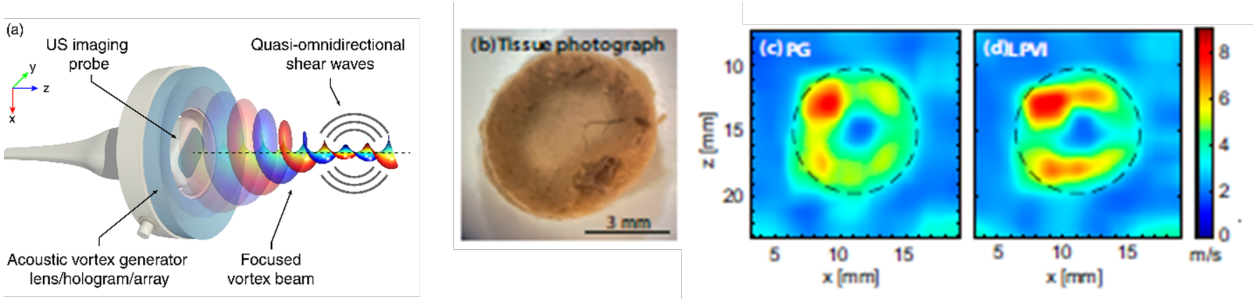


(a) Scheme of the device, (b) photograph of the ex-vivo liver inclusion, (c) shear wave speed using phase gradient and (d) using LPVI method [1].

# PRECLINICAL VIBRATIONAL SHEAR WAVE ELASTOGRAPHY: A REPEATABILITY STUDY

*J Civale*[1,*], *V Parasaram*[1], *JC Bamber*[1], *E Harris*[1]

[1]Institute of Cancer Research, London, UK.

**Background:** Ultrasound Shear Wave Elastography (SWE) provides a quantitative and convenient method to image the viscoelastic properties of tissue. Shear wave speed (SWS), and SWS dispersion are related to the storage (elastic) and loss (viscous) moduli of tissue. These properties are of interest in preclinical studies as they can inform on response to treatment. Preclinical SWE is challenging due to the small size of tumors, and sedation methods are required to obtain reliable measurements of shear wave speed (SWS). We introduce Vibrational SWE (VSWE), a system we have developed at the ICR where the mechanical impulse is generated by an external shaker and applied by contact to subcutaneous tumors.
**Aims:** To determine the degree of repeatability of VSWE measurements in 3D preclinical tumor models, and to determine whether the repeatability can be improved by choice of tumor orientation and anesthetics.

**Methods:** Tumor cells (MDA-MB cell line) were injected subcutaneously on the flank of athymic nude mice (n=4). Tumors were left to grow, and when they reached approximately 10mm in diameter were ready for imaging using 3D VSWE [1]. The system comprises an external shaker (Bruel & Kjaer model 4810, Denmark) and a research ultrasound system (Verasonics Vantage 256, USA) working with a linear high frequency imaging probe (L22-14vX) giving a 12mm square field of view. The probe was linearly translated in the elevational direction to capture 3D data. Acoustic coupling between the probe and tumor was achieved by placing a layer of acoustic gel over the entire tumor volume to be scanned. A modified line-by-line US imaging sequence was used to image shear wave oscillations [2]. The 3D shear wave field was filtered using a set of directional filters, from which local SWS values were estimated using an autocorrelation method [3]. Data was acquired at three different vibration frequencies (500, 700 and 1000 Hz). Tumors were imaged in two orientations (top vs side), over three consecutive days during which mice were sedated in separate sessions using injectables (fentanyl cytrate, Hypnorm, midazolam) or breathable (Isoflurane 2%) anesthetic. 3D tumor volume outlines were used to determine the spatial transformation required to register a pair of 3D SWS data sets. This allowed calculation of repeatability metrics, namely normalized cross correlation (NCC) and the mean and standard deviation of the difference between registered SWS sets.

**Results:** An analysis of variance of mean SWS measurements (2–5 m/s across tumors and vibration frequencies) revealed significant differences between the tumors ($p<0.001$), and vibration frequencies ($p<0.001$). Mean SWS values were not found to be significantly affected by the choice of anesthetic or tumor alignment relative to the imaging probe. Repeatability of SWS spatial distributions was assessed by spatial registration of 3D SWS data sets obtained over consecutive days. Data sets showed improved repeatability when obtained from the same tumor (+76% increase in NCC), the same orientation (+39%), and when using a side orientation at 500 Hz (+18%). The breathing motion in the US axial direction was affected by the choice of anesthetic, with larger amplitude (<0.3mm) and more rapid ( 140 bpm) motion observed for breathable and injectable anesthetic respectively. Side orientation also showed a reduction in motion amplitude compared to the top orientation. These differences in breathing motion due to the choice of orientation and anesthetic however showed no significant impact on SWS measurements or their repeatability.

**Conclusions:** We conclude VSWE is a repeatable and feasible technique for in-vivo preclinical studies, our findings regarding repeatability with regards to the orientation of the tumor and choice of anesthetic may also be relevant to other forms of preclinical elastography.
**Acknowledgements:** Craig Cummings from the ICR mechanical workshop.

**References:**
[1] Parasaram V, Civale J, Bamber JC, Robinson SP, Jamin Y, Harris E. Preclinical Three-Dimensional Vibrational Shear Wave Elastography for Mapping of Tumour Biomechanical Properties In Vivo. Cancers. 2022 Oct 3;14(19):4832.
[2] Loupas T, Powers JT, Gill RW. An axial velocity estimator for ultrasound blood flow imaging, based on a full evaluation of the Doppler equation by means of a two-dimensional autocorrelation approach. IEEE transactions on ultrasonics, ferroelectrics, and frequency control. 1995 Jul;42(4):672-88.
[3] Civale J, Parasaram V, Bamber JC, Harris EJ. High frequency ultrasound vibrational shear wave elastography for preclinical research. Physics in Medicine & Biology. 2022 Dec 7;67(24):245005.

# ADAPTIVE FILTER FOR REMOVAL OF SUBORDINAL SHEAR WAVES IN CONTINUOUS SHEAR WAVE ELASTOGRAPHY FOR LIVER IMAGING.

*N Tano*[1,*], *R Koda*[2], *S Tanigawa*[3], *N Kamiyama*[3], *Y Yamakoshi*[1,2], *M Tabaru*[1]

[1]Tokyo Institute of Technology, Yokohama, Kanagawa, JAPAN; [2]Gunma University, Kiryu, Gunma, JAPAN; [3]GE HealthCare, Hino, Tokyo, JAPAN.

**Background:** Continuous shear wave elastography (C-SWE) is a technique that employs an external mechanical vibrator to continuously excite shear waves [1]. While C-SWE achieves high signal-to-noise ratio and frame rate due to the large shear wave amplitude and the absence of cooling during shear wave generation. Moreover, given the liver's deeper location within the human body, the influence of these subordinal shear waves cannot be ignored, particularly in liver elastography.
**Aims:** This study aims to design an adaptive filter to mitigate the effects of these subordinal shear waves.

**Methods:** The process of the proposed adaptive filter begins with peak detection in the spatial wave number domain after a 2D Fourier transformation. The detected peaks are then categorized into signal and noise components. The peak coordinates of the signal component determine the center of the Gaussian filter matrix. Subsequently, parameter fitting is applied to ascertain the standard deviations of the Gaussian filter matrix before multiplying the resulting filter matrix with the Fourier-transformed signals. To validate the proposed filter and understand subordinal shear waves in liver C-SWE, a simulation study on subordinal shear waves was conducted. This study considered subordinal waves from reflection and rib vibration. Following the simulation study, phantom experiments and analysis of healthy volunteer measurement results were also performed to evaluate the effect of the proposed adaptive Gaussian filter.

**Results:** As shown in Figure a, a comparison between the simulation results and the measurements from healthy volunteer revealed that subordinal shear waves from rib vibrations are more significant than reflected waves. Figure b demonstrates that the proposed filter can effectively mitigate the subordinal shear wave from rib vibration, as evidenced by both simulation and phantom studies. Finally, as depicted in Figure c and d, the analysis of volunteer measurements at a shear wave frequency of 77.9 Hz showed a significant reduction in errors from previously reported shear wave velocities in healthy liver [2].
**Conclusions:** Our results shows that the proposed adaptive filter, combined with peak detection and parameter fitting, can effectively reduce the impact of subordinal shear waves.
**Acknowledgments:** Part of this work was supported by JSPS KAKENHI Grant Number 22K04134 and the Cooperative Research Project of Research Center for Biomedical Engineering.

**References:**

[1] Tano, N., Koda, R., et al., "Continuous Shear Wave Elastography for Liver Using Frame-to-Frame Equalization of Complex Amplitude", Ultrasonic Imaging, 46(3):197-206, (2024).
[2] Madhok, R., Tapasvi, C., et al., "Acoustic Radiation Force Impulse Imaging of the Liver: Measurement of the Normal Mean Values of the Shearing Wave Velocity in a Healthy Liver", Journal of Clinical and Diagnostic Research, 7(1), 39, (2013).

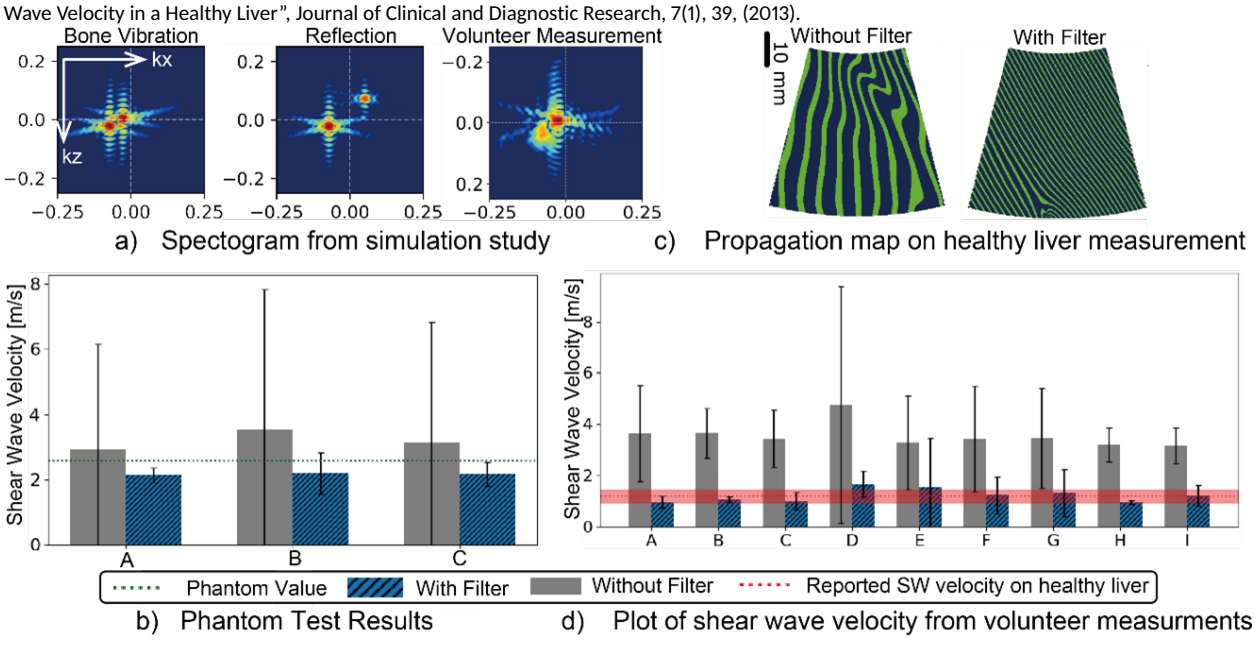

# AN EXPERIMENTAL STUDY ON THE DIAGNOSIS OF SKIN LESIONS USING TORSIONAL WAVE PROPAGATION AND RECONSTRUCTION ALGORITHMS.

*YS Almashakbeh*[1,2,3,*], *H Shamimi*[2,3], *IH Faris*[2,3,4], *JL Martín-Rodríguez*[3,5], *RR Villaverde*[3,5], *A Callejas*[2,3], *G Rus*[2,3,4].

[1]The Hashemite University, Zarqa, JORDAN;[2]University of Granada, Granada, SPAIN; [3]Biosanitary Research Institute, Granada, SPAIN; [4]Excellence Research Unit, Granada, SPAIN; [5]San Cecilio Clinical University Hospital of Granada, Granada, SPAIN.

**Background**: The mechanical properties of human skin serve as important markers for diagnosing skin diseases and assessing the effectiveness of dermatological treatments. Traditional techniques for measuring these properties, such as suction [1], torsion [2], and traction [3], often alter the skin's natural tension state, making it difficult to obtain accurate measurements. Dynamic Mechanical Analysis (DMA) is precise but limited to in vitro or ex vivo applications and faces constraints at higher frequencies due to the inertial limitations of the rheometer [4]. Torsional Wave Elastography (TWE) presents a modern alternative that can measure the viscoelastic properties of skin tissue in vivo, providing more reliable data for clinical use [5].
**Aims**: The purpose of this study is to develop a novel method for the diagnosis of skin lesions using the Probabilistic Inverse Problem (PIP) techniques and the Torsional Wave Elastography (TWE) rheological modeling. The primary objective is the identification of the most effective rheological model, either the spring pot (SP) model or the Kelvin Voigt Fractional Derivative (KVFD) model, for the simulation of skin tissue behavior.
**Methods**: The methodology involved several steps. Two rheological models, the Spring Pot (SP) and the Kelvin Voigt Fractional Derivative (KVFD), were selected for simulation. The FDTD method was used to implement these models. Experimental data were collected using a TWE sensor developed by the Ultrasonics Lab. The sensor generated and received shear waves within the frequency range of 0.4 to 1 kHz. Data was collected from 19 patients between the ages of 46 and 72 using the TWE sensor. The collected data were analyzed using PIP techniques to reconstruct the viscoelastic parameters of the skin tissue. Equipment and software used included the TWE sensor from Ultrasonics Lab and MATLAB® (Release 2018a) with the Parallel Computing Toolbox from The MathWorks, Inc.
**Results**: The results show that this approach effectively reconstructs skin tissue parameters and diagnoses skin lesions. The SP model revealed $\eta$ values from 7.5 to 12 Pa.s for control tissue and 14 to 67.5 Pa.s for pathological tissue, while the KVFD model showed $\eta$ values of 3.5 to 9.5 Pa.s for control tissue and 10 to 47 Pa.s for pathological tissue. For the KVFD model, control tissue had $\mu$ values of 0.93 to 8.7 kPa, and pathological tissue had $\mu$ values of 7.04 to 197.56 kPa. The SP model, requiring only two parameters compared to KVFD's three, proved more efficient and straightforward.
**Conclusions**: The SP model, combined with the TWE and PIP, is effective for reconstructing skin biomarkers and detecting skin lesions. It offers precise depiction of viscoelastic tissues, which is essential for various applications. Cost and usability are also significant considerations. Our study did not investigate the effects of sex and age on skin biomarkers due to the limited number of patients. Future research should explore these factors to advance personalized medicine. The KVFD and SP models can distinguish between control and pathological skin, showing potential for diagnostic use. However, they currently cannot specify the type of pathology, which should be addressed in future studies. Integrating advanced imaging technologies with TWE analysis could further improve the detection of skin lesion biomarkers, enhancing diagnostic accuracy and early detection.
Acknowledgements: This research was funded by the Ministerio de Educación, Cultura y Deporte (grants DPI2017-83859-R, EQC2018-004508-P), Ministerio de Ciencia e Innovación (grants PID2020-115372RB-I00, PYC20 RE 072 UGR), Ministerio de Sanidad, Servicios Sociales e Igualdad (grants DTS15/00093, PI16/00339), Instituto de Salud Carlos III y Fondos Feder, Junta de Andalucía (grants PI-0107-2017, PIN-0030-2017, IE2017-5537), and other supporting bodies.
**References**:
[1]S Diridollou, F Patat, F Gens, L Vaillant, D Black, JM Lagarde, Y Gall, and M Berson. In vivo model of the mechanical properties of the human skin under suction. Skin Research and technology, 6(4):214–221, 2000.
[2]R Sanders. Torsional elasticity of human skin in vivo. Pflügers Archiv, 342:255–260, 1973.
[3]T Sugihara, T Ohura, K Homma, and HH Igawa. The extensibility in human skin: variation according to age and site. British journal of plastic surgery, 44(6):418–422, 1991.
[4] Simon Chatelin, Jennifer Oudry, Nicolas Périchon, Laurent Sandrin, Pierre Allemann, Luc Soler, and Rémy Willinger. In vivo liver tissue mechanical properties by transient elastography: Comparison with dynamic mechanical analysis. Biorheology, 48(2):75–88, 2011.
[5] Yousef Almashakbeh, Hirad Shamimi, Inas H Faris, José M Cortés, Antonio Callejas, and Guillermo Rus. Healthy human skin kelvin voigt fractional and spring-pot biomarkers reconstruction using torsional wave elastography. Physical and Engineering Sciences in Medicine, pages 1-13, 2024.

# EXPLORING THE LIMITS TO QUANTITATIVE ELASTOGRAPHY: SUPERSONIC SHEAR IMAGING IN STRETCHED SOFT STRIPS.

*S Croquette*[1,*], *A Delory*[1,2], *DA Kiefer*[1], *C Prada*[1], *F Lemoult*[1]

[1]Institut Langevin, ESPCI, Paris, FRANCE; 2PMMH, ESPCI, Paris, FRANCE.

**Background:** Shear wave elastography has enriched ultrasound medical imaging with quantitative tissue stiffness measurements. However, limitations persist, related to viscoelasticity [1], guiding geometry [2] or static deformation [3].
**Aims:** We tackle those limitations, introducing frequency-dependent mechanical parameters and taking into consideration strong dispersion and prestress.
**Methods:** To explore these limits, a nearly-incompressible soft elastomer strip is chosen to mimic the mechanical behavior of an elongated tissue [4, 5]. A supersonic shear wave scanner measures the propagation of shear waves within the strip. By repeating the experiment on the same sample for different orientation and static strain, the scanner provides a wide range of shear wave velocities from 2 to 6 m/s.
**Results:** The guided wave effect is highlighted and the spatiotemporal Fourier transform of the data provides the dispersion diagrams. We provide a theoretical model which accounts for the static deformation and allows the extraction of the mechanical parameters of the sample, including its rheology and hyperelastic behavior.
**Conclusions:** To overcome some limitation of current elastography, we present a method which allows for the simultaneous characterization of the viscoelastic and hyperelastic properties of soft tissues, paving the way for robust quantitative elastography of elongated tissues.

**References:**

[1] Ralph Sinkus, Elasticity of the Heart, Problems and Potentials, Current Cardiovascular Imaging Reports, 7(9):9288, 2014.
[2] Mitchell A. Kirby, Ivan Pelivanov, Shaozhen Song, Lukasz Ambrozinski, Soon Joon Yoon, Liang Gao, David Li, Tueng T. Shen, Ruikang K. Wang and Matthew O'Donnell. Optical coherence elastography in ophthalmology, Journal of Biomedical Optics, 22(12):121720, 2017.
[3] Thomas Elgeti and Ingolf Sack. Magnetic Resonance Elastography of the Heart, Current Cardiovascular Imaging Reports, 7(2):9247, 2014.
[4] Alexandre Delory, Fabrice Lemoult, Maxime Lanoy, Antonin Eddi and Claire Prada. Soft Elastomers: a playground for guided waves, The Journal of the Acoustical Society of America, 151(5):3343-3358, 2022.
[5] Alexandre Delory, Daniel A Kiefer, Maxime Lanoy, Antonin Eddi, Claire Prada and Fabrice Lemoult. Viscoelastic dynamics of a soft strip subject to a large deformation, Soft Matter, 20(9):1983-1995, 2024.

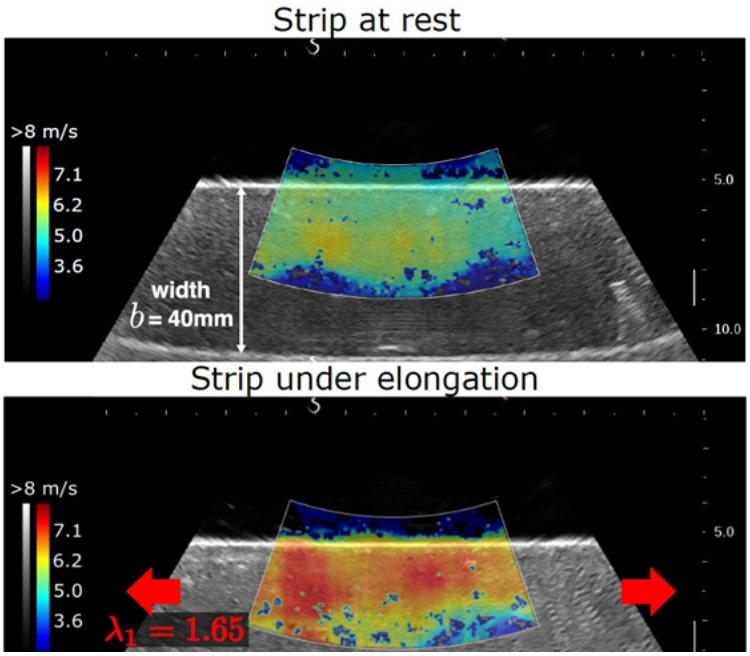

# NON-INVASIVE SKIN PATHOLOGY DIAGNOSIS USING TORSIONAL WAVE ELASTOGRAPHY BIOMARKERS

*H Shamimi*[1,3], *R Ruiz-Villaverde*[2,3], *A Martin-Castro*[2], *JL Martin*[2], *G Rus*[1,3,4,*]

[1]University of Granada, ETS Caminos, Calle Dr Severo Ochoa, Granada, Granada, 18001, SPAIN; [2]Hospital Universitario San Cecilio, Av. del Conocimiento, Granada, Granada, 18016, SPAIN; [3]Biosanitary Research Institute of Granada, 15, Madrid Ave, Granada, Granada, 18012, SPAIN;

**Background:** Skin is one of the organs whose viscoelastic properties is not fully understood. Besides being highly nonlinear and dependent on the orientation of Langer's lines [1], they are mainly governed by the collagen, elastin, and cell structure, which strongly changes under pathological conditions (Keratoacanthoma, Basal cell carcinoma, Squamous cell carcinoma, melanoma). It supports our hypothesis that elastography has the potential to non-invasively predict histopathology of skin tumors. Thus, we have developed both a new concept of torsional shear waves ideally suited to interrogate surface and subsurface stiffness, as well as a new set of mechanical biomarkers.
**Aims:** A novel elastography method, known as Torsional Wave Elastography (TWE), is introduced, and investigated for non-invasive diagnosis of skin cancer and characterization of the mechanical properties of the skin. This technique incorporates biomarkers such as viscosity and elasticity to facilitate the diagnosis of skin-related diseases.
**Methods:** A new Torsional Wave Elastography (TWE) device has been developed for diagnosing skin cancer, inspired by a previously created TWE device for evaluating cervical mechanical properties [3]. This portable device features an emitter producing shear elastic waves and a sensor capable of detecting waves within the 50 Hz to 20 kHz range. The study included 31 patients with suspected malignant skin lesions, adhering to specific inclusion/exclusion criteria, ethics committee approval, and informed consent. Out of these, 20 patients with no history of pre-surgical therapy or cancer recurrence were chosen for testing. Initially, the stiffness of the affected tissue was assessed by measuring the shear wave velocity in the 0.4 to 1 kHz frequency range. For comparative purposes, tests were also performed on healthy tissue either on the symmetrical side of the body or near the suspected lesion. The Histopathology test was considered the gold standard for the study. The results were then compared to the histopathology examination of the same lesion after surgical removal.
**Results:** Results obtained from the tests done on both pathological and healthy tissue were analyzed and a classification of the lesion as benign or malignant was determined based on the changes in the velocity of the shear wave. The obtained results were then compared to the histopathology reports and a statistical analysis utilizing ROC (Receiver Operating Curve) was done correlating the histopathology report and the TWE results with the AUC of 0.91, demonstrating the accuracy of TWE technique in non-invasive diagnosis of skin cancer by avoiding false negatives in diagnosis.
**Conclusions:** The promising initial results suggest TWE could be a useful tool for diagnosing skin pathologies. Further research will evaluate its robustness and reliability. Moreover, the TWE technology has shown potential for noninvasive screening and precise extraction of skin mechanical properties by considering various biomarkers.
**Acknowledgements:** MS2022-96 Ayudas para la recualificación del sistema universitario Español; INTRAIBS-2022-05; Ministerio de Ciencia e Innovación. PID2020-115372RB-100, PYC20 RE-072 UGR; Listen2Future funding by 101096884 in HORIZON-KDT-JU-2021-2-RIA and by PCI2022-135048-2.

**References:**

[1] Kalra et al. (2016). "An Overview of Factors Affecting the Skins Youngs Modulus". J Aging Sci 2016, 4:2
[2]. Callejas et al, "Kelvin–Voigt Parameters Reconstruction of Cervical Tissue-Mimicking Phantoms Using Torsional Wave Elastography", Sensors, vol. 19, 3281, 2018.

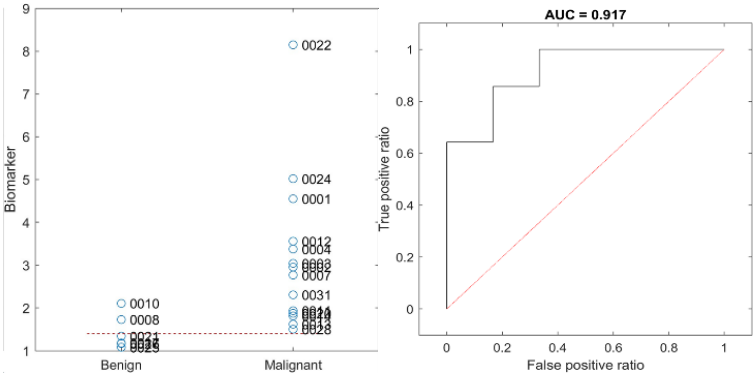


Figure1. Statistical analysis based on the correlation of the TWE biomarkers with the histopathology reports.

# HIGH-RESOLUTIONAL SHEAR WAVE PHASE ESTIMATION WITHIN SMALL ROI AND ITS APPLICATION IN MULTI-LAYERED ELASTIC STRUCTURES EVALUATION.

*N Tano*[1,*], *R Koda*[2], *Y Yamakoshi*[1,2], *M Tabaru*[1]

[1]Tokyo Institute of Technology, Yokohama, Kanagawa, JAPAN; [2]Gunma University, Kiryu, Gunma, JAPAN.

**Background:** Continuous shear wave elastography (C-SWE), with an external vibrator to excite a continuous wave, employs spectral calculation for the reconstruction of propagated shear waves [1]. While it provides a better understanding of wave components and multiple filters for noise reduction, it can reduce the spatial resolution. Observing muscles for inflammation, which is caused by fascia adhesion, requires high spatial resolution measurements [2]. Here, we propose the approximation differential calculation method for shear wave reconstruction in C-SWE to obtain local changes in mechanical properties.
**Aims:** This study aims to establish a high-resolution analysis of shear wave propagation and phase enhancement for thin layer adhesion analysis.

**Results:** As shown in Figure b, a simulation study on a multi-layered structure was performed. By simulating the adhesion condition by inserting the adhesion coefficient, a "phase jump", dynamic shift in the phase of shear wave, occurred. This phenomenon was only observed using the proposed calculation method. Fine elastic structure of a healthy volunteer was also detected using the proposed method, with a similar phase jump to the simulation study, as presented in Figure c.

**Conclusions:** The proposed method allows for the detection of different layers based on phase information. By combining the phase view with shear wave velocity, it may be possible to measure thin-layer hardness in different anatomical structures.

**Acknowledgements:** Part of this work was supported by JSPS KAKENHI Grant Number 22K04134 and the Cooperative Research Project of Research Center for Biomedical Engineering.

**References:**
[1] Tano, N., Koda, R., et al., “Continuous Shear Wave Elastography for Liver Using Frame-to-Frame Equalization of Complex Amplitude”, Ultrasonic Imaging, 46(3):197-206, (2024).
[2] Ma, X., Gao, H., et al., “Increased expression of cell adhesion molecules in myofasciitis”, Frontiers in Neurology 14:113404, (2023)

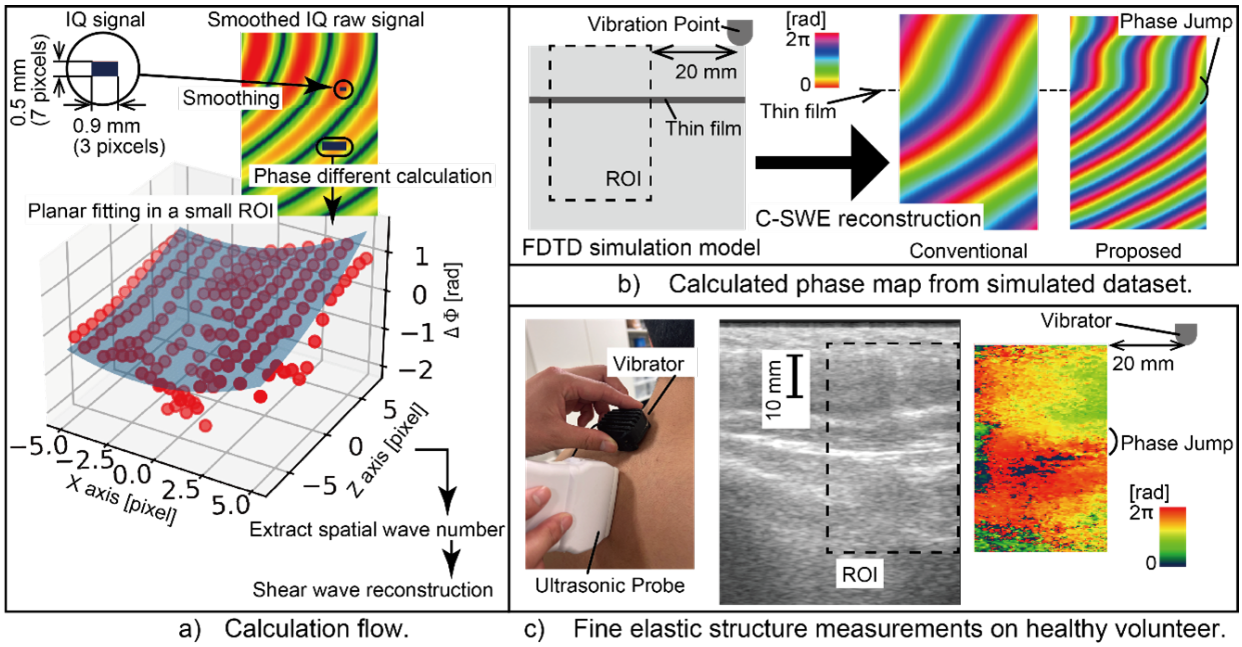

# EVALUATING CORNEAL ELASTICITY: A NONLINEAR APPROACH USING TORSIONAL WAVE TECHNOLOGY.

*Inas H Faris*[1,2,3,*], *Antonio Callejas*[1,2,3], *Jorge Torres*[4], *Guillermo Rus*[1,2,3]

[1]UltrasonicsLab, Dept of Structural Mechanics, University of Granada, Granada 18071, SPAIN; [2]TEC-12 Group, Instituto de Investigación Biosanitaria, ibs.Granada Granada 18001, SPAIN; [3]Excellence Research Unit "ModelingNature" (MNat), University of Granada, Granada 18001, SPAIN; [4]INSERM LabTAU U1032, Lyon, FRANCE.

**Background:** Measuring the mechanical nonlinear properties of the cornea remains challenging due to the lack of consensus in methodology and models that effectively predict its behavior[1]. This study aims to develop a procedure to reconstruct nonlinear fourth-order elastic properties of the cornea using torsional wave elastography (TWE). Understanding tissue elasticity, which varies with context and scale, is crucial as it influences cell structure and responses. Corneal mechanics are particularly important for diagnosing diseases related to intraocular pressure (IOP) alterations, such as glaucoma and ocular hypertension.
**Aims:** Our goal is to enhance elastography techniques to characterize the dynamic elastic properties of the cornea. We aim to distinguish between healthy and damaged corneas by measuring nonlinear parameters [2]. Specifically, we seek to identify differences in the Lamé parameter, third-order elastic constant, and fourth-order elastic constant using TWE at various IOP levels [3]. **Methods:** We used a torsional wave device to measure in-plane corneal samples (Figure1-Left), incrementally increasing IOP from 5 to 25 mmHg in 5 mmHg steps. Samples included non-treated and ammonium hydroxide (NH4OH)-treated porcine corneas. The shear wave speed was measured, and a mathematical model based on Hamilton's theory was applied to determine nonlinear elastic parameters. Data were collected using a multichannel AD/DA converter and a high-speed MATLAB® environment (Release 2018, MathWorks, Natick, United States).
**Results:** Our study measured the shear wave speed of both control and NH4OH-treated cornea samples at various IOP levels (Figure1-Right). The results showed a nonlinear variation in shear wave speed with higher values for higher IOPs. Control group samples exhibited higher shear wave speeds compared to treated samples. Significant differences were found between control and treated groups in the Lamé parameter (25.9–6.52 kPa), third-order elastic constant (215.09–44.85 kPa), and fourth-order elastic constant (523.5–129.63 kPa), with p-values of 0.010, 0.024, and 0.032 respectively.
**Conclusions:** Our torsional wave elastography system effectively measured and analyzed the nonlinear elastic properties of the cornea at the microscopic level. It captured detailed viscoelastic values across a range of IOPs, demonstrating significant differences between healthy and chemically treated corneas. This advancement in spatial resolution and physiological relevance enhances our ability to diagnose diseases related to intraocular pressure, such as glaucoma. Future applications will focus on in vivo tissues, providing deeper insights into corneal mechanics and disease mechanisms.
**Acknowledgements:** Ministerio de Ciencia e Innovación grant numbers PID2020-115372RB-I00, PYC20 RE 072 UGR; Junta de Andalucía - Consejería de Universidad, Investigación e Innovación- proyecto (P21_00182); Listen2Future funding by 101096884 in HORIZON-KDT-JU-2021-2-RIA and by PCI2022-135048-2 by Ministerio de Ciencia e Innovación; Proyectos Intramurales IBS.Granada INTRAIBS-2022-05; Ministerio de Universidades Ayudas para la recualifcación del sistema universitario español, MS2022-96 (Co funded by European Union Next GenerationEU/PRTR).

**References:**

[1] Wang Y, Cao H. Corneal and scleral biomechanics in ophthalmic diseases: an updated review. Med Novel Technol Devices. 2022.
[2] Gennisson J-L, Rénier M, Catheline S, Barrière C, Bercoff J, Tanter M, Fink M. Acoustoelasticity in soft solids: assessment of the nonlinear shear modulus with the acoustic radiation force. J Acoustical Soc Am. 2007;122(6):3211–3219.
[3] Torres J, Faris IH, Callejas A, Reyes-Ortega F, Melchor J, Gonzalez-Andrades M, Rus G. Torsional wave elastography to assess the mechanical properties of the cornea. Sci Rep. 2022;12(1):1–11.

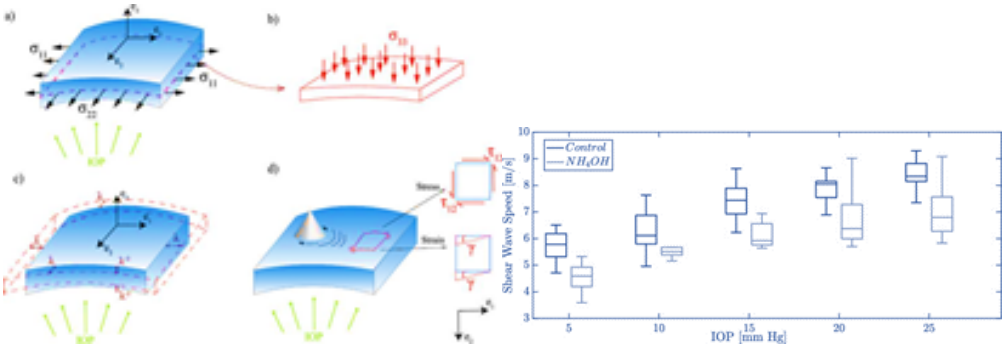


Figure1: (Left) Scheme of the stress and strain field. (Right) SWS from TWE for control and NH4OH vs IOP

# TOWARDS A CLINICAL USE OF ROBOTIZED TRANSIENT OPTICAL COHERENCE ELASTOGRAPHY IN HUMAN SKIN

*A. Marmin*[1], *G. Regnault*[1], *A. BS*[1], *B. Anderson*[1], *R. K. Wang*[1], *M. O'Donnell*[1], *I. Pelivanov*[1]

[1]University of Washington, Seattle, Washington, United States.

**Background:** Certain pathologies, such as malignant tumors and inflammatory diseases, alter the structure of biological tissues, thereby modifying their mechanical properties. For example, in skin, injuries often require grafting, and monitoring elastic properties of replaced tissue in the recipient site helps in managing its healing. Recently, transient elastography using phase-sensitive optical coherence tomography (OCT) for the detection of propagating mechanical waves has demonstrated substantial clinical potential, providing quantitative, noncontact stiffness measurements in skin and ocular tissues [1]. In addition, multiple OCT modalities (polarization-sensitive (PS) OCT and OCT angiography) can be combined with OCE to provide comprehensive micron-scale resolution data about structural and functional properties of the investigated skin region [2]. Experimental studies have focused on addressing mechanical anisotropy to reduce biases related to sample orientation and to improve precision in elasticity measurements. Some approaches utilize diffuse wave fields to retrieve anisotropy [3], though they are limited by approximations in boundary conditions and energy partition. Alternatively, other studies have employed directional shear-wave sources and multi-angle acquisitions [2,4]. Those first studies on anisotropy imaging using optical systems have yielded promising results, indicating that transient OCE can effectively reconstruct anisotropic mechanical moduli. However, previous approaches necessitated manual sample rotation, leading to increased acquisition times and a lack of spatial resolution.

**Aims:** To develop a fiber-optic, robotized, fully automated, investigational clinical system for non-contact monitoring of skin graft surgeries based on co-registered four OCT modalities (structural OCT, PS-OCT, OCT angiography and OCE).

**Methods:** An 1310nm fiber-optic swept-source OCT has been integrated on a cart. The sample arm of the interferometer was mounted on a robotic arm with an objective (Thorlabs, LSM03) achieving 16 um lateral and 12 um axial resolutions in air with a dynamic range around 92 dB. and the field of view is 8x8 mm with an A-line rate of 400 kHz. A custom cylindrical acoustic micro-tapping transducer [5] was added to the imaging head to provide a line-source excitation for launching plane surface mechanical waves over skin surface. Contrary to point sources, the plane waves allow direct measurement of the phase velocity required for the reconstruction of mechanical moduli in skin [4].

**Results:** Nineteen-angle propagation in plane of the skin was used as the robotic arm automatically aligned the imaging head, performed its rotation and compensated for tissue motion. All four OCT-based images (structural OCT, PS-OCT, OCT angiography and OCE) were acquired. In OCE, the wave field is then reconstructed for different angles followed the reconstruction of all three anisotropy mechanical moduli ($G$, $\mu$ and $\delta$) based on a nearly incompressible transversely isotropic model (NITI) [6]. All measurements were performed in-vivo on healthy volunteers in different skin sites.
**Conclusions:** Our preliminary results show that the approach proposed herein can provide comprehensive quantitative metrics regarding skin's structural, functional and mechanical properties which gives a promise for its clinical translation.

**Acknowledgements:** This work was funded by NIH (R01EY035647, R01AR077560) and the Department of Bioengineering at The University of Washington.

**References:**

[1] Wang S, Larin KV. "Optical coherence elastography for tissue characterization: a review". J. Biophotonics. 8(4):279-302 (2015).
[2] M. Kirby, P. Tang, H. Liou et. al. "Probing elastic anisotropy of human skin in vivo with light using non-contact acoustic micro-tapping OCE and polarization sensitive OCT," Sci. reports 12, 1–17 (2022).
[3] A. Marmin, F. Facca, S., Catheline and al., "Full-field noise-correlation elastography for in-plane mechanical anisotropy imaging." Biomedical optics express, 15(4), 2622-2635 (2024).
[4] G. Regnault, R. Wang, M. O'Donnell et. al. ''Line source excitation for accurate reconstruction of all three shear moduli in skin using non-contact OCE.", Optical Elastography and Tissue Biomechanics X, SPIE. (2024).
[5] Ł. Ambroziński, S. Song, S.J. Yoon SJ et. al. "Acoustic micro-tapping for non-contact 4D imaging of tissue elasticity." Sci Rep. 6:38967 (2016)
[6] J. Pitre, M. Kirby, D. Li, et. Al. "Nearly-incompressible transverse isotropy (NITI) of cornea elasticity: model and experiments with acoustic micro-tapping OCE." Sci Rep. 10(1):12983 (2020).

# NON-LINEAR ELASTICITY OF THE BRACHIAL ARTERY IN KOROTKOFF SOUNDS GENERATION

*Jerome Baranger*[1,*], *Olivier Villemain*[1], *Guillaume Goudot*[1,2], *Alexandre Dizeux*[1], *Heiva Le Blay*[1], *Tristan Mirault*[2], *Emmanuel Messas*[2], *Mathieu Pernot*[1], *Mickael Tanter*[1]

[1]Physics for Medicine Paris, Inserm U1273, ESPCI, PSL Paris, CNRS UMR 8063, Paris, France [2]Université Paris Cité, Inserm U970, PARCC, Vascular Medicine Department, Hôpital Européen Georges-Pompidou, Assistance Publique des Hôpitaux de Paris, Paris, France.

**Background:** Blood pressure measurement is a critical clinical procedure for predicting cardiovascular risk and guiding treatment. The gold standard for noninvasive assessment is the auscultatory method, which relies on detecting Korotkoff sounds (KSs) using a stethoscope placed at the outlet of a pneumatic arm cuff. Despite their widespread clinical use, the fundamental mechanisms generating KSs are still debated, posing limitations to the accuracy of blood pressure measurements.

**Aims:** This study aims to elucidate the fundamental mechanisms behind the generation of Korotkoff sounds, with a particular focus on the role of the non-linear elasticity of the brachial artery. Understanding these mechanisms could provide insights into arterial biomechanics in vivo [1].

**Methods:** We employed ultrafast ultrasound imaging (UUI) using an Aixplorer system (Supersonic Imagine, Aix-en-Provence, France) with a linear transducer to capture in vivo images of the brachial artery under the pressure cuff at frame rates up to 10,000 frames per second. The arterial wall motion, tissue displacements, blood flow, and tissue stiffness were measured. An electronic stethoscope (Littmann 3200, 3M, St. Paul, MN, USA) was used to acquire the KSs simultaneously. Data were analyzed using MATLAB (MathWorks, Natick, MA, USA) for signal processing and correlation analysis.

**Results:** Our results demonstrate that the Korotkoff sounds are not traditional sound waves emanating from the brachial artery but are instead shear vibrations transmitted through surrounding tissues. These vibrations are induced by the non-linear pulse wave propagation in the compressed artery segment under the cuff, that engenders wall motions of high amplitudes. As the pulse wave propagates, its wavefront steepens until it reaches a shock that can be observed inside the cuff at high cuff pressure levels. We matched these observations with a new theoretical pressure-area relationship for the artery involving fluid mechanics and acousto-elasticity.

**Conclusions:** This study provides a detailed mechanistic insight into the generation of Korotkoff sounds, highlighting the critical role of the non-linear elasticity of the brachial artery and the formation of shock waves. These findings challenge the traditional understanding of KSs and suggest that our work may help to better understand arterial biomechanics in vivo.

**Reference:**

[1] J. Baranger. O. Villemain et al., « The fundamental mechanisms of the Korotkoff sounds generation », Science Advances, vol. 9, no 40, p. eadi4252, oct. 2023, doi: 10.1126/sciadv.adi4252.

# EXPERIMENTAL CHARACTERIZATION OF YOUNG'S MODULUS USING OPTICAL ELASTOGRAPHY IN A SOFT ELASTIC STRING.

*Jiayuan Zhu, François Legrand, Sibylle Grégoire, Frédéric Turquier, Aline Bel-Brunon, Stefan Catheline, Bruno Giammarinaro*

LabTAU, INSERM, Centre Léon Bérard, Université Claude Bernard Lyon 1, F-69003, LYON, France; University of Lyon, INSA Lyon, CNRS, LaMCoS, UMR5259, 69621 Villeurbanne, France

**Background:**When playing string instruments, people usually adjust the tension on the strings to control the pitch. Strings, both physically and mathematically, are considered at first sight the simplest and most intuitive model for studying waves. We revisit the subject with soft strings of quasi-incompressible materials. However, based on experimental research, the waves propagating on strings are not as simple as we might think.
**Aims:**This study aims to characterize three types of waves propagating on hyper-elastic strings under tension and to extract the mechanical parameters of the strings.
**Methods:** Experiments are performed on strings made in Eco-Flex 00—20 Fast. Waves are then excited by a shaker and are analyzed using optical elastography is, a technology based on image processing algorithms and noise correlation algorithms. We use a high-speed camera to record the propagation process of the three types of waves in the medium and then use MATLAB-based image processing algorithms and noise correlation algorithms to ultimately obtain the wave speeds in the medium [1]. The extracted wave speeds are then compared to theoretical models from beam theory to estimate the useful mechanical parameters.
**Results:** We successfully observed the different types of waves on the cylinder and extracted the mechanical parameters of the strings for different tensions. We found that the wave speed of the Young waves is not sensitive to changes in tension within the cylinder contrary to the other ones. However, the wave speed obtained using optical elastography is slightly higher than that of static mechanical reference experiments. We introduced the viscoelastic Voigt model to reduce the gap between the two.
**Conclusions:** The successful measurement of Young waves propagating in a one-dimensional medium using optical elastography fills the previous gap in the research of these waves. It also lays the foundation for subsequent studies on bending waves and string waves in cylinders. Additionally, the study of waves on cylinders contributes to the application research of medical imaging in tensioned organs such as tendons and ligaments. However, it is essential to consider the viscous effects of the medium on the wave propagation when using this method to determine the Young's modulus.
**Acknowledgments:** With financial support from ITMO Cancer of Aviesan within the framework of the 2021-2030 Cancer Control Strategy, on funds administered by Inserm.

**References:**

[1] G. Laloy-Borgna, L. Puyo, H. Nishino, M. Atlan, et S. Catheline, « Observation of natural flexural pulse waves in retinal and carotid arteries for wall elasticity estimation », Sci. Adv., vol. 9, no 25, p. eadf1783, juin 2023, doi: 10.1126/sciadv.adf1783.

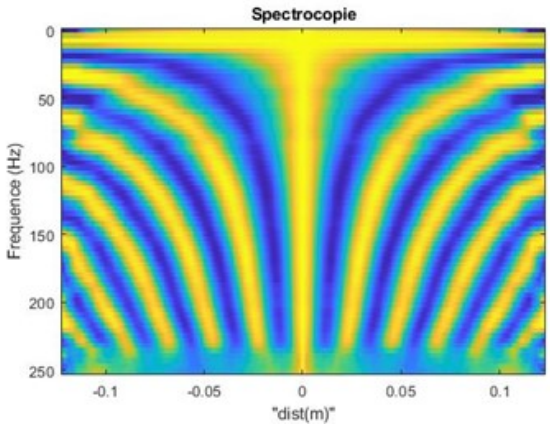


Figure: Correlation Spectroscopy: experimental measurement of wavelength (x axis) as function of frequency (y axis).

# FLEXURAL PULSE WAVE VELOCITY IN BLOOD VESSELS

*Sibylle Gregoire*[1,*], *Gabrielle Laloy Borgna* [2], *Johannes Aichele* [3], *Fabrice Lemoult* [4], *Stefan Catheline* [1]

[1]LabTAU, INSERM, Universite Lyon 1, Lyon, 69003, France, [2]ImPhys, Technische Universiteit Delft, Delft, 2628 CJ, The Netherlands, [3]Institute of Geophysics, ETH Zurich, Zurich, 8092, Switzerland, [4]Institut Langevin, CNRS, Universite PSL, Paris, 75005, France

**Background:** Arteriosclerosis is a major risk factor for cardiovascular disease and results in arterial vessel stiffening [1]. Velocity estimation of the pulse wave sent by the heart and propagating into the arteries is a widely accepted biomarker. This symmetrical pulse wave propagates at a speed which is related to the Young's modulus through the Moens Korteweg equation [2, 3]. Recently, an antisymmetric flexural wave has been observed in vivo [4]. It offers promising applications for monitoring arterial stiffness and early detection of atheromatous plaque. However, to our knowledge, no equivalent of the Moens Korteweg equation exists for flexural pulse waves linking its velocity to arterial stiffness. This work aims to bridge this gap.
**Methods:** To bridge this gap, a beam based theory was developed, and approximate analytical solutions were reached. An optical experiment in soft polymer artery phantoms was built to observe the dispersion of flexural waves. Moreover, finite elements (FE) simulations were develloped to study the flexural waves dispersion.
**Results:**After a heart beat, all modes of propagation can exist within a blood vessel. Two were observed experimentally, the symmetric mode and the flexural mode. The symmetric mode, which travels at the Moens Korteweg's velocity, is well known and used to probe the elasticity of arteries. This mode is not dispersive, and propagation is thus independent of frequency. Unlike the symmetric mode, the flexural mode is dispersive. In this work the link between the phase velocity of the flexural wave and the elasticity of the blood vessels was characterized. Figure 1 displays the evolution of the phase velocity with frequency for the flexural mode. The dots represent optical experimental data, while the solid curves represent FE simulations. The dashed curves represent the analytic approximations, for a cylinder (a), a tube (b) and a fluid filled tube (c).

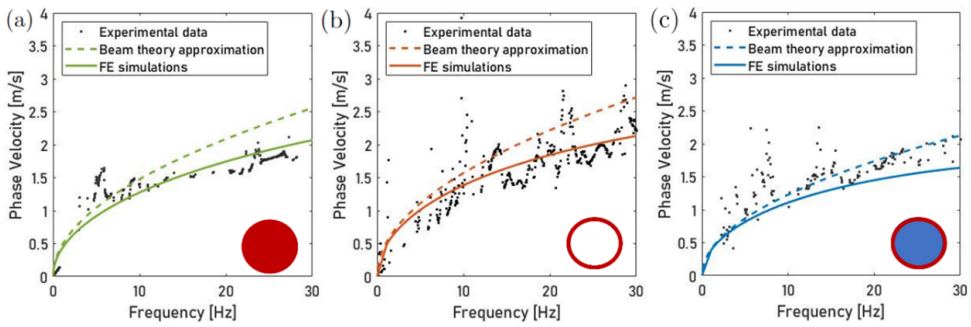


*Figure 1 Dispersion curves of the flexural mode in a cylinder in PVA (a), a hollow tube of PVA (b), and in a water filled tube of PVA(c). Dots represent experimental data, plain curves are finite elements simulated data and dotted curves are the analytic results.*

**Conclusions:** The validity of the analytic expression was verified both experimentally and in FE simulations for physiological frequencies. Thanks to its dispersive behaviour the flexural mode travels slower at low frequencies. With fast imaging devices, like ultrafast ultrasound imaging, precision on the measured flexural pulse wave speed is thus higher than that of the symmetric mode. Local, precise, noninvasive measurement of blood vessel elasticity could be reached. The slowness of the flexural wave makes elasticity measurements with X-rays, MRI, or FF-OCT possible. Finally, an accurate, noninvasive estimation of arterial pressure is also envisioned.
**Acknowledgments:** With financial support from ITMO Cancer of Aviesan within the framework of the 2021-2030 Cancer Control Strategy, on funds administered by Inserm.

**References:**

[1] Arterial Elastic Properties and Cardiovascular Risk/Event. K. S. Cheng, C. R. Baker, G. Hamilton, A. P. G. Hoeks, A. M. Seifalian. 2002, European Journal of Vascular and Endovascular Surgery.
[2] Die Pulscurve. Moens, A. A. Isebree. 1878.
[3] Ueber die Fortpflanzungsgeschwindigkeit des Schalles in elastischen Rohren. Korteweg, D. J. 1878, Annalen der Physik und Chemie.
[4] Observation of natural flexural pulse waves in retinal and carotid arteries for wall elasticity estimation. G. Laloy-Borgna, L. Puyo, H. Nishino, M. Atlan, S. Catheline. 2023, Science Advances.

# EXPLORING BIOMECHANICAL PROPERTIES OF THE ANTERIOR BLADDER WALL: PRELIMINARY STUDY ON SHEAR WAVE ELASTICITY IMAGING FOR BLADDER CANCER TUMOR GRADE ASSESSMENT.

*Iyad Chaoui*[1,*], *Damien Fouan*[1], *Ali Bourgi*[2], *Franck Bruyère*[2], *Ayache Bouakaz*[1], *Frédéric Patat*[1], *Jean-Pierre Remenieras*[1]

[1]Université de Tours, INSERM, Imaging Brain & Neuropsychiatry iBraiN U1253, 37032, Tours, France ; [2]Département d'Urologie, Centre Hospitalier Universitaire, Tours, France.

**Background:**Accurately estimating the pathological grade of bladder cancer (BCa) tumors preoperatively is crucial for determining appropriate adjuvant treatment options. Early single instillation of intravesical chemotherapy (SICI) is beneficial for low-grade tumors, reducing recurrence rates. With poor diagnostic sensitivity [1], the absence of preoperative high-grade cytology is the only method to predict tumor grade [2]. There is a need for a non-invasive preoperative evaluation of BCa to better determine the eligibility of patients for SICI. Assessing BCa stiffness using Shear Wave Elasticity (SWE) is a potential method to differentiate high-grade from low-grade tumors [3].
**Aims:** To validate our suprapubic approach for measuring bladder tumor elasticity, we aim to compare the shear elastic modulus$\mu_{eff}$ of the non-tumoral anterior bladder wall to the applied stress $\sigma$during bladder filling.
**Methods:** Since February 26, 2024, patients admitted to the Urology Department at Tours University Hospital with a bladder tumor and no history of bladder resection have been recruited. Measurements were taken under general or spinal anesthesia, in the operating room just before transurethral resection.
- *Conventional ultrasound and SWE Examinations* : Suprapubic bladder ultrasound at different filling volumes were performed using the Aixplorer system® (SuperSonic Imagine) equipped with a convex XC6-1 probe. Parameters such as wall thickness e, minor $r_1$, and major radii $r_2$ were measured on a cross-section of the bladder's largest axis. Laplace's law was used to calculate the stress applied to the bladder wall. Shear elastic modulus maps of the tumor and anterior non-tumoral bladder wall were recorded, segmented, filtered and analyzed using MATLAB® software.
- *Intravesical pressure assessment* : Intravesical pressure p was monitored using the SmartDyn® urodynamic system (Creo Medical). The bladder was catheterized with a 24 Fr resectoscope system, connected to a water sensor and a roller pump irrigation system. Bladder was filled from 0 to 400mL. The resection was then performed, allowing histopathological analysis of the bladder tumor.
**Results:** Bladder shear elastic modulus $\mu_{eff}$ is linearly related to bladder wall stress induced by the intravesical pressure. Among the 10 patients included, a strong correlation coefficient was observed (individual patient $r^2$ ranged from 0.55 to 0.91, overall $r^2$ = 0.51, p < 0.001). Additionally, there was a significant increase in the shear elastic modulus $\mu_{eff}$ throughout bladder filling, with a multiplicative factor ranging from 4 to 18.
**Conclusions:** Preliminary in-vivo results validate the use of SWE imaging with a suprapubic approach in the bladder model. We are currently developing a physical model of nonlinear bladder behavior that explains our experimental results. With an increased sample size, our objective is to evaluate the difference in shear elastic modulus between low- and high-grade bladder urothelial carcinoma and to assess the influence of intravesical pressure on tumor stiffness.
**Acknowledgments:** I.C. is funded by a research year scholarship from the Centre-Val de Loire Regional Health Agency.

**References:**

[1] Reid et al. Accuracy of grading of urothelial carcinoma on urine cytology: an analysis of interobserver and intraobserver agreement. Int J Clin Exp Pathol. Oct 2020.

[2] Neuzillet Y et al. French AFU Cancer Committee Guidelines - Update 2022-2024. Prog Urol. Nov 2022.

[3] Huang et al. Shear Wave Elasticity differentiation between low- and high-grade bladder urothelial carcinoma and correlation with collagen fiber content. J Ultrasound Med. Jan 2021

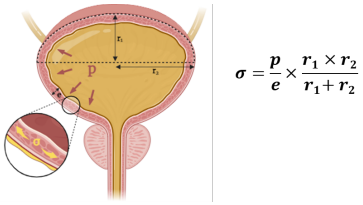


Fig1: Bladder anatomy and stress distribution in the bladder wall.

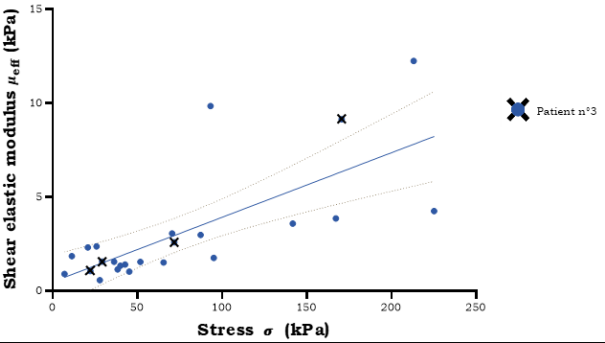


Fig 2: Scatter plot showing the correlation between shear elastic modulus (kPa) and bladder wall stress (kPa).

# DIRECT IN VIVO CHARACTERIZATION OF TENSILE ANISOTROPY AND SHEAR ANISOTROPY OF SKELETAL MUSCLE BY ULTRASOUND SHEAR WAVE ELASTOGRAPHY

*Ricardo J. Andrade[1,*], Apolline Racapé[1] Mar Hernández-Secorún[1], Ha-Hien-Phuong Ngo[2], Alice Lemoine[3], Nicolas Etaix[3], Thomas Frappart[3], Christophe Fraschini[3], Antoine Nordez[1,4], Jean-Luc Gennisson[2]*

[1]Nantes Université, Mouvement - Interactions - Performance, MIP, UR 4334, Nantes, France ; [2]Université Paris-Saclay, CEA, CNRS, Inserm, BioMaps, Orsay, France ; [3]Supersonic Imagine, Aix-en-Provence, France ; [4]Institut Universitaire de France (IUF), Paris, France.

**Background:** In vivo imaging assessment of skeletal muscle structure and function enables longitudinal quantification of tissue health. Conventional ultrasound shear wave elastography (SWE) has shown promise as a noninvasive method to estimate tissue mechanical properties in response to tissue loading and disease. In clinical implementation of conventional SWE, the medium is commonly assumed to be isotropic; yet muscles are anisotropic due to their fiber arrangement. Consequently, three independent parameters are needed to fully characterize muscle tissue as an elastic, incompressible, transversely isotropic material: the longitudinal shear modulus ($\mu_{//}$), the transverse shear modulus ($\mu_{\perp}$), and the tensile anisotropy ($X_E$). The ability to measure $X_E$, corresponding to the ratio of the Young's moduli, may therefore provide a unique biomarker for muscle mechanical characterization. Previous work has demonstrated that $X_E$ can be estimated through Green's function simulations.
**Aims:** Herein we developed a methodology to experimentally quantify $X_E$ by combining a novel steered pushing beam (SPB) elastography sequence with SWE during passive muscle axial loading.
**Methods:** All measurements were performed on the fusiform human biceps brachii muscle of 9 healthy participants. Ethical approval was obtained from local institutional board. Two different measurements were conducted to capture shear wave wavefronts using SPB and conventional SWE sequences. Muscle tensile load was modulated by passively varying the elbow joint from 70° to 180° (180°=full extension) by increments of 5°. An ultrafast ultrasound scanner (Mach30, Supersonic Imagine) driving a 7.5 MHz central frequency transducer array (SL18-5, 256 elements) was used for all data acquisitions. First, the ultrasound transducer was aligned with the muscle shortening direction (longitudinal to the muscle fibers). In this configuration, the SPB method was used to quantify both the elastic parameter $X_E\dot{\mu}_{\perp}$ and $\mu_{//}$ (Figure A1) by capturing the shear vertical (SV) propagation mode. Second, the transducer was rotated 90° in respect to the muscle fibers. In this configuration, conventional SWE was used to track the shear horizontal (SH) propagation mode and, thus, to quantify $\mu_{\perp}$ (Figure A2). Finally, tensile ($X_E$) and shear anisotropy ($X_{\mu}$) factors were calculated as follows: $X_E = (X_E\dot{\mu}_{\perp})/\mu_{\perp}$ and $X_{\mu} = \mu_{//}/\mu_{\perp}$.
**Results:** Averaged $X_E$ across all elbow angles varied from 3.1±0.9 to 6.5±3.7 (Figure B). At the slack angle (85°), $X_E$ was 3.3±1.5, being greater (p = 0.01) than $X_{\mu}$ (2.8±1.4). These findings are in line with previous literature, where $X_E$ was estimated by means of simulations; and experimentally confirms that $X_{\mu}$ is an additional independent parameter.
**Conclusions:** This study demonstrates that $X_E$ can be directly quantified without the need of time-consuming simulations, enabling the full and direct characterization of anisotropic muscle tissues with a fusiform geometry. We speculate that the ability to measure both $X_E$ and $X_{\mu}$ may provide a novel and promising biomarker for muscle health characterization and warrants further studies. The behavior of the shear moduli and $X_E$ during passive muscle lengthening also indicates the involvement of non-linear elasticity in shear wave propagation, highlighting the need to take it into account in future studies.
**Acknowledgments:** This work was funded by ANR INNOVAN under grant number ANR-19-CE19-001

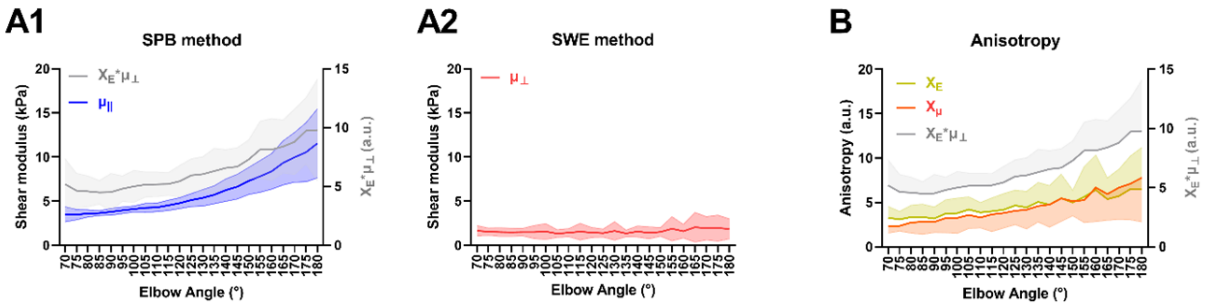

# SPEED-OF-SOUND AS A NOVEL TISSUE CHARACTERIZATION METHOD

*CD Bezek*[1,*], *O Goksel*[1]

[1]Uppsala University, Uppsala, SWEDEN.

**Background:** Typical B-mode ultrasound (US) images display the reflectivity of tissue structures, which provides only qualitative information. Most quantitative US imaging research aims to image the Young's modulus, estimated from vibrational displacements or shear-wave speed measurements. Speed-of-sound (SoS) is an alternative quantitative biomechanical marker that relates to the bulk modulus and may provide complementary and/or independent information on tissue composition and pathological states, such as breast cancer [1]. Therefore, tissue can be fully characterized using both SoS and elastography. SoS is also important for other ultrasound imaging modalities that depend on beamformed images, such as shear-wave elastography [2] and local SoS imaging [3].
**Aims:** A novel and effective global SoS estimation method is proposed.
**Methods:** After two different transmissions ($T_x$), radiofrequency (RF) echo images are beamformed using an assumed constant SoS. These two images are then compared using a displacement estimation (speckle tracking) algorithm to identify apparent inter-frame speckle shifts, denoted as $\Delta x$. Any discrepancy between the assumed beamforming SoS (cbf) and the actual tissue SoS (cgt) creates a specific spatial-variation in $\Delta x$, which can be modeled as a function of differential distances to any beamformed point N, as $\Delta x = (c_{bf}/c_{gt} - c_{gt}/c_{bf})(d_{N2} - d_{N1})/2$. By concatenating these measurements (and potentially multiple $T_x$), a single linear model is solved, cf. Fig(a). SoS is found by iteratively running beamforming, speckle tracking, and model fitting.
**Results:** Our method finds the effective SoS value after a few iterations in tissue-mimicking phantoms, regardless of the initial assumed SoS, cf. Fig(b). Using the correct SoS also improves the quality of B-mode images, cf. Fig(c). Our results also show improved accuracy in local SoS reconstructions when using the estimated global SoS value for the image area instead of a pre-set generic value. Additionally, we demonstrate that SoS is promising for breast density classification, achieving 100% specificity and 78% sensitivity with an area under the curve (AUC) of 0.924 for dense breast classification. Extremely dense breasts were classified with 100% specificity and 75% sensitivity, with an AUC of 0.906.
**Conclusions:** Our SoS estimation method effectively finds the tissue SoS. These values can then be used for tissue characterization, improving B-mode image resolution and local SoS reconstruction accuracy.
**Acknowledgments:** Funding was provided by the Uppsala Medtech Science and Innovation Centre.

**References:**

[1] Ruby, L., et al., "Breast cancer assessment with pulse-echo speed of sound ultrasound from intrinsic tissue reflections: Proof-of-concept," Invest Radiol. 54(7), 2019.
[2] Chintada, B.R., et.al., "Phase-aberration correction in shear-wave elastography imaging using local speed-of-sound adaptive beamforming," Front. Phys. 9, 2021.
[3] Bezek, C.D., and Goksel O. "Analytical estimation of beamforming speed-of-sound using transmission geometry." Ultrasonics 134, 2023.

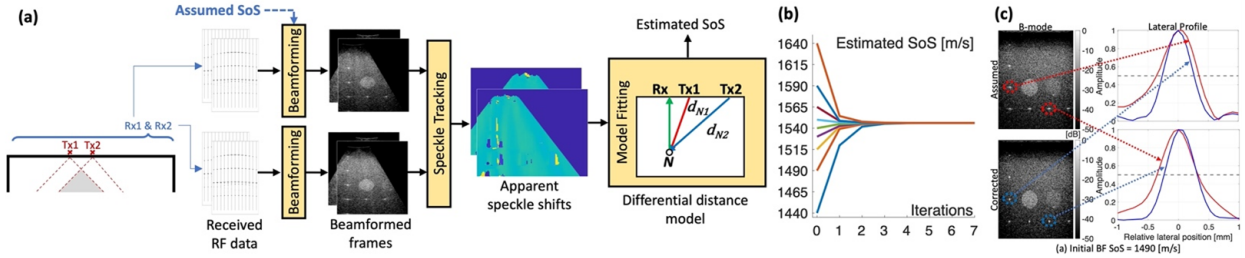


Fig. (a) Schematic of the proposed method. (b) Iterative estimation of SoS for a tissue-mimicking phantom from different initial SoS assumptions. (c) Improvements in B-mode image of the tissue-mimicking phantom.

# ELUCIDATING THE EFFECT OF FLUID CONTENT ON MODEL-FREE ELASTOGRAPHY ESTIMATES USING VISCOELASTIC PHANTOMS

*SR Bisht*[1,*], *BP Marri*[1], *KP Mercado-Shekhar*[1].

[1]Indian Institute of Technology (IIT) Gandhinagar, Gandhinagar, Gujarat, INDIA.

**Background:** Viscoelastic properties of tissues are commonly estimated by shear wave elastography based on fitting a rheological model to the shear wave dispersion curve. However, there is a lack of consensus about rheological models that best represent tissue behavior [1]. The choice of the model may create bias in viscoelasticity estimates [2]. Therefore, model-free elastography approaches, such as shear wave attenuation (SWA) and dispersion slope analyses, have been investigated. The amount of fluid in tissues changes during tumor progression [3], which may affect model-free elastography estimates, and hence, has been assessed in this study.
**Aims:** The current study aims to evaluate the effect of fluid content on SWA and dispersion slope estimates using viscoelastic tissue-mimicking phantoms.
**Methods:** Four phantom types were prepared using a mixture of low-viscosity polyvinyl alcohol (PVA, 5% w/v, Elvanol 71-30, Kuraray America, Inc., Houston, USA) and high-viscosity PVA (5, 6, 8, and 10% w/v), a cryoprotectant (20% v/v concentration, Waxpol Industries Ltd, Ranchi, India), silicon carbide (SiC) particles (1% w/v, 600 grit), and distilled water (69, 68, 66, and 64% v/v, respectively). Phantoms (8% w/v PVA, 2% w/v SiC) with and without cryoprotectant (20% v/v) were also tested. Scanning electron microscopy was conducted to test the differences in microstructure of all phantom types. A Vantage 128 system (Verasonics, Kirkland, WA, USA), equipped with an L11-5v transducer (acoustic radiation force push frequency: 5.2 MHz, plane wave imaging frequency 7.6 MHz, frame rate 10 kHz) was used for shear wave elastography data acquisition. The frequency-shift method was used to estimate SWA coefficients [4], and phase velocity dispersion curves were employed to compute the dispersion slope [5].
**Results:** Estimated SWA increased with the increase in water content in the phantoms (Figure A). However, no significant differences between dispersion slope estimates were observed in PVA phantoms with 66, 68, and 69% v/v water (Figure B). Phantoms without cryoprotectant had higher SWA estimates compared to phantoms with cryoprotectant and had a more porous microstructure as per SEM analyses, which could have led to more water entrapment. No significant differences in dispersion slope estimates were observed.
**Conclusions:** This work with phantoms in controlled conditions showed that SWA was more sensitive than dispersion slope analysis in differentiating between phantoms with varying concentrations of fluid. SWA was also sensitive to changes in phantom porosity in contrast to dispersion slope as evaluated in phantoms with and without cryoprotectant. These findings indicated that SWA estimation can potentially be used to differentiate between normal and pathological tissues based on fluid content.
**Acknowledgments:** The authors thank Dr. Himanshu Shekhar for helpful discussions. This work was supported by the Science and Engineering Research Board (Grant No. SRG/2021/001222), Government of India.

**References:**

[1] Parker, K. J., Szabo, T. & Holm, S. Phys. Med. Biol. (2019) doi:10.1088/1361-6560/AB453D.
[2] Zhou, B. & Zhang, X. J. Mech. Behav. Biomed. Mater. (2018) doi:10.1016/j.jmbbm.2018.05.041.
[3] Munson, J. M. &Shieh, A. C. Cancer Manag. Res. (2014) doi:10.2147/CMAR.S65444.
[4] Bernard, S., Kazemirad, S. & Cloutier, G. IEEE T-UFFC 64, (2017). doi:10.1109/TUFFC.2016.2634329.
[5] Ormachea, J. & Parker, K. J. UMB 46, 3448–3459 (2020). doi:10.1016/j.ultrasmedbio.2020.08.023.

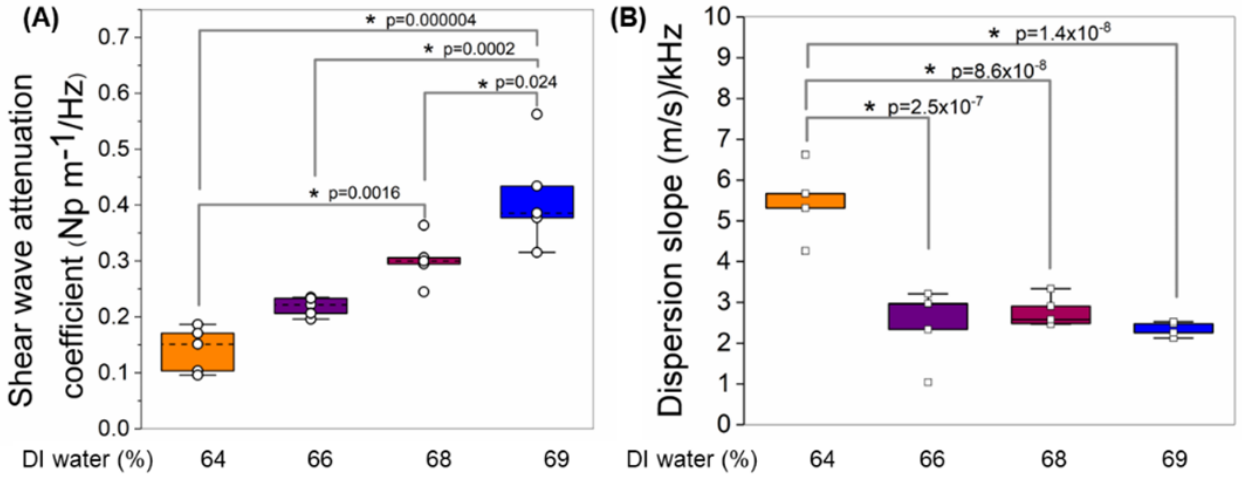


Figure (A) SWA coefficient and (B) dispersion slope estimates of the four different types of PVA phantoms. Each data point represents the mean estimate from five imaging planes per phantom sample. Five samples per phantom type were assessed. * p<0.05.

# IN VIVO ASSESSMENT OF SHEAR MODULUS ALONG THE FIBERS OF PENNATE MUSCLE DURING PASSIVE LENGTHENING AND CONTRACTION USING STEERED ULTRASOUND PUSH BEAMS

*Ricardo J. Andrade*[1,*], *Ha-Hien-Phuong Ngo*[2], *Alice Lemoine*[3], *Apolline Racapé*[1], *Nicolas Etaix*[3], *Thomas Frappart*[3], *Christophe Fraschini*[3], *Antoine Nordez*[1,4], *Jean-Luc Gennisson*[2]

[1]Nantes Université, Mouvement - Interactions - Performance, MIP, UR 4334, Nantes, France ; [2]Université Paris-Saclay, CEA, CNRS, Inserm, BioMaps, Orsay, France ; [3]Supersonic Imagine, Aix-en-Provence, France ; [4]Institut Universitaire de France (IUF), Paris, France.

**Background:** Ultrasound shear wave elastography (SWE) has emerged as a promising non-invasive method for muscle evaluation by assessing the propagation velocity of an induced shear wavefront. In skeletal muscles, the propagation of shear waves is complex, depending not only on the mechanical and acoustic properties of the tissue but also upon its geometry.
**Aims:** This study aimed to comprehensively investigate the influence of muscle pennation angle on the shear wave propagation, which is directly related to the shear modulus.
**Methods:** A novel elastography method based on steered pushing beams (SPB) was used to assess the shear modulus along the fibers of the gastrocnemius medialis (pennate) muscle in twenty healthy volunteers. Ultrasound scans were performed during passive muscle lengthening (n=10) and submaximal isometric contractions (n=10). The shear modulus along the fibers was compared to the apparent shear modulus, as commonly assessed along the muscle shortening direction using conventional SWE sequences.
**Results:** The shear modulus along the muscle fibers was significantly greater than the apparent shear modulus for passive dorsiflexion angles, while not significantly different throughout the range of plantar flexion angles (i.e., under any or very low tensile loads). The concomitant decrease in pennation angle, along with the gradual increase in the difference between the two methods as the muscle lengthens, strongly indicates that non-linear elasticity exerts a greater influence on wave propagation than muscle geometry. In addition, significant differences between methods were found across all submaximal contractions, with both shear modulus along the fibers and the pennation angle increasing with the contraction intensity. Specifically, incremental contraction intensity led to a greater bias than passive lengthening, which could be partly explained by distinct changes in pennation angle.
**Conclusions:** The new SPB sequence provides a rapid and integrated geometrical correction of shear modulus quantification in pennate muscles, thereby eliminating the necessity for specialized systems to align the ultrasound transducer array with the fiber's orientation. We believe that this will contribute for improving the accuracy of SWE in biomechanical and clinical settings.
**Acknowledgments:** This work was funded by ANR INNOVAN under grant number ANR-19-CE19-001

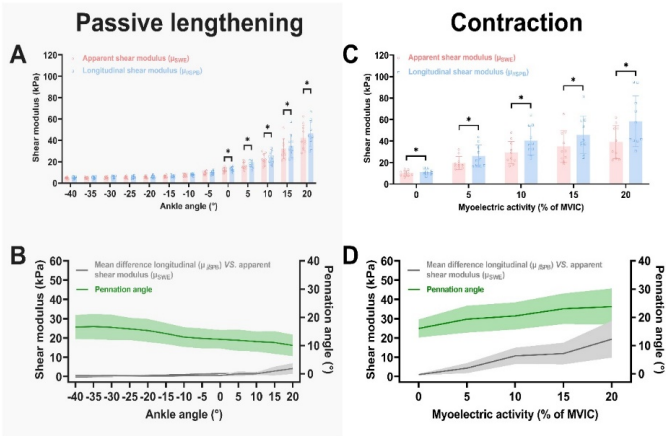


Gastrocnemius medialis longitudinal shear modulus measured by SPB method, and the apparent shear modulus, as assessed by conventional SWE. A. Averaged shear modulus quantified by SPB (blue) and SWE (red) methods during a passive ankle rotation. Negative ankle angles correspond to plantar flexion angles (gastrocnemius medialis shortened) and positive ankle angles correspond to dorsiflexion angles (gastrocnemius medialis under passive tensile loading). Circle (O) and square (□) symbols denote individual data. B. Averaged difference in shear modulus between both methods (gray) and pennation angle (green) throughout muscle lengthening. C. Averaged shear modulus quantified by SPB (blue) and SWE (red) methods for different levels of submaximal isometric contractions, expressed as percentage of myoeletric activation (EMG-RMS). Circle (O) and square (□) symbols denote individual data. D. Averaged difference in shear modulus between both methods (gray) and pennation angle (green) as a function of contraction intensity. *p value < 0.05.

# EXPLORING THE RELATIONSHIP BETWEEN CARDIAC-INDUCED BRAIN STRAIN AND BOTH GLOBAL BOUNDARY CONDITIONS AND LOCAL MICROSTRUCTURE

*M. Burman Ingeberg*[1,*], *M. Froeling*[2], *E. van Houten*[3], *J.J.M. Zwanenburg*[1]

[1]Translational Neuroimaging Group, [2]Highfield MRI Group, Center for Image Sciences, UMC Utrecht, Utrecht, The Netherlands; [3]University de Sherbrooke, Sherbrooke, Canada.

**Background:** Measuring the mechanical properties of the brain is challenging, as traditional mechanical testing methods face significant obstacles when applied to brain tissue [1]. Consequently, computational modeling is often used to simulate and analyze the brain's mechanical behavior. However, these models depend on accurate mechanical representations that capture the complex underlying structure of the brain. One property of particular interest is the mechanical anisotropy of the brain. Despite extensive research, the extent to which the brain is mechanically isotropic or anisotropic remains unresolved in the literature1. Recent work has provided a different means of investigating the mechanical behavior of the brain through *strain tensor imaging* [2], where the 3D strain tensor is calculated from precise displacement measurements of cardiac-induced brain deformations. This technique allows for in vivo exploration of how local brain tissue strains emerge, and how they are affected by global boundary conditions and local microstructure.
**Aims:** To explore to what extent the principal strain directions can be explained by both global boundary conditions and the local microstructure (including mechanical anisotropy) in vivo in the human brain.
**Methods:** We used data from a previously described 7T MRI study [2], where DENSE (3 mm isotropic) and diffusion tensor imaging (DTI) (2 mm isotropic, b = 800 s/mm$^2$) data were acquired during the same scan for 8 healthy subjects. The displacement measurements were used to reconstruct the peak-systolic strain tensor of brain tissue (relative to diastole). The dependency of tissue strain on macro- and microstructure was investigated separately through the means of the first and third principal strains, respectively. In the first case, a simplified brain model of was constructed which considers the funnel-like systolic forces previously described [1]. The model consists of a weighted sum of a vector field that is directed perpendicular to the skull and a vector field that is pointing towards the foramen magnum. This model was voxel-wise compared with the direction of the first principal strains (FPS). In the second case, DTI was compared on a voxel-wise basis with the third principle strain (TPS) by computing the angle between the TPS and principal diffusion direction. A subselection and orthogonalization technique was employed to avoid bias on the TPS introduced by the fact that the TPS is perpendicular to the FPS: only voxels were selected in which the angle between FPS and DTI allowed approximately any angle between TPS and DTI.
**Results:** The FPS maps displayed good resemblance with the model strains (see Figure 1a-1f) with the majority of corresponding angle probability distribution centered around 0° (Figure 1g). A tendency for TPS to align perpendicularly to the principal diffusion direction was observed in white matter but not in gray matter (Figure 1h-1j).
**Conclusions:** The majority of FPS patterns could be described by the model, suggesting that expansion patterns primarily depend on the global boundary conditions. Meanwhile, a tendency for TPS to align perpendicular to the principal diffusion direction was observed, suggesting that compression effects occur across white matter tracts which highlights a source of mechanical anisotropy. As these findings indicate that mechanical anisotropy emerges as a second-order effect in the third principal strain, they may help resolve the ongoing debate on brain mechanical isotropy.
**Acknowledgments:** This work was supported by a Vici Grant from NWO under grant agreement no.18674

**References:**

[1] Budday, S., Ovaert, T.C., Holzapfel, G.A. et al. Fifty Shades of Brain: A Review on the Mechanical Testing and Modeling of Brain Tissue. Arch Computat Methods Eng 27, 1187–1230 (2020).

[2] 4. Sloots JJ, Zwanenburg JJM. Strain Tensor Imaging: Cardiac-induced brain tissue deformation in humans quantified with high-field MRI. Neuroimage. 2021 Aug 1;236:118078.

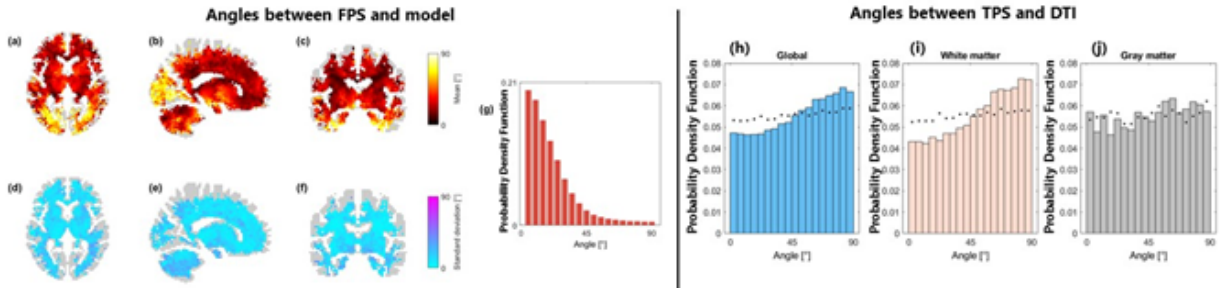

# NONE-INVASIVE QUANTIFICATION OF PORTAL PRESSURE BY COMBINED 3D MRI DEFOMRATION MAPPING AND MR ELASTOGRAPHY

*Noah Jaitner*[1,*], *Yasmine Safraou*[1], *Matthias Anders*[1], *Jakob Schattenfroh*[1], *Tom Meyer*[1], *Biru Huang*[1], *Jakob Jordan*[1], *Oliver Boehm*[1], *Jing Guo*[1], *Ingolf Sack*[1]

[1]Charité – Universitätsmedizin Berlin, Berlin, GERMANY

**Background:** Magnetic resonance elastography (MRE) is clinically established for quantification of hepatic stiffness and liver fibrosis detection. However, even small modulations of blood volume or abdominal pressure by water intake or breathing affect liver stiffness [1, 2]. This mixed sensitivity to solid-fluid properties limit the specificity of liver stiffness as a disease marker in fibrosis or for the detection of elevated portal pressure. Separate contrasts for shear modulus and pressure in MRE of the liver would be highly desirable. While stiffness a tissue property, pressure denotes compressive stress, which is compression modulus times volumetric strain. Non-invasive measurement of pressure requires measurement of volumetric strain and knowledge of the tissue intrinsic compression modulus. Typically, MRE cannot measure the compression modulus of the liver, but can exploit the sensitivity of the shear modulus to changes in vascular pressure and fluid volume as a proxy for changes in compression modulus [3].
**Aims:** Non-invasively quantify the physiological changes in portal pressure in healthy human subjects induced by drinking water or breathing, for the first time.
**Methods:** Five ex vivo rat livers were studied by MRE and volumetric MRI at known portal pressures. To study in vivo changes in liver pressure, 11 healthy volunteers (9 men, 2 women; age range 18 to 53 years) without any history of liver disease were studied with MRE and volumetric MRI in three different physiological states: (i) overnight fasting and end-expiration, (ii) overnight fasting and end-inspiration, (iii) after drinking 1.5L of water and 45min wait period. Imaging examinations were performed in a 3T MRI scanner (Magnetom Lumina, Siemens, Erlangen, Germany) using an 18-channel knee coil for the rat experiments and a 12-channel receiver coil for the human study. For the rat livers T2-weighted images and MRE at four vibration frequencies (130-160 Hz) were acquired. For the human subjects T1-weighted images and MRE at three vibration frequencies (25-40 Hz) were acquired. Shear wave speed maps (SWS) were generated using k-MDEV inversion [4]. Volumetric strain was determined using two methods: First by quantifying relative volume change in different states for rat livers as well as by 3D image registration. By multiplying changes in shear modulus with volumetric strain hepatic pressure could be determined. For rat livers, measurements of hepatic pressure were correlated with known portal pressure measurements to determine a calibration function. The function was then used to calibrate in vivo hepatic pressure measurements to calculate portal pressure.

**Results:** Figure 1 shows volumetric strain maps averaged for all patients and SWS maps for one healthy volunteer for every state. Water ingestion induced liver expansion (volumetric strain: 2 ± 1.2%, $p < 0.001$) and stiffening (differential shear modulus: 3.9±3.9kPa, p=0.001) while end-inspiration gave mixed effects in strain and shear modulus ($p>0.05$). However, positive and negative strains were associated with stiffening and softening, respectively, resulting in portal pressure magnitudes of approximately 1kPa for both water ingestion and breathing (p=0.001).

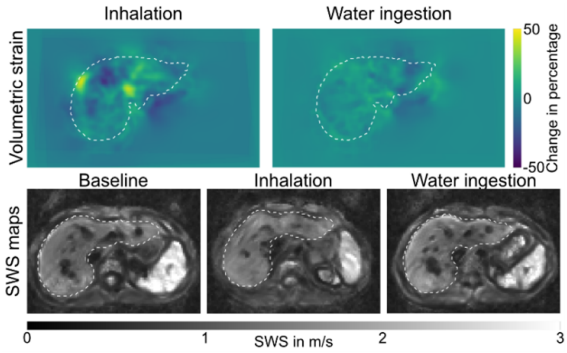


Figure 1 Average volumetric strain over all healthy subject and SWS maps for one subject.

**Conclusions:** The combination of 3D image registration with MRE in different scenarios of in-vivo liver deformations and its calibration with controlled ex-vivo experiments non-invasively probed hepatic pressure changes. In clinical applications, combined MRE and volumetric MRI after breathing or drinking could provide mechanical contrast for hepatic pressure-related disease.
**Acknowledgments:** German Research Foundation (FOR5628, CRC1340 and GRK2260).
**References:**
[1] Wang, K., et al., Repeatability and reproducibility of 2D and 3D hepatic MR elastography with rigid and flexible drivers at end-expiration and end-inspiration in healthy volunteers. Abdom Radiol (NY), 2017. 42(12): p. 2843-2854.
[2] Ipek-Ugay, S., et al., Time Harmonic Elastography Reveals Sensitivity of Liver Stiffness to Water Ingestion. Ultrasound Med Biol, 2016. 42(6): p. 1289-94.
[3] Hirsch, S., J. Braun, and I. Sack, Magnetic Resonance Elastography: Physical Background And Medical Applications. 2017: Wiley-VCH. [4]Tzschatzsch, H., et al., Tomoelastography by multifrequency wave number recovery from time-harmonic propagating shear waves. Medical Image Analysis, 2016. 30: p.1-10.

## October 22nd

## MAGNETIC RESONANCE ELASTOGRAPHY: BASIC PRINCIPLES AND APPLICATIONS

*Richard L. Ehman, MD*

Mayo Clinic

Many disease processes cause profound changes in the mechanical properties of tissues. Magnetic Resonance Elastography (MRE) is an imaging technique that uses propagating shear waves to quantitatively assess mechanical properties such as stiffness, viscosity, attenuation, and anisotropic behavior, providing access to a new range of previously unexplored tissue imaging biomarkers. MRE has a range of established, emerging, and potential applications in hepatic, brain, cardiac, gastrointestinal, pulmonary, and musculoskeletal systems.

The most established clinical application of magnetic resonance elastography (MRE) technology is for detection of hepatic fibrosis. Current research is focusing on using additional MRE-derived biomarkers to discriminate between inflammation, fibrosis, venous congestion, and portal hypertension.

The major emerging application of MRE in clinical practice is brain imaging. Preoperative assessment of the mechanical stiffness of meningiomas and skull-base tumors has great practical value in surgical planning. MRE-based biomarkers in malignant brain tumors are correlated significantly with histologic stage and with genetic mutation status. Other research has shown that brain stiffness is a novel biomarker of neurodegenerative disease, with spatial patterns that reflect the known regional distributions of different dementing diseases

# MULTIFREQUENCY MR ELASTOGRAPHY FOR GRADING LIVER INFLAMMATION IN VOLUNTEERS AND PATIENTS WITH METABOLIC DYSFUNCTION-ASSOCIATED FATTY LIVER DISEASE: A PILOT STUDY

*Amirhosein Baradaran Najar* [1,2,*] , *Guillaume Gilbert* [3,4], *Elige Karam* [2,4], *Anton Volniansky* [4], *Emmanuel Montagnon* [2], *Bich N. Nguyen*[5], *Guy Cloutier* [2,4,6,7], *An Tang* [2,4,8], *Elijah Van Houten* [1,9]

[1]Département de génie mécanique, Université de Sherbrooke, Sherbrooke, Québec, CANADA; [2]Centre de recherche du Centre hospitalier de l'Université de Montréal (CRCHUM), Montréal, Québec, CANADA; [3]MR Clinical Science, Philips Healthcare, Mississauga, CANADA; [4]Department of Radiology, Radiation Oncology and Nuclear Medicine, Université de Montréal, Montréal, Québec, CANADA; [5]Service of Pathology, Centre hospitalier de l'Université de Montréal (CHUM), Montréal, Québec, CANADA; [6]Institute of Biomedical Engineering, Université de Montréal, Montréal, Québec, CANADA; [7]Laboratory of Biorheology and Medical Ultrasonics (LBUM), Centre de recherche du Centre hospitalier de l'Université de Montréal (CRCHUM), Montréal, Québec, CANADA; [8]Laboratoire clinique de traitement de l'image (LCTI), Centre de recherche du Centre hospitalier de l'Université de Montréal (CRCHUM), Montréal, Québec, CANADA; [9]Centre de recherche du Centre hospitalier de l'Université de Sherbrooke (CRCHUS), Sherbrooke, Québec, CANADA.

**Background:** Metabolic dysfunction-associated fatty liver disease (MAFLD) is the most prevalent chronic liver disease. The presence of inflammation and ballooning characterizes metabolic dysfunction-associated steatohepatitis (MASH), the progressive form of MAFLD [1]. Noninvasive detection and grading of inflammation are critical for early characterization of CLD [2].
**Aims:** This study aimed to assess the diagnostic value of multifrequency MR elastography for grading inflammation in the liver.
**Methods:** This prospective cross-sectional study was approved by the institutional review board. The study included volunteers and patients with MAFLD. Their livers were examined by biopsy and multifrequency MR elastography (MF-MRE) at 30, 40, and 60 Hz. The shear modulus dispersion coefficient ($\alpha$) was calculated via a non-linear inversion. The measurements were compared to biopsy for inflammation using Spearman correlations and multiple regression analysis. Comparisons were assessed with Kruskal-Wallis test and diagnostic accuracy with area under the receiver operating characteristic curve (AUC).
**Results:** The study included 11 volunteers and 36 patients. Mean values of $\alpha$ decreased with higher inflammation grades, with a mean of 1.12 ± 0.04 (standard deviation) for A0; 1.05 ± 0.08 for A1; 1.01 ± 0.04 for A2; and 0.96 ± 0.03 for A3. Univariate analysis showed a significant negative correlation between $\alpha$ values and inflammation (Spearman's $\rho$ = -0.562, p < 0.0001), while the multivariate analysis revealed a significant regression coefficient for inflammation (Estimate = -0.041, p = 0.003). MF-MRE $\alpha$ values were significantly different between inflammation grades (p = 0.001) and AUC of 0.81 for $\geq$ A1 and 0.84 for $\geq$ A2.
**Conclusions:** The measurement of the multifrequency dispersion coefficient via MF-MRE has the potential to grade liver inflammation in the MAFLD-MASH disease spectrum.
**Acknowledgments:** This work was funded by a research scholarship from the Fonds de recherche du Québec en Santé (#298509) and a grant from the Canadian Institutes of Health Research (CIHR #389385).

**References:**

[1] Lefebvre, T., et al., Intravoxel incoherent motion diffusion-weighted MRI for the characterization of inflammation in chronic liver disease. European Radiology, 2021. 31: p. 1347-1358.
[2] Garteiser, P., et al., Necro-inflammatory activity grading in chronic viral hepatitis with three-dimensional multifrequency MR elastography. Scientific reports, 2021. 11(1): p. 19386.

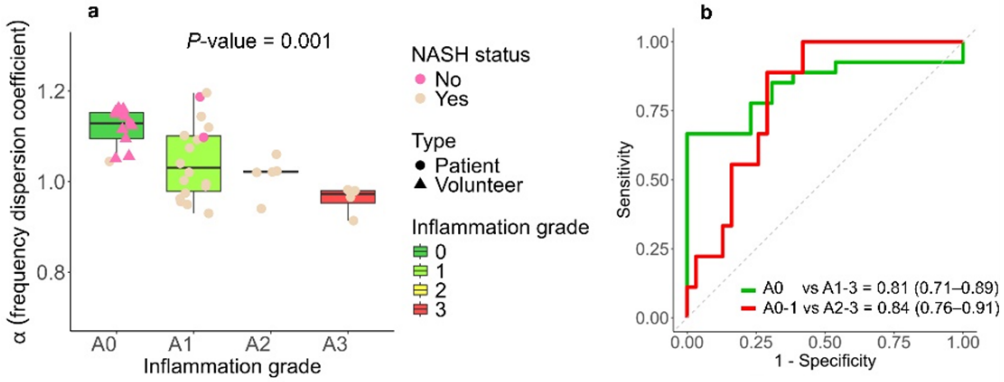


Figure 1. (a) Boxplot of the frequency dispersion coefficient ($\alpha$) versus inflammation grades, including data categorized by patients (circles) and volunteers (triangles), and non-alcoholic steatohepatitis status. The p-value for the Kruskal-Wallis test is reported, comparing the results between each grade of inflammation. (b) Receiver operating characteristic (ROC) curves show the categorization of dichotomized groups of inflammation grades based on $\alpha$ values in the liver.

# QUANTIFICATION OF BRAIN TUMORS STIFFNESS BY MAGNETIC RESONANCE PASSIVE ELASTOGRAPHY: FROM SEISMOLOGY TO MEDICAL DIAGNOSIS.

*G Pagé[1,*], K Rachid[1], B Larrat[2], B Giammarinaro[3], J Aichele[3], G Lacoin[4], I Zemoura[4], F Mauconduit[2], A Nemeth[1], L Barantin[4], A Vignaud[2], JP Remenieras[4], S Catheline [3], JL Gennisson[1]*

[1]Université Paris Saclay, CNRS, Inserm, BioMaps, Orsay, France; [2]Université Paris Saclay, CNRS, CEA, NeuroSpin/BAOBAB, Gif-sur-Yvette, France; [3]Labtau, Inserm, Université Claude Bernard, Lyon, France; [4]iBrain, Inserm, Université de Tours, Tours, France.

**Background:** Knowledge of brain mechanical properties can be a major asset for physicians and neuroscientists in basic or clinical research. Then, elastography has been developed to in ultrasound or magnetic resonance imaging (MRI) to explore organization or some degeneration of the brain [1,2]. However, skull is a strong aberator and a complicated barrier to ultrasound propagation; while brain is very isolated from external vibrations thanks to the cerebrospinal fluid which imply to generate high intensity vibrations that can be potentially unpleasant for the patient. To face these issues, MR passive elastography has been proposed [3]. The technique was inspired by seismic noise tomography to extract from natural vibrations (such as heart beatings or respiratory motion) the velocity of elastic waves [3]. Therefore, no MR synchronized external vibrators are required.

**Aims:** The purpose of this study was to apply the MR passive elastography sequence to patients with diagnosed brain tumor. Mechanical properties measured by the passive methods were compared to ultrasound shear wave elastography (SWE) considered, here, as a clinical standard

**Methods:** The study was performed in 18 patients with brain tumors (10 high grade gliomas, 2 low grade gliomas, 4 meningiomas, 2 metastasis). MR acquisitions were performed before surgery with a 3T Magnetom Prisma fit (Siemens Healthineers). A unique home-made MR passive elastography 2D spin-echo echo planar was developed with two bipolar sinusoidal gradient schemes placed around the refocusing pulse to sensitize the sequence to motion. In the end, TE = 53 ms, TR per slab = 1.5s and it was played 200 times for a total acquisition time of 5min06s. Ultrasound acquisitions were performed during surgery by using a programmable ultrafast ultrasound device (Aixplorer V12.3, 192 elements, Supersonic Imagine). SWE commercial sequence described in [4] was used and passive elastography was constituted of an ultrasound plane wave acquisition of 9 angles acquired at 8000 frames/s ad 6 MHz central frequency (3 half-cycle) during 1s. Shear wavelength was estimated from MR passive elastography method described by Zorgani et al. [3] and velocity and shear wavelength were measure from ultrasound passive elastography using a homemade algorithm. Passive elastography results obtained with both methods were compared to SWE.

**Results:** Tumors wavelength values quantified with SWE are significantly correlated to MR and US passive elastography ($r = 0.59$, $p = 0.009$ and $r = 0.75$, $p = 0.0004$, respectively). Moreover, results obtained from both passive methods were significantly correlated ($r = 0.56$, $p = 0.01$). A subgroup analysis is shown in Figure 1 to observe tissue wavelength and tissue stiffness determined with US-elastography (Fig. 1.a), MRE (Fig. 1.b) and passive-US (Fig. 1.c). For each method a similar pattern is observed and Mann-Whitney test shows significative difference between meningiomas (Fig.1.d) and normal brain shear wavelength values.

**Conclusions:** In conclusion, the present study demonstrates noninvasive quantification of brain mechanical parameters using intrinsic displacements of the human body with values correlated to a clinical standard method.

**Acknowledgments:** This work was funded by Plan Cancer INCA 2018.

**References:**

[1]. Liao J. et al. J Ultrasound Med (2020). [2] Bunevicius A. et al. Neuroimage Clin (2020). [3] Zorgani et al. PNAS (2015).

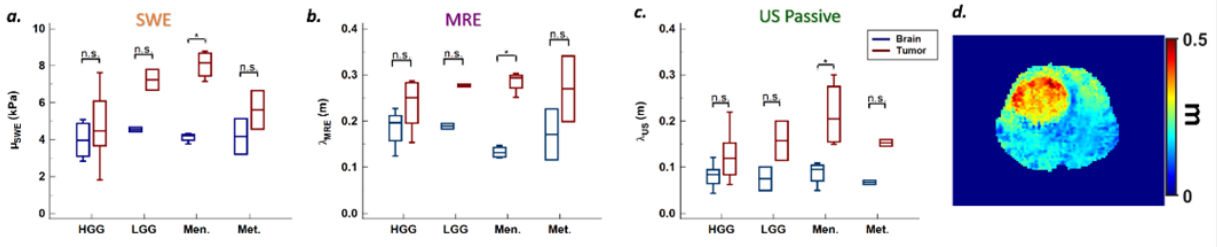


Fig. 1. Shear modulus (a.), shear wavelength from passive MRE (b.) and ultrasound (c.) of both tumor and normal brain for the four analyzed types of tumors: high grade glioma (HGG), low grade glioma (LGG), meningioma (Men.) and metastasis (Met.) d. Shear wavelength map obtained from passive MR elastography

# MAGNETIC RESONANCE ELASTOGRAPHY (MRE) LUNG STIFFNESS: APPLICATION TO LONG-COVID PATIENTS

*Sabine F Bensamoun*[1,*], *Kiaran P McGee*[2], *Mashhour Chakouch*[1], *Philippe Pouletaut*[1], *Fabrice Charleux*[3]

[1]Université de technologie de Compiègne, CNRS, BMBI, UMR 7338, 60200 Compiègne, FRANCE; [2]Mayo Clinic & Foundation, Radiology Department, Rochester, Minnesota, USA; [3]ACRIM-Polyclinique Saint Côme, Radiology department, 60200 Compiègne, FRANCE.

**Background:** Long-COVID patients revealed more or less respiratory difficulties [1]. During the pandemic, CT scan was the main medical test to evaluate the features of the COVID lung represented with ground class opacity [2-3]. However, CT uses X-rays, limiting the regular follow-up of patients. Thus, alternative imaging modalities (MRI, US) enable to subjectively characterize the structural properties of lung tissue.
**Aims:** The purpose of the present study was to quantify the functional behavior with personalized cartographies of lung stiffness for long-COVID patients and to follow up the evolution of this quantitative mapping over time.
**Methods:** Seven healthy and seven long-COVID participants referred for a lung CT test were recruited (#A01496-33) at the ACRIM department. All participants underwent CT and MRE tests. CT was performed with pixel size 0.73 mm, slice thickness 0.62 mm and 100-140 kV. A senior radiologist subjectively analyzed the structural properties (bronchial thickness,...). Moreover, the slice level where the intermediate trunk was clover-shaped in appearance was identified for future MRE assessment of the same lung region. CT density was calculated by converting the measured Hounsfield number into density units [4]. Less than one month later, a first MR lung density test followed by a first MRE test were performed. MR lung density obtained from a fast gradient-echo sequence was calibrated with a Gadolinium-doped water phantom placed on the sternum, and validated with the CT density values. MRE test was performed on a 1.5 T MRI, with a 22 s breath-hold, and a driver placed on the right lung inducing mechanical shear waves (50 Hz). A spin-echo echo-planar sequence, including a motion-encoding gradient, was applied with four offsets to obtain four axial phase images. The mechanical properties of the right lung were measured within a contour drawn by 2 operators. The true lung stiffness was then calculated from the phase images using multi-model direct inversion and a homemade post-processing (pixel-wise correction for density...). The monitoring (lung density, stiffness) was carried out after 4.7 to 11.2 months for each COVID patient.
**Results:** The density for COVID patients were significantly (P = 0.047) greater (170 kg.m-3) compared to healthy (125 kg.m-3) subjects. The evolution of the MR lung density over time, i.e from MR test N°1 to N°2, varies differently from one patient to another. In the first MRE test, the stiffness for the healthy subjects was always in the same range (about 1 kPa) while the COVID patients showed a larger range (from 1.39±0.04 kPa to 2.05±0.02 kPa). After a minimum delay of 4 months, the stiffness decreased (from 22% to 40%) for every COVID subject (Fig 1-2). Inter-operator correlation coefficient was excellent (0.78-0.97).

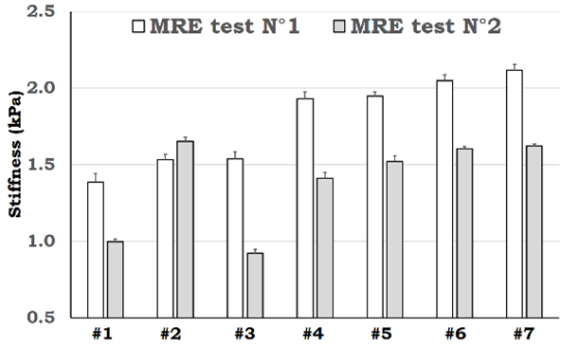


**Fig 1.** Evolution of the lung stiffness values in the MRE test N°1 and MRE test N°2 for the 7 long-COVID patients.

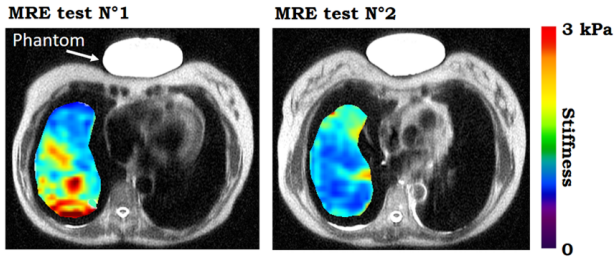


**Fig 2.**Evolution of the personalized lung stiffness for the patient #3 (cf. Fig 1).

**Conclusions:** MRE test is enough sensitive to monitor disease-induced change in lung stiffness. This non-invasive modality could yield complementary information as a new imaging biomarker to follow up long- COVID patients.
**Acknowledgments:** This work was supported by the CPER TECSANTE

**References:**

[1] Christopher et al PLOS Global Public Health 2024
[2] Hani et al Diagnostic and Interventional Imaging 2020
[3] Chakouch et al State of Art in Bioengineering 2022
[4] Schneider et al PMB 1996.

# OBSERVATION OF POROELASTIC WAVES USING MR ELASTOGRAPHY

*T Deruelle*[1,2], *J Aichele*[1,2], *S Catheline*[1,2], *R Souchon*[1,2,*].

[1]INSERM, LabTAU laboratory, Lyon, FRANCE; [2]Université Claude Bernard Lyon 1, Lyon, FRANCE.

**Background:** Poroelastic waves were first observed in earth science while probing soil layers composed of rocks and fluids (water, oil, gas, ...) [1]. They are typically described as a second, slow compression wave that comes in addition to the well known compression wave and shear wave. Poroelastic waves were also observed in trabecular bone [2]. A recent publication demonstrated that this wave exists in a water-filled soft foam [3], but the existence of such waves in soft biological tissues has not been demonstrated yet.
**Aims:** To investigate the existence of poroelastic waves in tissue-mimicking materials.
**Methods:** Experiments were carried out in the same water-filled foam that had been used previously [3] and in an agar gel. We used magnetic resonance elastography (MRE) to acquire the three components of the wave field, in the entire volume of the samples, so that the full displacement field was known at any time. The vibration frequencies ranged from 40 Hz to 200 Hz. The divergence operator was used to remove the shear field. The 3D Local Frequency Estimator (LFE) algorithm was used to measure the wave speed. The experiments were repeated in two different MR scanners (GE Healthcare & Siemens).
**Results:** In the foam and in the agar gel, the divergence field showed waves with short wavelength (a few centimeters) progressing through the medium. The observation is consistent with slow compression waves. Shear wave speed and slow compression wave speed measured in the foam phantom were consistent with values obtained independently using ultrasound in the same sample [3].
**Conclusions:** The observations were consistent with poroelastic waves previously described in the literature. This study opens the way for noninvasive measurement of the poroelastic properties of tissues.

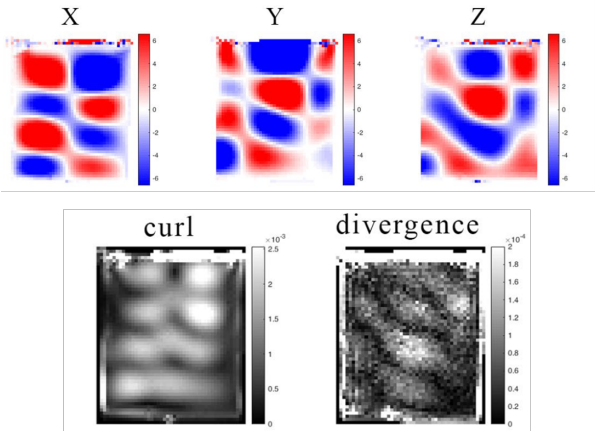


**Fig 1.** Waves in agar phantom (100 Hz).

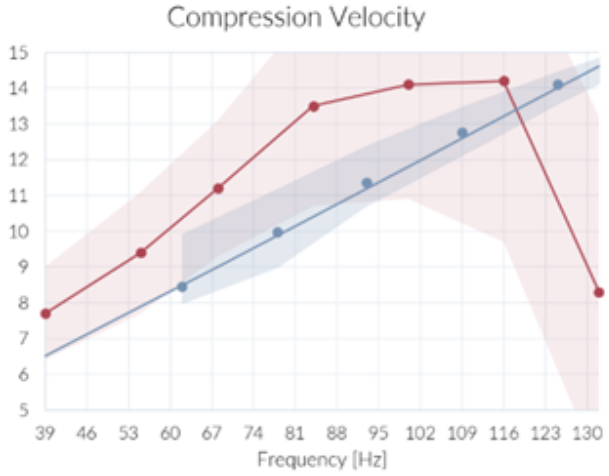


**Fig 2.**Compression Wave Speed (m/s) in foam phantom. Red = MRE, Blue = Ultrasound from Reference [3]. Good correspondence was found between 40 and 116 Hz. Wave attenuation precluded MRE measurement at 130 Hz.

**Acknowledgments:** We thank Pr Ehman (Mayo Clinic, Rochester MN) and Pr Sack (Charité, Berlin) for providing the MRE sequences. This work was supported by the RHU PERFUSE (ANR-17-RHUS-0006) led by Université Claude Bernard Lyon 1 (UCBL), within the program "Investissements d'Avenir" operated by the French National Research Agency (ANR).

**References:**

[1] Plona TJ, Observation of a second bulk compressional wave in a porous medium at ultrasonic frequencies. Appl. Phys. Lett. 36, 259–261 (1980).
[2] R. Lakes R et al. Slow compressional wave propagation in wet human and bovine cortical bone. Science (80-. ). 220, 513–515 (1983).
[3] Aichele J et al. Capturing the Shear and Secondary Compression Waves: High-Frame-Rate Ultrasound Imaging in Saturated Foams. Phys. Rev. Lett. 123, 148001 (2019)

# MAPPING MICROSCALE VISCOELASTICITY: CHARACTERIZATION THROUGH A 2D BOUNDARY-CONDITION-FREE NONLINEAR INVERSION TECHNIQUE

*Sajad Ghazavi*[1,2,*], *Hari S. Nair*[1,2], *Guillaume Fle*[1,2], *Boris Chayer*[1], *Ruchi Goswami*[3], *Salvatore Girardo3*, *Jochen Guck*[3], *Guy Cloutier*[1,2,4], *Elijah E. W. Van Houten*[5]

[1]Laboratory of Biorheology and Medical Ultrasonics, University of Montreal Hospital Research Center, Montreal, QC, CANADA;[2]Institute of Biomedical Engineering, University of Montreal, Montreal, QC, CANADA; [3]Max Planck Institute for the Science of Light & Max-Planck-Zentrum für Physik und Medizin, Erlangen, GERMANY; [4]Department of Radiology, Radio-Oncology and Nuclear Medicine, University of Montreal, Montreal, QC, CANADA; 5University of Sherbrooke, Sherbrooke, QC, CANADA

**Background:** Optical microelastography (OME) has emerged as a new technique for quantifying cellular mechanical properties [1, 2]. However, accurately reconstructing viscoelastic properties at the microscale level from noisy 2D displacement fields remains a challenge. This study introduces a 2D boundary-condition free nonlinear inversion (2D-NoBC-NLI) approach, addressing
**Aims:** To introduce and evaluate the effectiveness of the 2D-NoBC-NLI technique in OME for mapping the viscoelastic properties of microbeads and of a numerical model for validation.
**Methods:** OME involves inducing high-frequency harmonic shear waves within the cell [1, 2]. Here, the shear modulus distribution is recovered by analyzing wave-induced displacements through 2D-NoBC-NLI. This technique integrates viscoelastic constitutive parameters into the coupled adjoint field formulation applied to the nonlinear inversion process [3, 4], eliminating the need for explicit knowledge of boundary displacements. It was applied to experimental data obtained from homogeneous standardized polyacrylamide (PAAm) microbeads embedded with nanoparticles [5]. To mimic the experiment, a numerical model with the same diameter and vibration frequency of 40 kHz was used. The numerical model's viscoelastic properties were assigned based on the experimental results. Additionally, 5% Gaussian noise was introduced to the displacement data of the model to test the robustness of the reconstruction process.
**Results:** The homogeneous shear modulus for the PAAm microbeads (Figure 1a) was reconstructed as 1060+i400 Pa at 40 kHz, as shown in Figure 1b. The numerical simulation demonstrated high accuracy, with a 3% relative error from the ground truth for the storage modulus (Figure 1c), while the loss modulus displayed a 25% error. Even in the presence of up to 5% Gaussian noise, added as a fraction of the mean amplitude, the storage modulus maintained an error around 30% (Figure 1d). Noise had a smaller impact on the loss modulus reconstruction.
**Conclusions:** This study demonstrates the potential of using the 2D-NoBC-NLI technique for OME mapping of viscoelastic properties at the microscale level, even in the presence of noisy data, permitting cell micro-elastography.

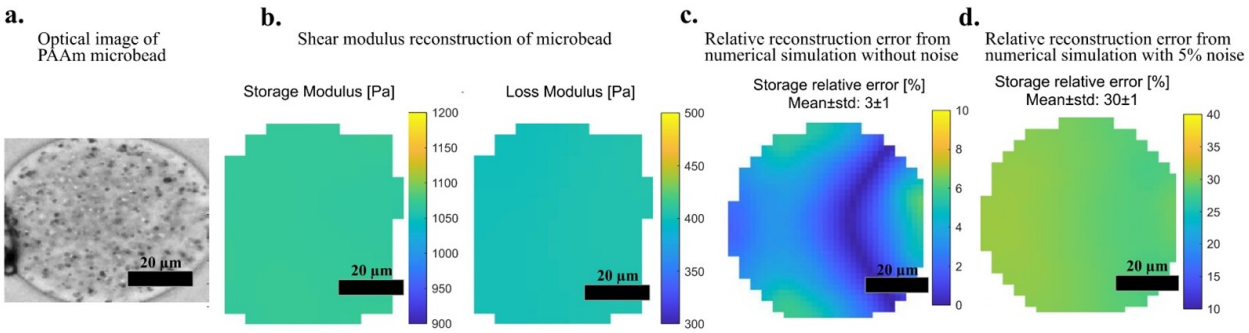


*Figure 1. (a) Optical image of a PAAm microbead. (b) Shear modulus reconstruction of the microbead. (c) Relative error of reconstruction of finite element model without noise. (d) Relative error of reconstruction of finite element model with noise*

**Acknowledgments:** Funded by the Canadian Institutes of Health Research (grant # 497451-MPI-ADWY-22963).

**References:**

[1] Grasland-Mongrain, P., et al. 2018, Proc Natl Acad Sci USA, 115(5):861–6.
[2] Flé, G., et al. 2023, Proc Natl Acad Sci USA, 120(21), p.e2213836120.
[3] Kurtz S., et al. 2024, IEEE Trans. Med. Imaging, 43(3): 1138 - 1148.
[4] Van Houten, EEW., 1999, Magn. Res. Med., 42(4):779-786.
[5] Girardo, S., et al. 2018, J Mater Chem B, 6(39):6245–61.

# BRILLOUIN LIGHT SCATTERING REVEALS SUB-NANOMETRIC PORE MECHANICS IN CELLS

*L Vovard*[1], *A Viel*[1], *G Jardiné*[1], *S Monnier*[1], *T Dehoux*[1,*]

[1]Institut Lumière Matière, UMR5306, Université Lyon 1-CNRS, Université de Lyon, 69622 Villeurbanne, FRANCE

**Background:** Volume regulation is key in maintaining important tissue functions, such as embryogenesis or wound healing. Perturbation of volume homeostasis, by external forces applied to the tissue or abnormal regulation, has also been associated with the development of degenerative diseases, such as cancer. For this reason, a large body of research has been devoted to the implementation of local sensors to monitor stresses or forces in model tissues during hyperosmotic shocks (3, 4). Such approaches focus on stiffness regulation, but they cannot capture the role of water efflux that changes molecular crowding within individual cells.
In recent years, a new quantitative microscopy based on Brillouin light scattering (BLS) has been proposed that uses the interaction of a laser light with picosecond timescale density fluctuations in the sample (8). Variations in the scattering spectra can be interpreted as the response of the sample to an infinitesimal uniaxial compression and formally yield the longitudinal sound velocity at GHz frequencies. BLS has been successfully used for mechanical phenotyping and imaging with a contrast based on the stiffness, but its relevance from a physiological standpoint remains debated due to the lack of knowledge on the link between microscopic structure of the cells and acoustic propagation in the GHz range.

**Aims:** Here we aim at deciphering the link between molecular crowding in the nucleus of cells and acoustic properties (sound velocity and attenuation) probed by Brillouin light scattering in the GHz range.

**Methods:** We modulate the volume of single cells using osmotic shocks. Briefly, we replace the culture medium with a medium with increasing concentration in sucrose. Water is drawn out and the concentration of non-permeant molecules in the nucleus increases. We quantify the resulting change in volume with a combination of fluorescent imaging and fluorescent exclusion microscopy. To check the impact of reduced nuclear volume on molecular dynamics, we track the motion of 40 nm fluorescent nanoparticles. On these systems, we image Brillouin spectra across the nucleus, and extract the sound velocity and attenuation in the nucleus as a function of increasing molecular crowding.

**Results:** As nuclear volume decreases, we observe a slowing down of the diffusion of the fluorescent tracers, consistent with slowing down of the molecular dynamics. This is accompanied with a nonlinear increase in the sound velocity and in the attenuation probed by Brillouin microscopy. We fit successfully this data with poroelastic theory, and calculate an effective pore size.

**Conclusions:** The comparison of the Brillouin data with poroelastic theory, together with the slowing down of the motion of molecular tracers, suggest that the nucleus of the cell behaves as a multiscale poroelastic network that hinders molecular motion. This conclusion defines Brillouin spectroscopy as a powerful tool to study molecular dynamics and volume regulated events in cells, with application to pathological environments.

# DEEP NEURAL NETWORK FOR SHEAR MODULUS RECONSTRUCTION OF ELASTIC MATERIALS IN MICROELASTOGRAPHY

*Hari S. Nair*[1,2,*], *Sajad Ghazavi*[1,2], *Guillaume Flé*[1,2], *Elijah E. W. Van Houten*[3], *Guy Cloutier*[1,2,4]

[1]Laboratory of Biorheology and Medical Ultrasonics, University of Montreal Hospital Research Center, Montreal, QC, Canada; [2]Institute of Biomedical Engineering, University of Montreal, Montreal, QC, Canada; [3]Department of Mechanical Engineering, University of Sherbrooke, Sherbrooke, QC, Canada; [4]Department of Radiology, Radio-Oncology and Nuclear Medicine, University of Montreal, Montreal, QC, Canada

**Background:** Optical microelastography (OME) has been proposed for the non-invasive assessment of mechanical properties at the micron scale [1,2,3]. OME utilizes elastic wave induction in cells and tracks them via high-speed optical imaging. The shear modulus is then reconstructed using various methods, such as passive elastography and non-linear inversion techniques [1,2]. While deep learning approaches have been previously explored for shear modulus reconstruction, these applications have primarily focused on datasets pertaining to macroscopic objects [4,5].
**Aims:** This study investigates the application of deep neural networks (DNNs) for shear modulus reconstruction of soft elastic materials in OME using high-frequency elastic wave induction.

**Methods:** The technique was validated on finite element model (FEM) datasets. The simulation model resembles a cell with a hemi-ellipsoid (mimicked cytoplasm, diameter = 100 $\mu$m) embedding an inclusion (mimicked cell nucleus - 30 $\mu$m) as depicted in Fig. 1 (a). Elastic waves at 36 kHz were induced on the model to extract displacements for the training dataset. Ground truth (GT) includes the shear elastic modulus of the background, hemi-ellipsoid and inclusion, as shown in Fig. 1(b). The shear elastic moduli within the simulated cells were varied across a range of 150 Pa to 4350 Pa, encompassing a range suitable for cells and soft tissues. The shear elasticity modulus ratio between the inclusion and the hemi-ellipsoid cell was varied from 0.6 to 2. We trained the DNN model on 207 simulated elastic data points and validated it on 31 additional data points. The simulation model employed in this stage was purely elastic, neglecting any viscoelastic behavior that might be present in real cells. A regression-based neural network architecture was chosen for this study [6]. The network was trained on the generated data using an Adam optimizer and Mean Squared Error (MSE) loss function to minimize the difference between the predicted and actual shear elasticity moduli. After training, the performance of the DNN model was evaluated on 25 unseen data points to assess its generalization capability. The mean error of the predicted shear moduli was then calculated by comparing it with the GT values.

**Results:** The DNN model achieved a mean error of 4.3% for predicting the shear elasticity modulus of the hemi-ellipsoid, 7% for the inclusion and 1% for the background.
**Conclusions:** High testing accuracy suggests the model learns the link between elastic wave propagation and shear elasticity modulus. The DNN successfully reconstructs the shear elastic modulus of soft micro-materials (like cells) from OME data. Next, the DNN will be tested experimentally on microbeads with known mechanical properties. Finally, the model will be enhanced to incorporate viscoelastic behavior.

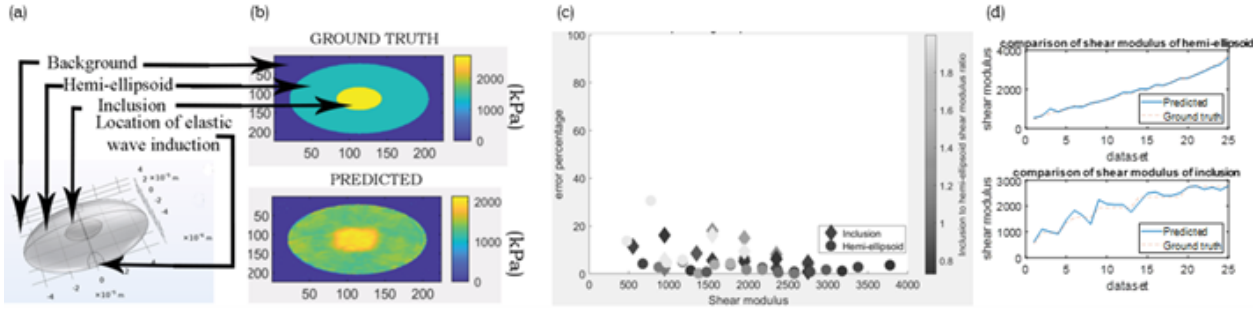


*Fig. 1: (a) Finite element model, (b) GT and predicted values of the FEM, (c) Error percentage from unseen dataset for different shear elasticity moduli, (d) Mean shear elastic modulus prediction for unseen datasets.*

**Acknowledgments:** Scholarship from the TransMedTech Institute of Montreal; grant from the Canadian Institutes of Health Research (# 497451-MPI-ADWY-22963).

**References:** [1] Grasland-Mongrain, P., et al. 2018, Proc Natl Acad Sci USA, 115(5):861–6. [2] Flé, G., et al. 2023, Proc Natl Acad Sci USA, 120(21), p.e2213836120. [3] Laloy-Borgna, G. et al. 2021, Appl Phys Lett, 118(11). [4] Tuladhar, U. R. et al. 2023, Proc SPIE Int Soc Opt Eng, 12470(26) [5]. Yin, Z., et al. IEEE Trans Med Imaging, 43(4). [6] Simonyan, K., 2014, 3rd ICLR 2015 - Conference Track Proceedings.

# MICRO-ELASTOGRAPHY OF BIOPSY TISSUE, APPLICATION TO ENDOMETRIOSIS

*Sibylle Gregoire*[1,*], *Bruno Giammarinaro*[1], *Axelle Brulport*[1], *Stefan Catheline*[1]

[1]LabTAU, INSERM, Université Lyon 1, Lyon, FRANCE

**Background:** Endometriosis affects 10% of women of childbearing age (Taylor, Kotlyar, & Flores, 2021). Patient quality of life may be significantly impaired mainly due to a wide range of painful symptoms and infertility. Due to the inflammatory component of the disease, fibrosis is a molecular feature of the pathophysiology of endometriosis (Burney, 2022). Fibrosis, by increasing tissue stiffness, can compromise the local diffusion of drugs used to treat the symptoms of the disease and make surgical management complex. Biopsy examination is notably used in endometriosis patients for diagnostic and follow-up purposes. The addition of mechanical characterization of the endometrium from the collected tissue could enable patients to be monitored without the need for additional invasive procedures.
**Aims:** Our aim is to use dynamic micro-elastography techniques to probe the elasticity of endometrium sample harvest from biopsy examination of patient affected with endometriosis. In this work, murine endometrial samples are considered as a proof of concept. A comparison is made with murine liver tissue.

**Methods:** The endometrium of 3 different mice was studied. For each individual, 3 samples were taken and an acquisition was performed on each sample. Similarly, the liver of 3 different mice was sampled. The mouse uterus and liver are harvested after death and stored on ice. The tissue is then cut into 1 $mm^3$ samples. Figure 1 illustrates the platform. An inverted microscope (Nikon Ti-S) coupled to an ultra-fast camera (Phantom v12.1) enables us to record x10 zoom films of the sample at 20 000 frames/s. A shaker (Cedrat APA100M) driven by a generator is placed in contact with the gel. The displacements are computed through a phase tracking algorithm. Shear wave velocity in the sample is computed using a noise correlation approach (Catheline, et al., 2013).

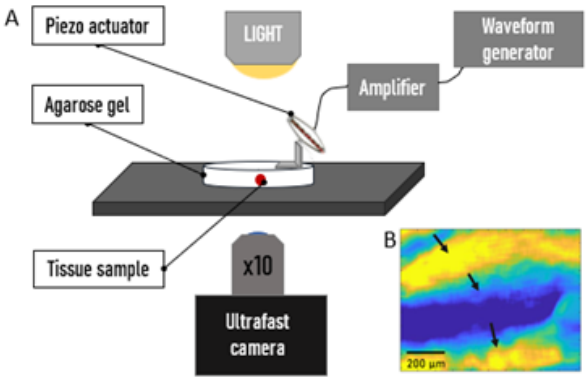


***Figure 1(A)*** *Micro-elastography platform: a wave field created with a shaker propagates in a gel containing a murine tissue sample. Film of the propagation is acquired using an ultrafast camera.* ***(B)*** *Displacements field inside an endometrium sample.*

**Results:** On the basis of preliminary data acquired, the liver appears significantly harder than the endometrium. Quantitative estimates of elasticity are forthcoming.
**Conclusions:** A method for the mechanical characterization of biopsy samples is proposed. Preliminary results obtained in murine liver and endometrial samples are very encouraging. There appears to be no barrier to the mechanical characterization of endometrium sample harvested from patient affected with endometriosis. What's more, this method can be used for all types of biological tissue, opening the way to rapid mechanical characterization of biopsies.
**Acknowledgments:** With financial support from ITMO Cancer of Aviesan within the framework of the 2021-2030 Cancer Control Strategy, on funds administered by Inserm. A.B is the recipient of a grant from the Fondation URGO for her work on endometriosis.

**References:**

Burney, R. (2022). Fibrosis as a molecular hallmark of endometriosis pathophysiology. Fertility and Sterility.
Catheline, S., Souchon, R., Rupin, M., Brum, J. Dinh, A., & Chapelon, J.-Y. (2013). Tomography from diffuse waves: Passive shear wave imaging using low frame rate scanners. Applied Physics Letters.
Saunders, P., & Horne, A. (2021). Endometriosis: Etiology, pathobiology, and therapeutic prospects. Cell.
Taylor, H., Kotlyar, A., & Flores, V. (2021). Endometriosis is a chronic systemic disease: clinical challenges and novel innovations. The Lancet

## FibroScan®: 23 Years at the Forefront of Liver Health

*Laurent Sandrin*

Echosens

Since its introduction in 2003, FibroScan® (Echosens, France), the first quantitative elastography device, has revolutionized the management of chronic liver diseases worldwide. For over two decades, liver stiffness measurement using Vibration-Controlled Transient Elastography (VCTE) has provided a non-invasive method for assessing liver fibrosis in both research and clinical practice, greatly reducing the need for liver biopsies.

In 2011, the Controlled Attenuation Parameter (CAP) was integrated into the FibroScan procedure, enabling the assessment of liver steatosis—just as metabolic dysfunction-related diseases began gaining more prominence. More recently, the introduction of Vibration-Guided VCTE in newer FibroScan models has further enhanced its ease of use and effectiveness, particularly for managing very obese patients.

Whether used alone or in combination with simple blood biomarkers like in the FAST and Agile scores, Echosens' solutions provide a strong foundation for comprehensive liver disease management.

# MAY THE FORCE BE WITH YOU – ELASTICITY IMAGING IN INFORMING CARDIO-VASCULAR DISEASE AND CANCER TREATMENT

*Elisa E. Konofagou*

Departments of Biomedical Engineering, Radiology and Neurological Surgery Columbia University, New York, NY

Since its inception more than 35 years ago, elastography has crossed to the clinic and is routinely applied for cancer detection and diagnosis among other applications on a routine basis wordwide. Elasticity imaging has been capable of expanding the role of ultrasound imaging in the clinic by providing quantitative information on the underlying mechanical properties. Emphases of this presentation will be given on cardiovascular elasticity imaging techniques such as Myocardial Elastography, Electromechanical Wave Imaging (Fig. 1A) and Pulse Wave Imaging for the characterization of mechanical and electrical cardiac properties and vascular mechanical properties, respectively, based on the intrinsic pulsational function of the heart and blood vessels. Elasticity imaging on preclinical and clinical tumor characterization in the breast and pancreas using the radiation-force technique of Harmonic Motion Imaging will also be presented. The power of the new information provided by elastographic techniques for highlighting and informing both the state of disease but also the success of the treatment thereof.

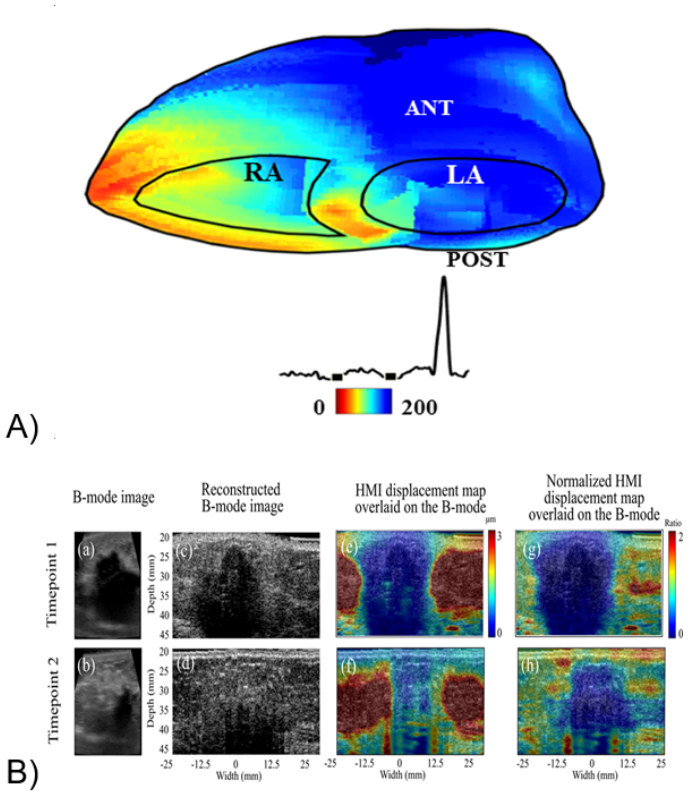


Figure 1: A) Electromechanical activation map of an atrial flutter in a patient before radio-frequency ablation; B) B-mode images of a 2.8-cm IDC (Patient 3) acquired with a commercial ultrasound scanner, Reconstructed B-mode images of the tumor acquired with the 7.8-MHz HMI imaging transducer, (e,f) 2-D HMI displacement maps overlaid on the B-mode images, (g-h) Normalized HMI displacement maps overlaid on the B-mode images. The B-mode images and HMI maps were acquired at two time-points of baseline and three weeks on neoadjuvant chemotherapy. The tumor could not be localized on the B-mode images at the third time- point. This subject achieved pCR according to the pathology reports.

# ULTRASOUND ELASTOGRAPHY TO PREVENT AGEING AND RUPTURE IN THE BREAST IMPLANTS

*Laetitia Ruffenach*[1,2], *Dimitri Heintz*[3], *Claire Villette*[3], *Denis Funfschilling*[1], *Frédéric Bodin*[1,2], *Nadia Bahlouli*[1], *Simon Chatelin*[1,*]

[1]University of Strasbourg, CNRS, Inserm, ICube UMR 7357, 1 place de l'hôpital, 67000 Strasbourg, FRANCE; [2]Service de chirurgie plastique esthétique et reconstructrice, CHRU Hautepierre, HUS, 1 avenue Molière, 67200 Strasbourg, FRANCE; [3]Plant Imaging & Mass Spectrometry (PIMS), IBMP, UPR 2357 CNRS, University of Strasbourg, 12 rue du Général Zimmer, 67000 Strasbourg, FRANCE.

**Background:** More than 58,000 people are affected by breast cancer every year in France (Institut Curie), a third of whom will undergo total surgical removal of the breast (mastectomy). Breast reconstruction is an integral part of breast cancer treatment. However, this reconstruction is not eternal, and patients will have to be re-operated, on average every 10 years, depending on the surgeon's estimate. To date, there are no quantitative criteria for deciding to replace an implant. Aims: In this study we propose to study their mechanical evolution, still largely unknown (1), by proposing possible explanations, using elastography and multiphysical approaches.
**Aims:** In this study we propose to study their mechanical evolution, still largely unknown (1), by proposing possible explanations, using elastography and multiphysical approaches.
**Methods:** A1/*Mechanical imaging*. 51 breast explants from 6 manufacturers, implanted up to 18 years in patients, were characterized ex vivo using acoustic radiation force impulse (ARFI) elastography (Figure 1A). 2/*MALDI imaging*. Mass spectrometry imaging by Matrix Assisted Laser Desorption Ionisation (MALDI) imaging has been performed in the prosthesis gel to investigate the presence of potential unexpected molecules in the inner gel of the explants.

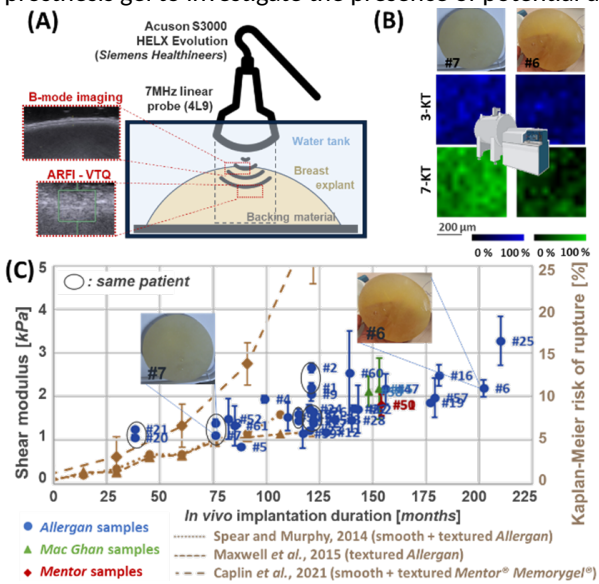


**Figure 1.** Illustration of the elastography (A) and MALDI (B) experimental setups and observations. Explant shear modulus is represented (C) as a function of implantation time (blue) and compared with that of rupture risk reported in the literature (brown).

**Results:** An increase in gel stiffness up to a factor of almost 3 with their implantation time was observed (Figure 1B). The evolution of the shear modulus (blue) is similar to that of the risk of rupture (brown) (2-3), initially low and beginning to increase after 6 to 8 years (4). What's more, traces of cholesterol metabolites (3- and 7-Keto Cholesterol) from breast tissue were widely detected by MALDI imaging in the prosthesis gel, confirming the permeability of the membrane. These biological metabolites are likely to be responsible for the degradation of PDMS. Cholesterol metabolites, detected for the very first time in prostheses, could have the effect of: (1) stiffening the gel inside the prostheses (as observed by elastography) and (2) allowing short PDMS chains to cross the membrane into the surrounding biological tissue, a potential source of inflammation and Autoimmune/inflammatory Syndrome Induced by Adjuvants (ASIA) syndrome (5). This latter hypothesis is reinforced not only by the frequent observation of inflammation in patients after 6 to 8 years (5-7), but also by the previous detection of foreign silicone debris in stained histopathological slides in the complex breast tissue matrix (8-9).

**Conclusions:** This preliminary study (10), which should be extended to further multiphysics and in vivo investigations, opens the way for an understanding of the physicochemical phenomena leading to the degradation of the implants. It gives perspective for the use of elastography as a quantitative indicator of the risk of breast implant rupture and help diagnose replacement.
**Acknowledgments:** This work was founded by the HealthTech ITI 2021-2028 program of the University of Strasbourg, CNRS and Inserm, by IHU Strasbourg (ANR-10-IAHU-02), by IdEx Unistra (ANR-10-IDEX-0002) with the IRIS techno. platform and by SFRI (ANR-20-SFRI-0012).

**References:**

(1) Bodin et al JMBBM 2015 (2) Spear and Murphy Plast Reconstr Surg 2014 (3) Maxwell et al Aesth Surg 2015 (4) Hillard et al Gland Surg 2017 (5) Cordel et al Gynéco Obst Fert & Séno 2020 (6) Rzymski et al Wideochir Tech 2011 (7) Prantl et al Clin Hemorheol Microcirc 2014 (8) Jung et al Clin Hemorheol Microcirc 2021 (9) Schaeberle et al Anal Chem 1996 (10) van Haasterecht et al JBiophot 2020 (11) Ruffenach et al J Biomech 2024.

# ULTRASOUND ELASTOGRAPHY OF BACK MUSCLE BIOMECHANICAL PROPERTIES: A SYSTEMATIC REVIEW AND META-ANALYSIS OF CURRENT METHODS

*Mercedes David*[1,2,*], *Karine Devantery*[3], *Bénédicte Nauche*[4], *Miguel Chagnon*[5], *Mark Keezer*[4,6], *Nathaly Gaudreault*[3], *Nathalie J Bureau*[4,7], *Guy Cloutier*[1,2,7]

[1]Laboratory of Biorheology and Medical Ultrasonics, University of Montreal Hospital Research Center, Montreal, Quebec, CANADA; [2]Institute of Biomedical Engineering, University of Montreal, Montreal, Quebec, CANADA; [3]University of Sherbrooke, Sherbrooke, Quebec, CANADA; [4]University of Montreal Hospital, Montreal, Quebec, CANADA; [5]Department of Mathematics and Statistics, University of Montreal, Montreal, Quebec, CANADA; [6]Department of Neurology, University of Montreal, Montreal, Quebec, CANADA; [7]Department of Radiology, Radio-Oncology and Nuclear Medicine, University of Montreal, Montreal, Quebec, CANADA.

**Background:** Muscle ultrasound elastography (UE) is a growing imaging method in rehabilitation therapy and physical medicine [1]. It enables to investigate the impact of musculoskeletal disorders (MSKd) on muscle elasticity [2].
**Aims:** To identify the actual UE methods used to quantify back muscles biomechanical properties in patients with MSKd and quantitatively sum up their reliability, validity (discrimination amongst MSKd and controls), and responsiveness (objectifying changes from one time to another) properties.
**Methods:** We searched the Cochrane, Embase, MEDLINE and CINAHL databases according to predefined study selection criteria. Grey literature was also screened. We employed the COSMIN tool to rate the quality of evidence in the included studies. A meta-analysis was conducted using a random-effect model, allowing the pool of intra-class correlation coefficients (pICC) for reliability and standardized mean differences (pSMD) for validity and responsiveness. Heterogeneity amongst studies was estimated using I-squared statistics.
**Results:** Of 8304 studies, 79 were meta-analyzed, totaling 3178 participants (see Figure). We inventoried three elastography methods: strain imaging (SI; the number of cohorts (n) =26), shear wave imaging (SWI; n =50) and vibration sonoelastography (VSE; n =3). Meta-analytic results demonstrated good reliability measurement properties for SI and SWI (pICC>0.70). A medium pSMD in discriminating MSKd from controls (validity) was found for SI and SWI (0.5; P$\leq$0.020). A medium pSMD (0.64; P=0.005) demonstrates SI's ability to moderately detect within-group changes (WG) over time, compared to a very high pSMD for SWI (1.25; P=0.005). Shear wave imaging also reported significant but small pSMD in detecting between-group changes (BG) over time (0.30; P = 0.003). Due to the insufficient number of cohorts, VSE studies were not meta-analyzed. I-squared statistics (> 90%; P<0.001) acknowledge high heterogeneity amongst studies.
**Conclusions:** Ultrasound elastography assessment of back muscles biomechanical properties in participants with MSKd showed good reliability and moderate validity. Strain imaging and shear wave elastography appear to be effective in detecting changes over time within the same group, but longitudinal studies are needed to confirm this. Future research should also determine the ability of ultrasound elastography to detect changes between different groups over time. The high heterogeneity among studies limited the conclusions that could be drawn from the meta-analyses.
**Acknowledgments:** We acknowledge funding from the Fonds de recherche du Québec – Nature et technologies (FRQNT, grant #302254).

**References:**

[1] Brandenburg JE et al (2014) Arch Phys Med Rehabil 95:2207-2219; [2] Cheung WK et al. (2020). Ultrasound Med Biol 46:1344-1358.

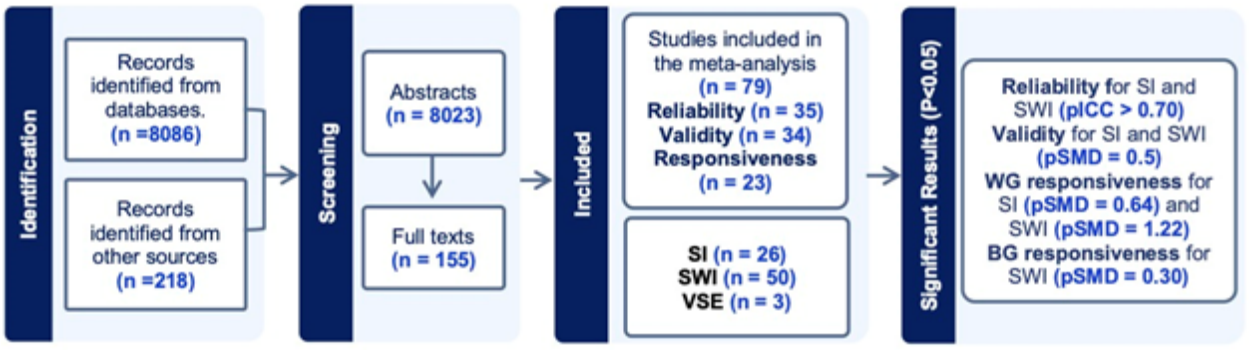

# 3D ROTATIONAL SWEI IN MUSCLE AND ANISOTROPIC PHANTOMS

*S Srinivasan*[1], *CT Paley*[1], *WE Wightman*[1], *DP Bradway*[1,*], *LD Hobson-Webb*[2], *KR Nightingale*[1]

[1]Duke University, Durham, NC, USA; [2]Duke University Hospital, Durham, NC, USA.

**Background:** There is an urgent and unmet clinical need for a low-cost, non-invasive biomarker to accurately assess muscle health, monitor neuromuscular disease progression, and determine treatment response. We are developing 3D rotational shearwave elasticity imaging (3D-RSWEI) with this goal in mind. In 3D-RSWEI, a linear array is rotated around its central axis to acquire shearwave speed (SWS) measurements during a 180-degree rotational movement. In developing the methods for the clinical study, it became apparent that standardizable, anisotropic elastic phantoms would be useful for comparison of elastography techniques.
**Aims:** We will present clinical data obtained in healthy volunteer subject's quadriceps exploring differences in shear anisotropy and nonlinearity across a range of joint flexion angles. In addition, we will present characterization of novel 3D-printed anisotropic phantoms that support imaging sequence development.
**Methods:** In a study of 10 healthy volunteers, we evaluated the effect of muscle passive stretch on the SWS along and across the muscle fibers [1]. The vastus lateralis muscle was passively stretched at 8 different knee flexion angles (controlled by a BioDex system) and 3D-RSWEI measurements were acquired.

Using 3D-RSWEI, we also characterized a set of 3D-printed, polyethylene diacrylate (PEGDA) scaled lattice-structure phantoms submerged in water, then again after embedding them in an isotropic polyvinyl alcohol (PVA) cryogel.
**Results:** In the clinical study, the median within-subject variability was found to be <16%, supporting feasibility as a repeatable clinical metric. Additionally, an unexpected result was found: shearwave signal amplitude along the fibers increased with increasing flexion and muscle stiffness, inconsistent with our expectations based upon material simulations. This observation may lead to an additional potential biomarker for muscle health or inform different material modeling choices for muscle.

In our phantom work, with the PEGDA lattice in water, we measured SWS of 6.3±0.7 m/s and 4.1±0.6 m/s parallel and perpendicular to the axis of rotational symmetry respectively. With the lattice embedded in PVA (SWS of 2.7 m/s), we measured SWS of 5.1±0.2 m/s and 3.1±0.2 m/s in those same directions. We estimated greater dispersion slopes parallel to the material symmetry axis in the lattice-PVA phantom compared to perpendicular to the axis or to PVA alone. These results demonstrate that 3D-RSWEI can quantify the anisotropy of lattice phantoms, that embedding lattices in softer isotropic PVA decreases SWS and measured anisotropy, and that wave dispersion in the lattice-PVA phantom is greater along the scaling direction compared to across.
**Conclusions:** Together the clinical study and novel phantom advance our goal of achieving shearwave-based quantitative biomarkers for skeletal muscle health and monitoring disease.
**Acknowledgments:** The funding source is NIH R01EB033064.
**References:**
[1] Paley, C.T., Knight, A.E., Jin, F.Q., Moavenzadeh, S.R., Rouze, N.C., Pietrosimone, L.S., Hobson-Webb, L.D., Palmeri, M.L. and Nightingale, K.R., 2024. Rotational 3D shear wave elasticity imaging: Effect of knee flexion on 3D shear wave propagation in in vivo vastus lateralis. *Journal of the Mechanical Behavior of Biomedical Materials*, 150, p.106302.

# ULTRASOUND SHEAR WAVE SPEED AND ATTENUATION ASSESSMENTS OF LIVER CANCERS: PRELIMINARY RESULTS

*Iman Rafati*[1,2,*], *Ladan Yazdani*[1,2], *Maxime Barat*[3], *Elige Karam*[3], *Audrey Fohlen*[3], *Bich N. Nguyen*[4], *Hélène Castel*[5], *An Tang*[3,6,7], *Guy Cloutier*[1,2,6]

[1]Laboratory of Biorheology and Medical Ultrasonics, University of Montreal Hospital Research Center, Montréal, Québec, CANADA; [2]Institute of Biomedical Engineering, University of Montreal, Montréal, Québec, CANADA; [3]Department of Radiology, University of Montreal Hospital, Montréal, Québec, Canada; [4]Department of Pathology, University of Montreal Hospital, Montréal, Québec, CANADA; [5]Departments of Hepatology and Oncology, University of Montreal Hospital, Montréal, Québec, Canada; [6]Department of Radiology, Radiation Oncology and Nuclear Medicine, University of Montreal, Montréal, Québec, CANADA; [7]Laboratory of Clinical Image Processing, University of Montreal Hospital Research Center, Montréal, Québec, CANADA.

**Background:** Liver cancer is a major health concern, with rising mortality rates worldwide. Diagnosis currently relies on CT and MRI scans, often supplemented by liver histopathology for confirmation in complex cases. However, diagnostic imaging is costly and liver biopsy is invasive. Because of the cost-effectiveness of ultrasound, there is a growing interest in improving ultrasound-based imaging techniques to improve early detection and characterization of liver cancer. This study focuses on investigating the potential of shear wave (SW) viscoelastography as a non-invasive approach for these applications.
**Aims:** To use elasticity and viscosity measures to distinguish between different types of liver nodules identified through MRI and biopsy.
**Methods:** This prospective cross-sectional study aims to enroll 100 patients with focal liver nodules. A Verasonics Vantage system with a C5-2 probe was used to acquire ultrasound radiofrequency images following radiation pressure pushes. Measurements focused on the largest liver nodule in patients undergoing diagnostic MRI. Two viscoelasticity parameters were measured (SW speed - SWS, and SW attenuation - SWA) in 35 patients (18 with benign and 17 with malignant nodules), to serve as a proof-of-concept preliminary study.
**Results:** Significantly lower SWS in benign (1.87 ± 0.57 m/s) than malignant nodules (2.35 ± 0.74 m/s) were measured ($p<0.05$). SWA values for benign and malignant nodules were 1.25 ± 0.44 and 0.57 ± 0.27 Np/m/Hz ($p<0.001$), respectively. Scatterplot analysis demonstrates the potential of the SWS to SWA ratio (proposed by others to detect liver transplant rejection [1,2] for distinguishing benign and malignant nodules (Fig.1 (a)) The combined SWS and SWA analysis outperformed individual parameters, exhibiting an area under the curve (AUC) of 0.96 compared to 0.70 for the SWS and 0.91 for the SWA in lesion classification (Fig.1 (b)). Further validation on the entire liver cancer cohort is ongoing.
**Conclusions:** The impact of this study lies in its potential to enhance liver nodule classification, offering an alternative screening method for patients with inconclusive conventional ultrasound exams.
**Acknowledgments:** Funded by the Oncotech consortium (Fonds de Recherche Québec, Oncopole, Medteq, Transmedtech, Cancer Research Society, and Siemens Healthineers). Now financed by the Canadian Institutes of Health Research.

**References:**

[1] Ultrasound Med Biol. 2019, 45(4):895-901; [2] Phys Med Biol. 2017, 62(2):484-500.

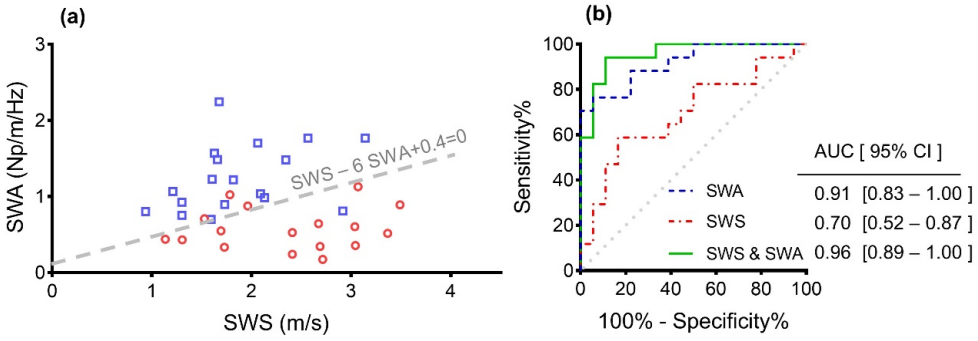


Fig.1. (a) The scatter plot of shear wave attenuation (SWA) and shear wave speed (SWS) for benign and malignant liver nodules. (b) ROC curve for benign and malignant classification using SWA, SWS and the combination of SWA and SWS.

# QUANTIFICATION OF VISCOELASTIC PARAMETERS WITH MRE IN A COHORT OF DIABETIC PATIENTS WITH NON-ALCOHOLIC STEATOHEPATITIS

*P Garteiser*[1,*], *G Pagé*[1,2], *P Manchon*[3], *V Paradis*[4], *L Castera*[1,5], *V Vilgrain*[6], *C Laouénan*[3], *D Valla*[5], *BE Van Beers*[1,6]

[1]Laboratory of Imaging Biomarkers,Center for Research on Inflammation, UMR 1149 Inserm / Université Paris Cité, Paris, France; [2]CEA, NeuroSpin/BAOBAB, Gif-sur-Yvette, France; [3]DEBRC, APHP, Paris, France; [4]Department of pathology, APHP, Clichy, France; [5]Hepatology department, APHP, Clichy, France; [6]Department of Radiology, APHP, Clichy, France

**Background:** Measurement of liver stiffness using magnetic resonance elastography (MRE) has been proposed in metabolic dysfunction-associated steatotic liver disease for diagnosing progressive forms, defined by significant fibrosis F $\geq$ 2 or steatohepatitis [1, 2]. While, in addition to stiffness, MRE is able to provide various mechanical parameters for a better characterization of tissue properties [3], the contribution of viscoelastic MRE parameters has been little studied [4].
**Aims:** In a cohort of type 2 diabetic patients, we evaluate the diagnostic performance of hepatic viscoelastic parameter measurements by MRE for diagnosing progressive forms of fatty liver disease.
**Methods:** 455 patients with diabetes and steatosis were included. MRE was performed using the Resoundant© system on a 3.0T (Philips) or a 1.5T (GE) MRI scanners with the following parameters: TR/TE: 50/20 ms (Philips) or 37/18 ms (GE), in-plane spatial resolution: 1.2 (Philips) or 1.9 (GE) mm, slice thickness: 10 mm, 3 slices, and 4 time steps at an excitation frequency of 60 Hz. Data were reconstructed using the MMDI method [5] (associated with the Resoundant system) and the MARS method [6]. In addition to stiffness (G*), MARS algorithm was applied to obtain measurements of viscoelastic properties (storage modulus G' and loss modulus G"). Measurement of values of mechanical parameters were obtained from a freehand region of the liver positioned on the central slice, excluding the gridded regions of low confidence provided in the MMDI algorithm. The performance of MRE in diagnosing metabolic dysfunction-associated steatohepatitis (MASH), significant fibrosis and fibrotic-MASH (MASH + F $\geq$ 2) was assessed by the area under the ROC curve (AUC). Parameters were assessed individually and by using bivariate analysis. The reference method was the histopathological examination of liver biopsies with central expert reading.
**Results:** Viscoelastic parameters could be determined in 307 patients. 161 patients (55%) had significant fibrosis (including 22 without non-alcoholic steatohepatitis), 133 patients had Fibrotic-NASH and 173 patients (53%) had steatohepatitis on histopathological examination. The AUCs for the diagnosis of significant fibrosis, NASH and fibrotic-NASH with stiffness (MMDI) and with stiffness, storage and loss moduli (MARS) are presented in Figure 1. Stiffness measured with the MMDI reconstruction method provided the highest AUCs values. Among the viscoelastic parameters obtained with MARS, the storage modulus provided the highest AUCs values. The association of viscoelastic parameters G' and G" had higher or equal AUC compared to any of the MARS parameters taken separately, with the exception of G' for NASH.
**Conclusions:** In patients with non-alcoholic fatty liver disease, determining storage and loss viscoelastic moduli using MRE demonstrates good performance in diagnosing significant fibrosis and moderate performance in diagnosing NASH.
**Acknowledgments:** [1]. Deffieux T. et al. J. Hepatology (2015). [2] Pagé G. et al. Frontiers in Phys (2022). [3] Kim et al. Acta Radiologica (2015). [4] Bernal M. et al. IEEE Trans Ultrason Ferroelectr Freq 2015). [5] Gennisson J.L. et al. JASA (2007). [6] Pagé G. et al. PMB (2023). [7]. Li et al. Zormpas-Petridis et al. Cancer Reseach (2019)
**References:**
[1]. Deffieux T. et al. J. Hepatology (2015). [2] Pagé G. et al. Frontiers in Phys (2022). [3] Kim et al. Acta Radiologica (2015). [4] Bernal M. et al. IEEE Trans Ultrason Ferroelectr Freq 2015). [5] Gennisson J.L. et al. JASA (2007). [6] Pagé G. et al. PMB (2023). [7]. Li et al. Zormpas-Petridis et al. Cancer Reseach (2019)

| | G*MMDI | G*MARS | G'MARS | G''MARS | G' + G'' |
|---|---|---|---|---|---|
| Significant fibrosis | 0.79 (95%CI: 0.73–0.83) | 0.74 (95%CI: 0.68–0.79) | 0.77 (95%CI: 0.70–0.82) | 0.60 (95%CI: 0.53–0.66) | 0.79 (95%CI: 0.74–0.84) |
| NASH | 0.71 (95%CI: 0.65–0.77) | 0.68 (95%CI: 0.62–0.74) | 0.69 (95%CI: 0.63–0.75) | 0.64 (95%CI: 0.57–0.70) | 0.68 (95%CI: 0.62–0.74) |
| Fibrotic-NASH | 0.74 (95%CI: 0.68–0.80) | 0.70 (95%CI: 0.64–0.76) | 0.72 (95%CI: 0.66–0.78) | 0.60 (95%CI: 0.53–0.66) | 0.73 (95%CI: 0.68–0.79) |

Figure 1. AUCs values corresponding of interest of mechanical parameters obtained from MRE to diagnose significant fibrosis, NASH and Fibrotic-NASH.

# QUANTIFYING SHEAR WAVE SPEED AND ATTENUATION AT THE COMMON EXTENSOR TENDON OF THE ELBOW: A FIRST STEP IN DIFFERENTIATING FIBROMYALGIA FROM PSORIATIC ARTHRITIS

*Arnaud Héroux*[1,2,*], *Mercedes David*[1,2], *Ladan Yazdani*[1,2,3], *Allen Steverman*[4,5], *Édith Villeneuve*[5,6], *Océane Landon-Cardinal*[5,6], *Nathalie J. Bureau*[7,8], *Guy Cloutier*[1,2,7]

[1]Laboratory of Biorheology and Medical Ultrasonics, University of Montreal Hospital Research Center, Montréal, QC, CANADA; [2]Institute of Biomedical Engineering, University of Montreal, Montréal, QC, CANADA; [3]now with the Department of Biomedical Engineering in Radiology, Weill Cornell Medicine, New York, NY, USA; [4]Department of Family Medicine and Emergency Medicine, University of Montreal, Montréal, QC, CANADA; [5]Department of Rheumatology, University of Montreal Hospital, Montréal, QC, CANADA;. [6]Department of Pharmacology and Physiology, University of Montreal, Montréal, QC, CANADA; [7]Department of Radiology, Radio-Oncology and Nuclear Medicine, University of Montreal, Montréal, QC, CANADA; [8]Department of Radiology and Research Center, University of Montreal Hospital, Montréal, QC, CANADA.

**Background:** There is a clinical overlap between fibromyalgia (FM) tender points and psoriatic arthritis (PsA) enthesitis contributing to misdiagnosis and mistargeted therapies [1]. The pathophysiology of FM tender points remains unclear. It is hypothesized that a biomechanical event, which induces enthesitis, triggers an immune-inflammatory response, leading to synovitis in PsA [2]. Research indicates that FM and PsA exhibit contrasting patterns of collagen turnover [3,4]. However, no biological markers can reliably discriminate between PsA and FM. We hypothesize that shear wave speed (SWS) and shear wave attenuation (SWA) [5] of tendons may provide new ultrasound biomarkers to dissociate FM from PsA.
**Aims:** To compare SWS and SWA of the elbow common extensor tendon between FM and PsA participants.
**Methods:** This pilot study examined 5 FM subjects, 5 PsA subjects and 5 controls from an ongoing cross-sectional prospective institutional review board-approved study. Ten acquisitions were acquired with the Virtual Touch elastography software of the Siemens ACUSON Sequoia scanner with the 10L4 probe in shear wave elastography (SWE) mode (software version: VA25b, Siemens Healthineers, Issaquah, WA, USA). A manually placed region-of-interest on the scanner interface allowed to extract clinical SWS values. In-phase and quadrature (I/Q) data were also exported for experimental SWS and SWA computations. First, displacements were computed with a 2D autocorrelation algorithm [6]. Experimental SWS was then computed by means of a phase velocity algorithm (average SWS between 100-300 Hz) [7]. Experimental SWA was computed according to the revisited frequency shift (R-FS) algorithm [8]. Tendons were manually segmented on all acquisitions. Median values of SWS and SWA were extracted from each parametric map, and finally, we considered the median value over all acquisitions. Wilcoxon rank sum tests were performed between groups.
**Results:** Results showed fair agreement between clinical and experimental SWS values (Fig. A), but no significant differences were observed between groups. Lower experimental SWA values were observed in FM subjects compared to controls (Fig. B, $p < 0.01$). However, no statistical differences were found between controls and PsA subjects ($p = 0.22$), nor between PsA and FM subjects ($p = 0.31$).
**Conclusions:** Results suggest that SWA may be a potential biomarker in the detection of FM, while the discrimination between FM and PsA using SWS and SWA may require a larger dataset.
**Acknowledgments:** We acknowledge funding from Société de l'Arthrite du Canada (#21-0000000089) and from Siemens Healthineers (Equipment loan - Siemens ACUSON Sequoia). We acknowledge the support from Fonds de recherche du Québec – Nature et Technologies (FRQNT) (#345635 for A. Héroux and #302254 for M. David) and from the University of Montreal (Doctoral Scholarship B) for A. Héroux
**References:** [1] Häuser, W. et al. (2019), Clin Exp Rheumatol; [2] McGonagle, D. et al. (2007), Arth. Rheum; [3] Jacobsen, S. et al. (1990), Br J Rheumatol; [4] Gudmann, NS. et al. (2017), Clin Exp Rheumatol; [5] Beuve, S. et al. (2021), IEEE IUS; [6] Loupas, T. et al. (1995), IEEE T-UFFC; [7] Deffieux, T. et al. (2009), IEEE TMI; [8] Yazdani, L. et al. (2022), IEEE T-UFFC.

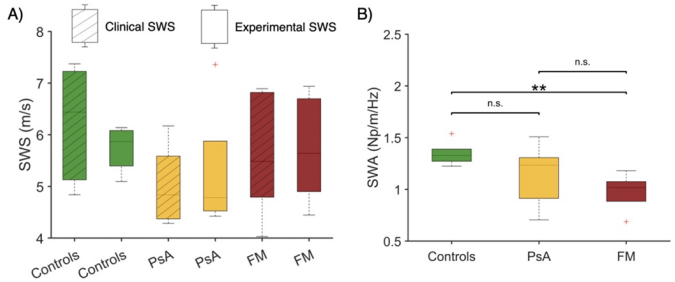


Figure 1: A) Comparison of shear wave speed (SWS) values for controls, psoriatic arthritis (PsA) and fibromyalgia (FM) subjects when using the Siemens ACUSON Sequoia shear wave elastography (SWE) mode (referred as clinical SWS) and when using our implementation of a shear wave phase velocity algorithm (referred to as experimental SWS). B) Comparison of experimental shear wave attenuation (SWA) values for controls, PsA and FM subjects. n.s.: not significant, **: $p < 0.01$

# COMPARING SHEARWAVE SPEED MEASUREMENT YIELD USING FUNDAMENTAL AND HARMONIC TRACKING IN SKELETAL MUSCLE.

*DY Chan*[1], *DP Bradway*[1,*], *LD Hobson-Webb*[2], *KR Nightingale*[1]

[1]Duke University, Durham, NC, USA; [2]Duke University Hospital, Durham, NC, USA.

**Background:** Tissue harmonic imaging (THI) is a nonlinear imaging modality that has been demonstrated in other shearwave elasticity (SWE) imaging applications (e.g., abdominal imaging) to reduce sources of acoustic noise that plague fundamental-mode imaging [1-4]. The factors contributing to the improvement in THI image quality include reductions of side-lobe levels, aberration, and reverberation clutter.

**Aims:** The study's primary objective is to obtain 2D-SWE measurements using fundamental and harmonic tracking along and across the fiber direction in the vastus lateralis muscle of subjects presenting to the Duke Neurological Disorders Clinic. We hypothesize that harmonic shearwave tracking will enable higher shearwave speed measurement yield than fundamental tracking for 2D-SWE imaging of skeletal muscle tissue.

**Methods:** This study was performed under Duke Health IRB protocol #Pro00115312. In patients meeting enrollment criteria who have consented to participate, 2D ultrasound SWE measurements were acquired in the quadriceps muscle using a modified commercial ultrasound system. Ten 2D-SWE acquisitions were obtained in the muscle for each of the following four imaging configurations: fundamental and harmonic SWE tracking along and across the muscle fibers. B-mode ultrasound was used to guide measurement location and orientation within the muscle.

**Results:** At the time of submission of this abstract, we have just completed accrual of ten subjects. Across these ten subjects, the imaging data showed a wide variation in the depth, thickness, structure, and degree of heterogeneity of the vastus lateralis muscle, resulting in a range of shearwave tracking quality for both fundamental and harmonic SWE tracking. While a full analysis of the data is ongoing, we have observed preliminary differences in shearwave speed measurement yield between fundamental and harmonic tracking, along and across the muscle fibers, that will be quantified when presented. Additionally, we observed qualitative improvements in B-mode image quality when harmonic imaging was used, enabling visualization of the muscle fibers with better spatial resolution.

**Conclusions:** When complete, the findings of this study will inform our design of a 3D-SWE imaging system to investigate SWE-derived biomarkers of muscle health.

**Acknowledgments:** The funding source is NIH R01EB033064. We thank Siemens Medical Solutions for in-kind support and technical assistance.

**References:**

[1] Irshid A, Anis M, and Ackerman SJ (2012). "Current role of ultrasound in chronic liver disease: surveillance, diagnosis and management of hepatic neoplasms", Curr Probl Diagn Radiol 41(2):43–51.

[2] Ortega D, Burns PN, Simpson DH, and Wilson SR (2001). "Tissue harmonic imaging: is it a benefit for bile duct sonography?", AJR Am J Roentgenol 176(3):653–659.

[3] Oktar SO, Yücel C, Ozdemir H, Ulutürk A, and Işik S (2003). "Comparison of conventional sonography, real-time compound sonography, tissue harmonic sonography, and tissue harmonic compound sonography of abdominal and pelvic lesions", AJR Am J Roentgenol 181(5):1341–1347.

[4] Hohl C, Schmidt T, Haage P, Honnef D, Blaum M, Staatz G, and Guenther RW (2004). "Phase-inversion tissue harmonic imaging compared with conventional B-mode ultrasound in the evaluation of pancreatic lesions", Eur Radiol 14(6):1109–1117.

# SPARSE EWI: TOWARDS AN AUTOMATED AND REAL TIME ARRHYTHMIA MAPPING TECHNIQUE.

*C Proestaki*[1,*], *M Tourni*[1], *YTT Ling*[1], *EE Konofagou*[1]

[1]Columbia University, New York, NY, USA.

**Background:** Electromechanical Wave Imaging (EWI) has been demonstrated as a viable noninvasive adjuvant echocardiography-based technique, shown to have 96% accuracy in arrhythmia localization against the invasive electroanatomic mapping clinical standard [1]. By employing high framerate ultrasound imaging, EWI displays cardiac electromechanical (EM) activation based on manual selection of axial strain zero-crossings that depict the EM activation times (EMAT). However, manual selection can be prohibitively time consuming for clinical translation. This study introduces an efficient, clinically applicable sparse EWI semi–automated method.
**Aims:** To demonstrate the feasibility and accuracy of sparse EWI and to compare with an existing automated algorithm.

**Methods:** Employing an electromechanical heart model and a 3D ultrasound simulation program [2], an automated algorithm [3] and sparse EWI methodologies were compared; the model's EMAT served as the ground truth, and using Field II [4], ultrasound RF signals were generated with a simulated transducer and scatterers, while single diverging wave imaging with a virtual source 4.8 mm behind the transducer enabled high volume-rate imaging via parallel beam-forming. The two methodologies were evaluated on a 2D slice of the volume corresponding to an apical 4-chamber view of the heart. Sparse EWI utilized recursive AT selection based on the strain correlation between adjacent points and reduced the number of required points that need to be selected by 90%. To evaluate the performance of sparse EWI against the automated algorithm, the Correlation Coefficient (CC) and the EMAT difference between the ground truth and each algorithm AT maps were computed. Additionally, an EMAT difference map was calculated, and EWI was iteratively applied while correcting the areas with the highest EMAT difference.

**Results:** The correlation coefficient (CC) between the EMAT maps of sparse EWI and the ground truth was 0.74, with 70.26% of the myocardium exhibiting an EMAT difference within 0-25 ms (15% error) in the first iteration. In the second iteration, sparse EWI achieved a CC of 0.78 and 70.67% of the myocardium within the same EMAT range. The automated algorithm exhibited a CC of 0.66 and 70.46% of the myocardium within the 0-25 ms EMAT difference range. This demonstrates that the sparse EWI method accelerates the process and achieves greater accuracy than the automated algorithm.

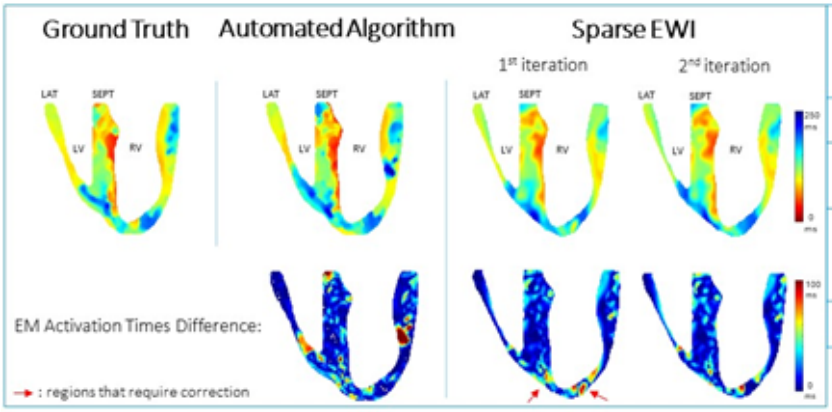


| | Automated Algorithm | Sparse EWI 1st iteration | Sparse EWI 2nd iteration |
|---|---|---|---|
| CC | 0.66 | 0.74 | 0.78 |
| EMAT difference | 70.46% | 70.26% | 70.67% |
| # of manual selected points | 1119 | 112 | 124 |
| Processing time | 61 sec | 677 sec | 749 sec |

*EMAT Difference: $t1-t2$ (t1, t2: activation times of common points between ground truth and automated/sparse maps), within 0-25 ms for a percentage of the myocardium mask.

**Figure:** Comparison of EM Activation Times (EMAT) between Ground Truth, Automated Algorithm, and Sparse EWI (1st and 2nd iterations). The top row shows the EMAT maps, while the bottom row displays the EMAT difference maps highlighting regions that require correction. LV: Left Ventricle, RV: Right Ventricle, ANT: Anterior, Post: Posterior.

**Conclusions:** Sparse EWI was hereby shown to achieve noninvasive, time-efficient and accurate EM mapping increasing its clinical potential to provide real-time feedback in arrhythmia localization towards ablative treatment.
**Acknowledgments:** This study was supported in part by NIH - R01 HL140646.

**References:**

[1] C.S. Grubb and L. Melki, Sci Transl Med, vol. 12, no. 536, pp. eaax6111, Mar. 2020.
[2] V. Gurev and T. Lee, Biomech Model Mechanobiol, vol. 10, no. 3, pp. 295-306, Jun. 2011.
[3] J. Grondin and D. Wang, Comput Biol Med, vol. 113, pp. 103382, Oct. 2019.
[4] J.A. Jensen and N.B. Svendsen, IEEE Trans Ultrason Ferroelectr Freq Control, vol. 39, no. 2, pp. 262-267, 1992.

# ULTRASOUND STIMULATION OF ULTRA-LOW CROSSLINKED HYDROGELS TO ENHANCE WOUND HEALING

*Aniket Beldar*[1], *Kirby Lattwein*[2]*„ Klazina Kooiman*[2], *Ashley Brown*[1]*„ Marie Muller*[1,*]

[1]North Carolina State University, Raleigh, NC, USA; [2] Erasmus Medical Center, Rotterdam, THE NETHERLANDS

**Background:** Chronic wounds affect over 6.5 million in the United States alone and result in health costs of more than $25 billion annually[1]. Aging, obesity and diabetes increase the risks of non-healing wounds[2]. Complications can be profound and include severe pain, septicemia, hospitalization and even amputation. Platelet-like particles are $\mu$gels comprising of ultra-low crosslinked (ULC) poly(N-isopropylacrylamide)[19] copolymerized with acrylic acid (AAc). These particles are similar in size to native platelets ($\approx$1 $\mu$m diameter in solution) and conjugated to a fibrin-binding antibody. Their high deformability allows them to mimic activated platelet morphology[20]. Platelet-like particles (PLPs) are a promising technology to address complications of non-healing wounds. However, the time scale of PLP-mediated clot retraction is an order of magnitude slower than with natural platelets (tens of hrs vs. four hrs). We hypothesize that ultrasound (US) stimulation can enhance PLP deformations and increase fibrin retraction and pro-healing activity.
**Aims:** This study had three objectives: i) to determine the optimal US stimulation settings to maximize PLP deformation; ii) to characterize the effect of PLP-US therapy on wound healing outcomes *in vitro* and *in vivo*; and iii) to elucidate the mechanisms at play in the interaction between PLP and US.
**Methods:** A variety of methods were used. First, a Verasonics US scanner was used to track displacements in a tissue-mimicking phantom in which PLPs were embedded, in order to indirectly evaluate the optimal stimulation frequency and PLP cross-linking for maximal deformations. Then, confocal microscopy and atomic force microscopy were used to evaluate the effect of US-PLP treatment on fibrin clot retraction in vitro. Then, a rodent model of laceration was used to demonstrate treatment efficacy *in vivo*. Finally, an ultra-high-speed camera (HPX-V2, Shimadzu Corp., Kyoto, Japan) coupled to a confocal microscope (A1R+, Nikon Instruments, Amsterdam, the Netherlands) was used to directly observe the effect of US on PLP deformations.

**Results:** We observed that the presence of $\mu$gels enhances the deformation observed within a tissue-mimicking phantom subjected to US stimulation. Deformation was maximum for a stimulation frequency close to 1 MHz and for the lowest degree of cross linking. In fibrin clots in vitro, US-simulated clot retraction is observed at an order of magnitude lower PLP concentration and on a much faster time scale than with PLPs alone. We also observed that this combined treatment enhances wound healing outcomes in vivo. PLPs+US treatment groups showed greater wound closure percentages at early time points relative to all other treatments. Histological analysis of wound tissues collected 9 days post-injury revealed significantly enhanced epidermal layer thickness and angiogenesis (via CD31 staining) for wounds treated with PLPs+US relative to all controls. Finally, the ultra-high-speed imaging revealed that the radius of PLPs tracked over time showed significant oscillations at the same frequency as that of the US stimulation. No such oscillations were observed in the absence of US stimulation.

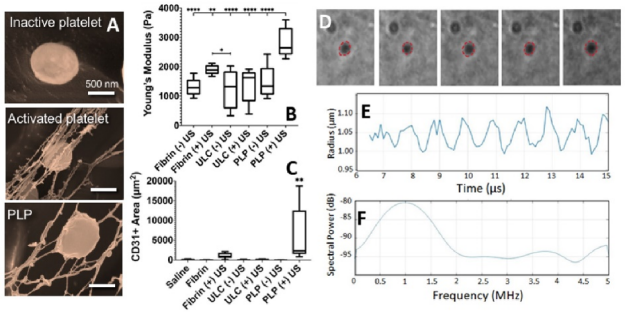


Platelets and PLPs imaged in situ using cryogenic SEM at 50,000X magnification (A). PLPs+US treatment creates stiffer fibrin clots in vitro (B) and higher markers of healing in vivo (C). US stimulation of PLPs induces oscillations at the applied US frequency (D-F).

**Conclusions:** Our results suggest a direct mechanical effect of US on PLPs, which seems to have significant impact on increased fibrin clot retraction and wound healing outcomes. However, the full nature of the mechanisms at play remains to be elucidated.
**Acknowledgments:** NIH R21HL154156 - NCSU Research and Innovation Seed Fund
**References:**
[1] Sen, C. K Advances in Wound Care 10, 281-292, doi:10.1089/wound.2021.0026 (2021).
[2] Guo, S. & DiPietro, L. A. Journal of Dental Research 89, 219-229, doi:10.1177/0022034509359125 (2010).
[3] Gao, J. & Frisken, B. J. Langmuir 19, 5212- 5216, doi:Doi 10.1021/La0269762 (2003).

# ON FRUGAL ELASTOGRAPHIES FOR ULTRAPORTABLE ULTRASOUND

*Adrien Besson*[1,*], *Baptiste Hériard-Dubreuil*[1], *François Maurice*[1], *Claude Cohen-Bacrie*[1].

[1]E-Scopics SAS, 235 rue Léon Foucault, Aix-en-Provence, FRANCE.

**Background:** Ultrasound-based elastography has been extensively studied since the end of the 90s with several clinical applications including liver disease assessment or breast cancer management. Dynamic methods e.g. transient and acoustic radiation force-based (ARF) elastographies are implemented on several cart-based systems. However, the feasibility of elastographies has not been studied

**Aims:** We explore the feasibility of two elastography techniques: the two-dimensional transient elastography (2DTE) and the ARF technique, on Hepatoscope®, a novel ultraportable ultrasound system. In this device, an ultrasound probe is connected to a portable laptop through USB-C without any external power supply. Hence, the power, data rate and computational resources are 10x lower than traditional cart-based systems. We demonstrate that with the adequate hardware and software design choices, both elastography methods are feasible and result in high in vitro performances.

**Methods:** Two key innovations enable frugal elastographies on ultraportable devices: optimized acquisition strategies enabling the transfer of raw data through USB-C and a fully software architecture leveraging GPUs to beamform at kHz frame rates.
Regarding the shear wave generation, 2DTE relies on a 50 Hz mechanical vibration of the probe, ensured by a resonating vibrator. ARF relies on the generation of 125us-long focused push beams (40Vpp, 4.5 MHz, F# 1.4) focused at different depths around 2cm. The processing pipelines perform ultrafast Doppler processing (pixel-based beamforming, displacement extraction, filtering) followed by 2D shear wave velocity estimation.

**Results:** Figure 1 displays the spatio-temporal diagrams obtained with the ARF technique on four calibrated phantoms (CIRS, Norfolk, USA) spreading a broad range of shear-wave speed (SWS) values. We visually identify the wavefronts of the shear waves corresponding to increasing SWS from (a) to (d). Box plots of independent SWS measurements (right plot) illustrate both the low variability of the two techniques and the ability to distinguish the different phantoms.
**Conclusions:** We have demonstrated the feasibility in vitro of two elastography techniques (2DTE and ARF) implemented on Hepatoscope®, a novel ultraportable ultrasound device. The two methods exhibit low variabilities on a wide range of SWS values which is promising for future in-vivo applications.

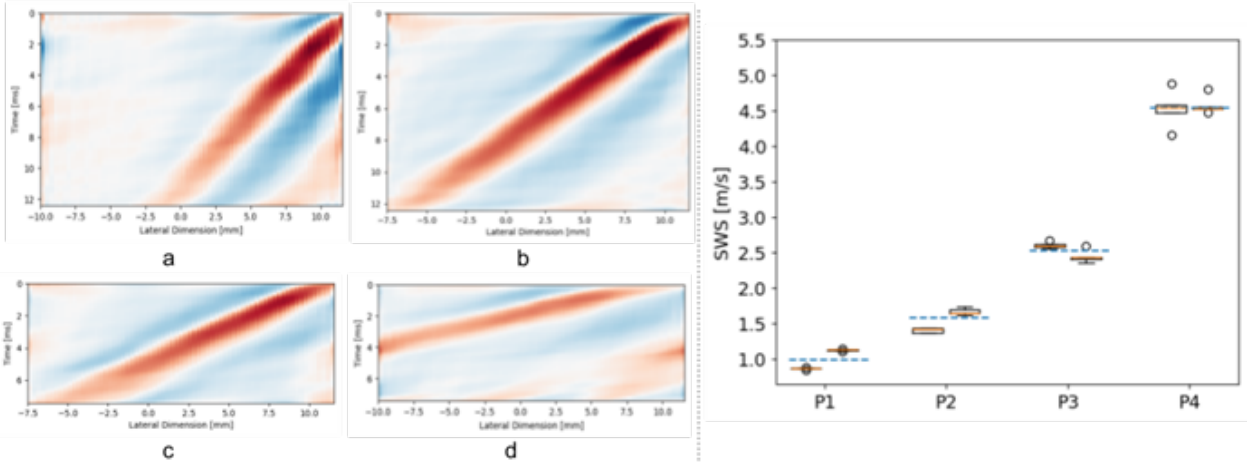


**Figure 1:** (Left) Spatio-temporal diagrams corresponding to a-0.97 m/s, b-1.58 m/s, c-2.52 m/s and d-4.53 m/s. (Right) Boxplots of SWS measurements performed with 2DTE (left box) and ARF (right box) techniques on the calibrated phantoms along with reference values (dashed blue line).

# In-vivo 3D ELASTIC AND BACKSCATTER TENSOR IMAGING USING A 128 ELEMENTS MATRIX TRANSDUCER.

*T Meki*[1,*], *J Reydet*[1], *O Pedreira*[1], *J Hanrard*[1], *M Tanter*[1], *C Papadacci*[1], *M Pernot*[1]

[1]Physics For Medicine, Paris, Ile-de-France, France.

**Background:** The assessment of musculoskeletal and myocardial disorders holds significant importance in the field of medical diagnosis. Elastic Tensor Imaging (ETI) based on 3D shear wave elastography (SWE) can provide quantitative analysis of the shear moduli in anisotropic soft tissues like skeletal muscles, or the myocardium. Backscatter Tensor Imaging (BTI) analyzes spatial coherence of backscattered echoes to provide structural information on the tissue anisotropy [1]. Both information are relevant to characterize quantitatively abnormal fiber tissues.
**Aims:** Current matrix transducers for these techniques are limited to lab research. This study aims to develop a clinical transposable ultrasound system combining 3D Ultrafast SWE and BTI to quantify elastic and coherence anisotropy.

**Methods:** A custom 128-element matrix transducer (Vermon, France) at 2.5MHz was designed and connected to a Vantage system (Verasonics, USA). It enabled 3D SWE using acoustic radiation force imaging with the emission of 3 diverging waves at 9kHz. In addition, volumetric BTI (Fig D) and B-mode (Fig B) was also implemented using diverging wave imaging with 100 virtual sources. Shear wave velocity (SWV) was computed in different spatial directions using tissue velocity from RF cross-correlation. 2D spatial coherence of backscattered echoes was computed using IQ signals at each voxel and fiber orientation was retrieved by applying an elliptic fit. Experimental validation was conducted on isotropic and anisotropic phantoms, and in-vivo measurements were performed on the biceps brachii muscle at varying contraction levels using weights held in the hand (Fig A).

**Results:** In-vivo results demonstrated increased SWV with muscle contraction, along fibers from 2.36±0.2m/s to 7.84±0.58m/s (p = 6e-4) (Fig C), leading to higher fractional anisotropy (FA) from 0.33±0.04 to 0.75±0.07 (p < 1e-4) (Fig E). BTI-derived fiber orientations aligned well with ETI estimates, showing a relative difference of 12.6%. FA retrieved from BTI data (Fig E) remained constant with contraction 0.68±0.05 (p = 0.21).
**Conclusions:** This novel device enables non-invasive characterization of anisotropic tissues, discerning stress and structural anisotropy in promising applications in musculoskeletal and myocardial pathologies.
**Acknowledgments:** This study was supported by ANR, ElastoHeart.

**References:**

[1] Papadacci, C., Pernot(2014). Ultrasound backscatter tensor imaging (BTI): analysis of the spatial coherence of ultrasonic speckle in anisotropic soft tissues. IEEE transactions on ultrasonics, ferroelectrics, and frequency control, 61(6), 986-996.

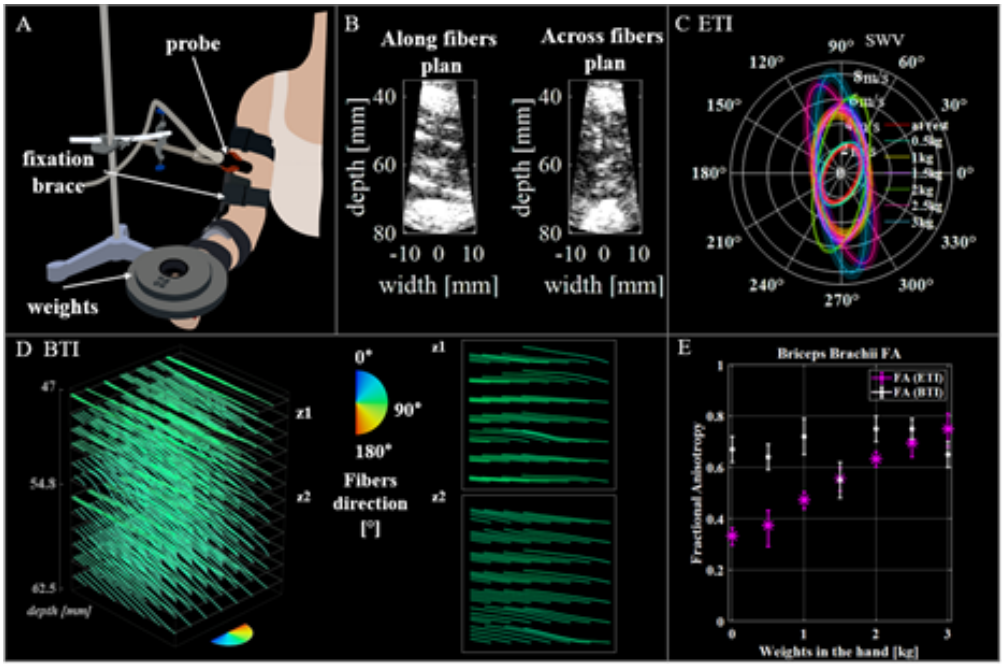

# FAST ULTRASOUND ELASTIC MODULUS RECONSTRUCTION USING DEEP NEURAL NETWORK.

*Utsav Ratna Tuladhar*[1,*], *Richard A. Simon*[1], *Michael S. Richards*[1]

[1]Rochester Institute of Technology, Rochester, NY, USA.

**Background**: Ultrasound (US) elastography is a technique that enables non-invasive quantification of material properties from ultrasound images of deforming tissue and often requires solving the inverse elasticity problem of identifying material properties from a measured displacement field. Traditional iterative techniques for solving the inverse problem are typically slow and computationally intensive while direct techniques are sensitive to measurement noise and require the full displacement field data.
**Aims**: We propose a deep learning (DL) approach, using neural networks trained with finite element (FE) simulated data, to recover the elastic modulus (E) from one component (axial) of the US measured displacement field. Additionally, we aim to implement this method for real-time application.
**Methods:** *Finite Element Simulation.* A FE forward model was used to generate lateral ($u_x(x,y)$) and axial ($u_y(x,y)$) displacement fields. The inputs for the FE model were the FE mesh with 128*128 cartesian grid of regularly spaced nodes in quadrilateral elements, tissue sample geometry, modulus distribution discretized at nodal locations, and boundary conditions. We use only the axial displacement field for DL model. *Depp Learning Model.* A U-net [1] based regression architecture for image-to-image translation was used to learn the mapping from the 2D displacement field to the modulus distribution. The mean square error (MSE) was chosen as the loss function,

$$MSE = \sum_{i=1}^{N} (E_i^t - E_i^p)^2,$$

where N is the number of pixels, $E^t$ is the true modulus and $E^p$ is the predicted modulus. Furthermore, this model was evaluated using both the MSE and the Mean Absolute Percentage Error (MAPE) metric,

$$APE = \sum_{i=1}^{N} |\frac{E_i^t - E_i^p}{E_i^t}|.$$

*Phantom and Clinical Data*. We collected ultrasound data at two different compression states using a tissue mimicking phantom, Elasticity QA Ultrasound Phantom CIRS 049, which contains both hard and soft inclusions. Furthermore, we employ 2 patient datasets from a study conducted by Hassan et al. [2].
**Results:** For the simulated data, we obtained a mean MAPE of 0.29 ± 0.13 % for hard inclusions and 0.35 ± 0.29 % for the soft inclusions. Similarly, for phantom data, an example of a hard inclusion is shown in Figure 1. The expected range of modular ratio of this inclusion is 2.19 to 4.48 and we obtained the ratio of 3.87 and the Contrast-to-Noise Ratio was 129.50. Similarly, a clinical example is also shown in Figure 2 which shows a hard inclusion.
**Conclusions**: We presented a deep learning method to solve the inverse problem of finding the elastic modulus distribution also evaluate its performance both quantitatively and qualitatively. We conclude that provided the simulated data is sufficiently diverse and representative of a wide variability, the algorithm trained on simulated data would generalize well to both phantom, as well as real-world clinical data.

**References:**
[1] Ronneberger, O., Fischer, P., and Brox, T., "U-net: Convolutional networks for biomedical image segmentation," in [International Conference on Medical image computing and computer-assisted intervention], 234–241, Springer (2015).
[2] H. Rivaz, E. M. Boctor, M. A. Choti, et al., "Real-time regularized ultrasound elastography," IEEE transactions on medical imaging 30(4), 928–945 (2010).

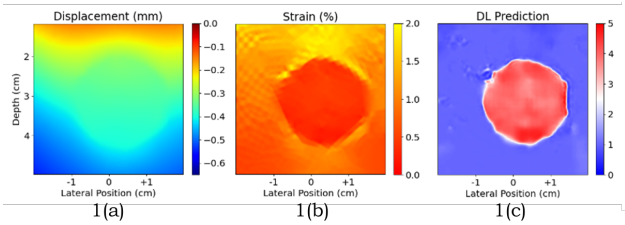


1(a) 1(b) 1(c)

Figure 1: Prediction for phantom data of hard inclusion

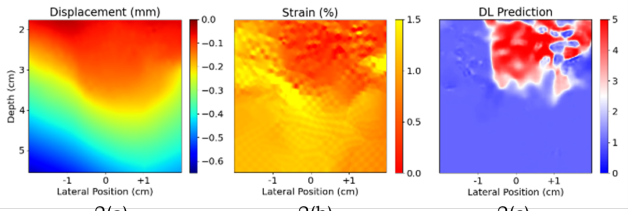


2(a) 2(b) 2(c)

Figure 2: Prediction for clinical

# POINT OF CARE CARDIAC TIME HARMONIC ULTRASOUND ELASTOGRAPHY USING PORTABLE VIBRATION PILLOWS

*Tom Meyer*[1,*], *Brunhilde Wellge*[1], *Gina Barzen1*[1], *Fabian Knebel*[2], *Katrin Hahn*[1], *Thomas Elgeti*[1], *Thomas Fischer*[1], *Jürgen Braun*[1], *Heiko Tzschätzsch*[1], *Ingolf Sack*[1]

[1]Charité – Universitätsmedizin Berlin, Berlin, GERMANY; [2]Sana Klinikum Lichtenberg, Berlin, GERMANY

**Background:** Heart failure, often associated with diastolic dysfunction (DD), is an increasing health problem in Western societies. DD is associated with increased myocardial stiffness, which is not directly measurable by standard echocardiography. Ultrasound-based elastography is an established method for non-invasive assessment of tissue stiffness. In the recent years, promising approaches to cardiac elastography have been proposed[1, 2]. Yet, clinical applications of cardiac elastography suffer from expensive hardware and limited penetration depth. Time harmonic elastography (THE) relies on conventional focused ultrasound synchronized to continuous vibrations which are induced by a bed-actuator device[3]. Novel cardiac THE (cTHE) with full field-of-view coverage up to 15 cm depth has recently been shown to be sensitive to abnormally increased myocardial stiffness in patients with amyloidosis[4].
**Aims:** To test in patients and healthy subjects the reproducibility and sensitivity of optimized THE based on a portable vibration device for use as point-of-care and cost-effective cardiac elastography technique.
**Methods:** 15 healthy volunteers (1 female, age range 19-54 years) underwent cTHE twice. The subjects were examined in a test-retest experiment in which they stood up and moved around between experiments. In addition, 10 patients with aortic stenosis (AS) (5 women, age range 61-85 years) and associated mild to moderate hypertrophy were examined to analyze the sensitivity of cTHE to this condition. Continuous multifrequency vibrations (60, 70, 80 Hz) were induced using a custom designed portable vibration pillow (Elastance Imaging, Columbus, Ohio, US) placed underneath the subject's thorax. A customized ultrasound scanner (GAMPT Merseburg, Germany) with a phased array transducer was used for image acquisitions in parasternal long axis view with 15 cm depth. Images were continuously acquired in breath-hold over 4s with 100Hz frame rate. Measurements were repeated three times. Time-resolved shear wave speed maps (SWS) were generated using k-MDEV inversion [5]. Diastolic frames were averaged to obtain a map of diastolic myocardial stiffness. Manually drawn regions of interest were placed within the septum and the posterior wall for SWS averaging. One-way intra-class correlation coefficient was used to assess reproducibility.

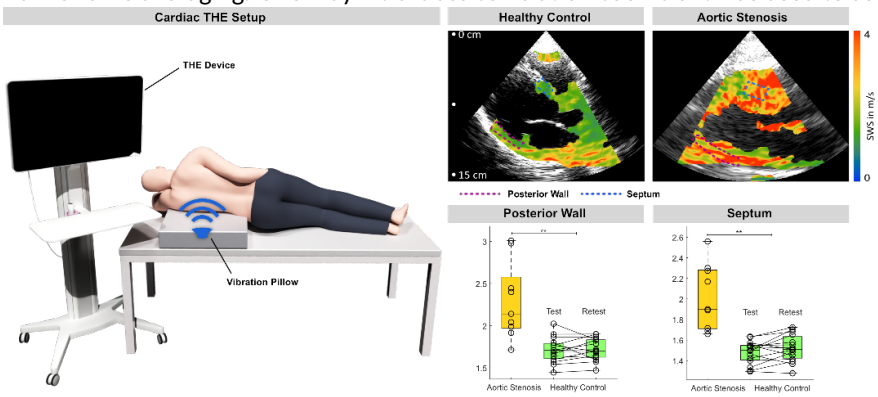


*Figure 1: Cardiac THE Setup with portable vibration pillow, together with representative elastograms of healthy controls and patients with aortic stenosis and group comparison.*
**Results:** In controls, diastolic SWS (septum: 1.5±0.1m/s, posterior wall: 1.7±0.2m/s) was highly reproducible with ICC=0.73 in the septum and ICC=0.72 in the posterior wall. Patients with AS showed markedly increased SWS values (septum: 2.0±0.3m/s, posterior wall: 2.3±0.5m/s, both p<0.001).
**Conclusions:** Novel cTHE with portable driver was highly reproducible and sensitive for elevated myocardial stiffness in aortic stenosis. With the recent advent of treatment options for DD, cTHE could be of clinical value as a point-of-care imaging modality for treatment monitoring in DD. Based on standard, low-cost ultrasound components, cTHE can be easily integrated into established clinical ultrasound systems.
**Acknowledgments:** German Research Foundation (FOR5628, CRC1340 and GRK2260) and Pfizer (WP2487656).
**References:**
[1]Villemain, O., et al., Myocardial Stiffness Assessment Using Shear Wave Imaging in Pediatric Hypertrophic Cardiomyopathy. JACC: Cardiovascular Imaging, 2018. 11(5): p. 779-781; [2]Santos, P., et al., Natural Shear Wave Imaging in the Human Heart: Normal Values, Feasibility, and Reproducibility. IEEE Transactions on Ultrasonics, Ferroelectrics, and Frequency Control, 2019. 66(3): p. 442-452; [3]Tzschatzsch, H., et al., Two-Dimensional Time-Harmonic Elastography of the Human Liver and Spleen. Ultrasound Med Biol, 2016. 42(11): p. 2562-2571; [4]Meyer, T., et al., Point-of-care cardiac elastography with external vibration for quantification of diastolic myocardial stiffness. medRxiv, 2024: p. 2024.01. 26.24301851.; [5]Tzschatzsch, H., et al., Tomoelastography by multifrequency wave number recovery from time-harmonic propagating shear waves. Medical Image Analysis, 2016. 30: p. 1-10.

## October 23rd

# GUIDED-WAVE OPTICAL COHERENCE ELASTOGRAPHY (OCE) TO QUANTIFY MACROSCOPIC ELASTICITY IN THE CORNEA

*Ivan (Vanya) Pelivanov*

Department of Bioengineering, University of Washington, Seattle, Washington, USA
ivanp3@uw.edu

Tissue elastography has spatially mapped the Young's modulus (or elasticity) of biological tissue for a few decades. Different deformation sources can create material displacement, and clinical imaging systems (US and MRI) can track the displacement leading to spatial elasticity maps. Existing elastography systems, however, are not well suited to characterize the eye because only fully non-contact methods have a chance for clinical translation. Dynamic Optical Coherence Elastography (OCE), in which externally generated propagating mechanical waves are tracked with phase-sensitive OCT, is the youngest elastography method. It is fully noncontact and noninvasive and is especially suited to elastography of external organs such as cornea or skin. An advantage of OCE is that OCT has recently become a standard of care in ophthalmology to image both structural and functional properties of ocular tissues. It does not require additional regulatory approvals which should be very helpful for fast OCE translation into clinical use.

We pioneered an acoustic micro-tapping (A$\mu$T) technique to launch shear waves in soft tissue with air- coupled acoustic radiation force, which to date provides the highest efficiency and resolution among noncontact excitation techniques in dynamic OCE.

Corneal elasticity is key to its biological function. OCT is currently the most accurate instrument in ophthalmology that can image all segments of the eye, including mapping corneal shape and thickness determining its refractive power, abnormalities, and ectasia. However, corneal geometry alone cannot predict disease progression nor guide corneal interventions such as LASIK and crosslinking therapies.

Mapping corneal elasticity with wave-based OCE can help guide interventions, but it is not an easy task. A realistic corneal mechanical model accounting for its physical bounding, pressurized state, curvature, and very strong mechanical anisotropy is key to quantitatively evaluating its elasticity and predicting deformational changes due to interventions. This talk will discuss the most elaborate and realistic corneal mechanical models and methods to reconstruct its elastic moduli with spatial resolution appropriate for clinical decision-making.

# OPTICAL TIME HARMONIC ELASTOGRAPHY

*Jakob Jordan*[1,*], *Noah Jaitner*[1], *Tom Meyer*[1], *Luca Brahmè*[2,3], *Mnar Ghrayeb*[4,5], *Julia Köppke*[2,3], *Stefan Klemmer Chandia*[1], *Vasily Zaburdaev*[6,7], *Liraz Chai*[4,5], *Heiko Tzschätzsch*[8], *Joaquin Mura*[9], *Anja I.H. Hagemann*[2,3], *Jürgen Braun8*, *Ingolf Sack*[1]

[1]Department of Radiology, Charité – Universitätsmedizin Berlin, GERMANY; [2]Department of Hematology/Oncology, Charité – Universitätsmedizin Berlin, GERMANY; [3]German Cancer Consortium-German Cancer Research Center, Heidelberg, GERMANY; [4]The Center for Nanoscience and Nanotechnology, The Hebrew University of Jerusalem, ISREAL; [5]Institute of Chemistry, The Hebrew University of Jerusalem, Jerusalem, 91901, ISREAL; [6]Department of Biology, Friedrich-Alexander Universität Erlangen, 91058 Erlangen, GERMANY; [7]Max-Planck-Zentrum für Physik und Medizin, 91058 Erlangen, GERMANY; [8]Institute of Medical Informatics, Charité – Universitätsmedizin Berlin, GERMANY; [9]Department of Mechanical Engineering, Universidad Técnica Federico Santa María, Santiago, CHILE

**Background:** Stiffness mapping using ultrasound elastography (USE) and magnetic resonance elastography (MRE) are routine diagnostic procedures for disease detection and treatment monitoring [1]. However, it is challenging to superimpose USE or MRE maps with light microscopy images due to different resolutions and unclear correlations of mechanical parameters with histological features. Powerful optical elastography methods exist [2-4], but comparison with MRE and USE is difficult due to the difference in approaches.
**Aims:** To develop optical multifrequency time-harmonic elastography (OMTHE) for superfast high-resolution, stiffness mapping from the surface of opaque samples or within the bulk of transparent biological tissues.
**Methods:** A high-speed camera (540K-S, Photron, Japan) was used to encode serial images of harmonic shear waves induced by a piezoelectric actuator (APA35XS, Cedrat, France) at frequencies between 800 and 2400 Hz. Each frequency was consecutively sampled with 8 dynamics over 3 periods with exposure times of 20$\mu$s, resulting in a total measurement time of 1.2 s. A custom optical flow algorithm was used to extract two in plane wave components from the image series. All frequencies and components were used for multifrequency wave inversion to generate maps of shear wave speed (SWS). OMTHE was validated with multifrequency MRE as ground-truth method in phantoms. Post-mortem zebrafish embryos were studied at 3, 24, 48, 72, 96, and 120 h post fertilization. Finally, bacterial biofilms of Bacillus subtilis were grown on two different substrates of 1.5wt.% and 3wt.% agar-water and studied after 24, 48 and 72 h time of growth.
**Results:** OMTHE agreed with MRE in phantoms across all studied frequencies (MRE 1.1±0.1 m/s, OMTHE 1.16±0.05 m/s). In zebrafish embryos, SWS was higher in the myotome than notochord (P<0.001), with a linear stiffness increase with age (R=0.65, P<0.001). In biofilms no stiffness difference between films grown on two different substrates was observed. Overall, the core region became softer than the periphery with age (core: 2.0±0.3, 1.3±0.3, 1.1±0.3 m/s, periphery: 1.9±0.3, 1.7±0.3, 1.6±0.3 m/s at 24, 48, 72 h, all p<0.005, age-related softening: R =-0.88, p<0.001).

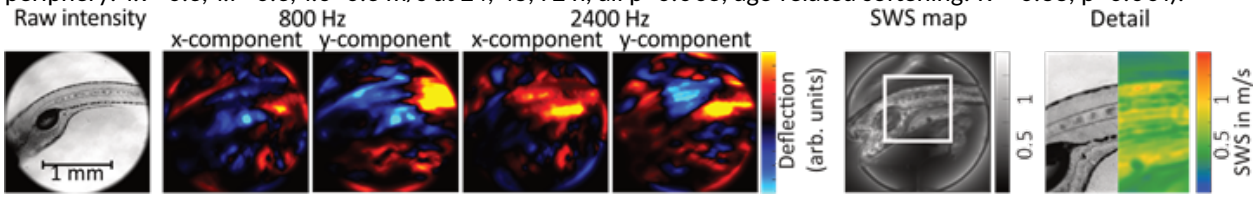


*Figure 1: From left to right: raw intensity images as captured by the high-speed camera, waveforms for the lowest and highest frequency measured in both x- and y-directions, SWS map, and magnified region of interest with camera image as comparison.*

**Conclusions:** OMTHE is a versatile platform that uses optical detection of surface waves or shear waves within transparent tissues. It provides solutions to several persistent problems in stiffness mapping in biomedical research over multiple length scales, including high optical resolution, ultrafast scanning, robust motion estimation of periodic tissue deflections, and multifrequency inversion of harmonic wavefields. As an in-plane mapping technique, OMTHE provides high-resolution stiffness maps in zebrafish embryos during development and at surfaces of growing biofilms.
**Acknowledgments:** German Research Foundation, GRK2260, FOR5628, CRC1340, CRC1540.

**References:**

[1] Sack, I., Magnetic resonance elastography from fundamental soft-tissue mechanics to diagnostic imaging. Nat. Rev. Phys., 2023. 5: p. 25-42.
[2] Grasland-Mongrain, P., et al., Ultrafast imaging of cell elasticity with optical microelastography. PNAS, 2018. 115(5): p. 861-866.
[3] Zorgani, A., et al., Optical elastography: tracking surface waves with digital image correlation. Phys. Med. Biol., 2019. 64(5): p. 055007.
[4] Laloy-Borgna, G., et al., Observation of natural flexural pulse waves in retinal and carotid arteries for wall elasticity estimation. Sci. Adv., 2023. 9(25): p. eadf1783.

# PASSIVE ELASTOGRAPHY USING SPECKLE CONTRAST IMAGING

*M Legrand*[1,*], *N Dufour*[1], *E Martins Seromenho*[1], *N Bahlouli*[1], *A Nahas*[1]

[1]University of Strasbourg, CNRS, ICube UMR 7357, Strasbourg, FRANCE.

**Abstract Body:** Stiffness estimation enhances the detection of tumor in tissues. For the colorectal cancer screening it is although difficult to mechanically touch the tissue and access this parameter, even with an endoscope.

**Background:** A first method previously developed in our laboratory is based on a digital holography setup [1] to image shear wave propagation. The elastography method used is noise correlation elastography, initially developed by Catheline et al. [2]. The method is used to estimate stiffness properties from a diffuse mechanical shear waves field. Thus it is possible to use shear wave noise already generated in vivo inside the patient to estimate the stiffnes which is particularly well adapted for endoscopic imaging.
**Aims:** The goal of this work is to provide a new approach that can fit in an endoscope, and with which it is still possible to retrieve the shear wave propagation and so the stiffness of the concerned area.

**Methods:** The noise correlation elastography [2] is a method that links temporal correlation of a diffuse shear wave field to Green function in each pixel of the concerned area. The Green function contains the wavelength, that can be directly linked to the speed of the wave. To apply this method on data and retrieve their celerity map, it is however necessary to record with high sensitivity the wave propagation. To avoid the size of the holographic setup that cannot fit in an endoscope, the experimental system use in this study is a LASER speckle contrast system. The sample is illuminated using a 637 nm LASER fiber with an camera acquisition frame rate of 200Hz. The back scattered light from the sample generates speckle patterns that is particularly sensitive to displacement within the sample. In order to generate a well control shear wave field to characterize the system, a low frequency piezo actuator (500-1000 Hz) has been used. Thus, while the mechanical wave propagates through the sample it will locally modulate the speckle patterns (see Fig.1). To retrieve the local displacement induced by the waves, differences between successive images is calculated. This algorithm is first tested and optimized on simulated data and then applied on different gelatin test samples with controlled optical properties that match skin optical properties and different mechanical properties (corresponding to different concentration of gelatin). We will also present a first proof-of-concept on ex-vivo pork tissues.

**Results:** Results of the successive differences algorithm is presented on figure 2 for simulated data and on figure 3 for acquired data. Qualitative difference of stiffness on heterogeneous acquired data is also observable. **Conclusions:** This method is particularly adapted to an endoscopic application.. The results obtained with this setup on acquired data are promising: the shear waves are visible, just like the difference of stiffness on a heterogeneous sample.

**References:**

[1] Marmin, A. et al. Time-of-flight and noise-correlation-inspired algorithms for full-field shear-wave elastography using digital holography. JBO 26, 086006 (2021).

[2] Catheline, S. et al. Tomography from diffuse waves: Passive shear wave imaging using low frame rate scanners. Applied Physics Letters 103, 014101 (2013).

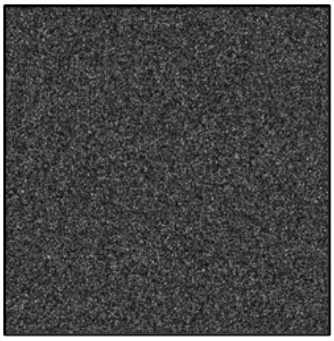

Figure 1: Initial data – speckle pattern combined with mechanical wave.

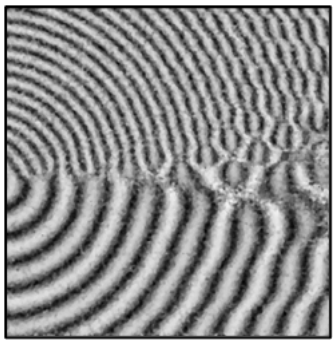

Figure 2: Wave propagation pattern on simulated data.

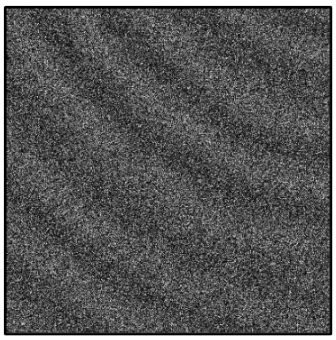

Figure 3: Wave propagation pattern on acquired data.

# RECONSTRUCTION OF ANISOTROPIC SHEAR MODULI USING NON-CONTACT OPTICAL COHERENCE ELASTOGRAPHY.

*G Regnault*[1,*], *M O'Donnell*[1], *I Pelivanov*[1]

[1]University of Washington, Department of Bioengineering, Seattle, WA, USA

**Background:** Skin grafting is often required to manage complex skin injuries and secondary aesthetic reconstructions. Factors associated with skin elastic properties (such as contractions and shearing forces) are among the most common causes of functional and cosmetic complications of graft procedures. Thus, determining tissue properties in vivo is critical to reconstructive success.
**Aims:** In a recent study [1], we introduced a non-contact, non-invasive air-coupled acoustic micro-tapping (A$\mu$T) technique to launch mechanical waves in soft media. By integrating A$\mu$T with real-time phase-sensitive Optical Coherence Tomography (OCT), we demonstrated a fully non-contact Optical Coherence Elastography (OCE) system that can image the propagation of mechanical waves in skin. However, quantitative reconstruction of elastic moduli and fiber orientation in skin accounting for its anisotropy is still a challenge.
**Methods:** Here we present a new method to reconstruct skin elasticity (considered as a nearly incompressible transversely isotropic (NITI) solid) based on Rayleigh wave propagation. Note that for a NITI material, three distinct elastic moduli are needed: G, the out-of-plane shear modulus; $\mu$, the in-plane shear modulus; $\delta$, a tensile anisotropy ratio. We conducted numerical simulations in OnScale for different excitation geometry (point- and line-shaped) and for NITI materials with different degrees of shear and tensile anisotropy to justify the method and inversion routine. The optimal protocol was then applied to reconstruct mechanical moduli of one anisotropic phantom and of human forearm skin in vivo.
**Results:** From simulations we show that propagation from a point-like source excitation (Fig. 1a) produces wave packets with speed not equal to either or phase velocity predictions for Rayleigh waves. In contrast, a line source excitation (Figs. 1b) enables direct measurement of phase velocity for most propagation directions, and is not affected by geometrical attenuation and can thus easily be used for elasticity reconstruction. All 3 shear moduli can be inverted from experimental A$\mu$T-OCE in a PVA NITI phantom (Fig. 1c) and in human skin in vivo (Fig. 1d). Note that multimodal imaging can be particularly interesting when investigating anisotropic properties of tissues. Indeed, polarization-sensitive (PS-) OCT (Fig. 1e), can be used to measure, in parallel to A$\mu$T-OCE, collagen fiber orientation. Here we show that both OCT-based modalities reveal the same principal axis of symmetry (Fig. 1d,e for A$\mu$T-OCE and PS-OCT, respectively).

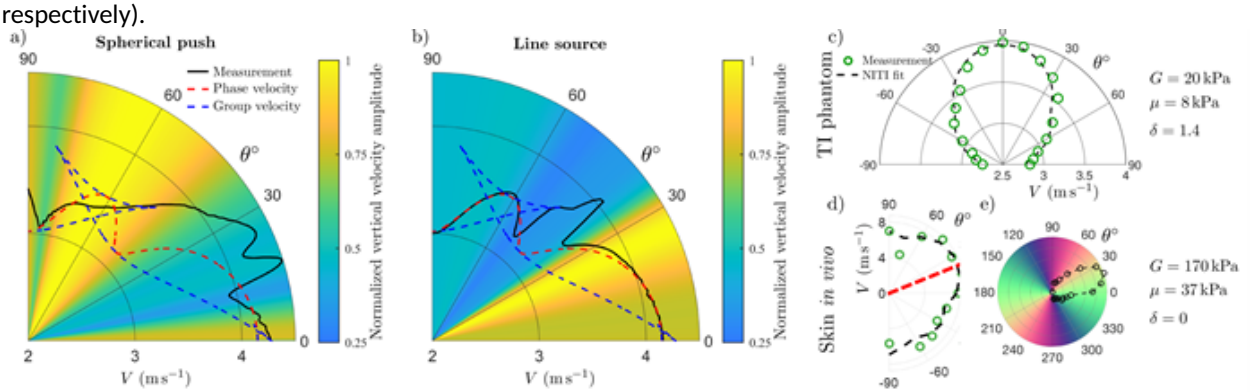


*Figure 1. Comparison of measured broadband wavepacket velocity following a), a spherical push or b) multiple line-shaped source with different orientation, with theoretical group and phase velocities for a NITI material with: G = 40 kPa, $\mu$ = 10 kPa and $\delta$ = 0. c) Measured anisotropic wavepropagation with A$\mu$T-OCE in a NITI PVA phantom. d) Measured anisotropic wavepropagation with A$\mu$T-OCE in human forearm in vivo. e) Measured collagen fiber orientation with PS-OCT for the same dataset as d).*

**Conclusions:** Conclusions: We show here that reconstruction of elastic moduli of anisotropic media, such as skin, from OCE measurements is not straightforward due to high geometric wave dispersion. Proper choice of the excitation geometry and signal processing routine is critically important for correct reconstruction of all 3 shear elastic moduli.
**Acknowledgments:** This work is supported by NIH grants R01EY035647, R01EY026532, R01EY028753, R01AR077560 and Life Sciences Discovery Fund 3292512.
**References:**
[1] Kirby et al., Scientific Reports (2022), 12.1, 3963.

# ASYNCHRONOUS, SEMI-REVERBERANT ELASTOGRAPHY

*G Schmidt*[1,2,*], *BE Bouma*[1,2], *N Uribe-Patarroyo*[1]

[1]Wellman Center for Photomedicine, Harvard Medical School and Massachusetts General Hospital, Boston, MA, USA; [2]Institute for Medical Engineering and Science, Massachusetts Institute of Technology, Cambridge, MA, USA.

**Background:** Optical coherence elastography measures elasticity– a property correlated with pathologies such skin cancer lesions and systemic sclerosis. Wave-based elastography, including reverberant elastography, leverages the properties of shear waves traveling through tissue primarily to infer shear modulus [1]. By leveraging a diffuse and dynamic shear wave field, reverberant elastography is relatively robust to motion, making it a promising candidate for translation in vivo [2]. Despite these potential benefits, existing implementations (as well as wave-based OCE methods in general) are fundamentally limited by their need to synchronize shear wave excitation with MB-mode imaging. Notably, this limitation is not due to the fundamental principles of reverberant elastography. Rather, it is a practical limitation unique to raster-scanned systems such as OCT and their slow frame rates relative to shear wave speeds. In order to address this, this work enables OCT elasticity measurements with the same acquisition time required for OCT angiography, greatly expanding the opportunity for widespread application of OCE in vivo.
**Aims:** This work represents the first successful demonstration of reverberant elastography in vivo with a conventional, raster-scanning OCT system without synchronization or complex custom hardware.
**Methods:** First, leveraging shear wave displacement rather than velocity removes temporal sampling requirements, thus enabling conventional raster-scanning. Second, the time delay between A-lines that arise from raster-scanning can be modeled as amplitude modulation, and therefore successfully demodulated to recover the coherent shear wave field without MB-mode synchronization. Finally, since demodulation only exists along the x-axis, we presented a novel shear wave-excitation scheme that only produces waves traveling in-plane along the B-scans.
**Results:** These advancements enabled reverberant elastography in vivo by drastically reducing acquisition time by two orders of magnitude for the same lateral sampling parameters typically used in previous work. For laterally Nyquist-sampled data, total imaging speed is still faster by an order of magnitude, while enabling a multitude of advanced signal processing techniques, such as non-linear speckle-based motion correction or optimum filtering.
**Conclusions:** We present a method for full recovery of the coherent shear wave field in an asynchronous, raster-scanning OCT system by modeling raster-scanning as an amplitude modulation of the displacement field. This technique recovers the entire spatially-coherent complex-valued shear wave field from just two B-scans, while reducing the time scale for sensitivity to motion from minutes to tens of milliseconds.

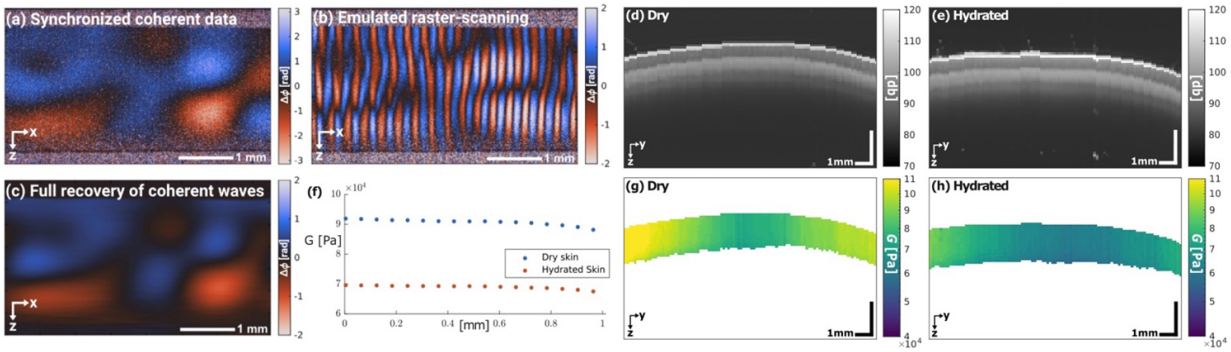


*Figure 1: (a) Ground truth shear wave field acquired via MB-mode scanning. (b) Emulated raster-scanning data produced by down sampling (a). (c) Recovered shear wave field using just 4% of the original data via our demodulation technique. (d) OCT reflectance image of human skin in vivo before and after (e) hydration. There is no remarkable difference. (f-h) Asynchronous, semi-reverberant elastography produces elastograms of stiffness before (g) and after (h) hydration. Data acquired with a convention, raster-scanning OCT system without MB-mode scanning. The depth averaged stiffness (f) reveals a notable reduction in stiffness after hydration.*

**Acknowledgments:** National Institutes of Health (R01EB033306, P41EB015903, K25EB024595); National Science Foundation (GRFP).

**References:**

[1] K. J. Parker, et al., "Reverberant shear wave fields and estimation of tissue properties," Phys. Med. Biol. 62, 1046–1061 (2017). [2] F. Zvietcovich, et al., "Reverberant 3D optical coherence elastography maps the elasticity of individual corneal layers," Nat Comm 10, 4895 (2019).

# EVALUATION OF MYOCARDIAL INFARCTION RECOVERY WITH ELECTROMECHANICAL ACTIVATION AND TIME TO PEAK PRINCIPAL STRAIN

*Hannah Schleifer*[1,*], *Tracy Yik-Tung Ling*[1], *and Elisa Konofagou*[1]

[1]Columbia University, New York, NY, USA

**Background:** Myocardial Elastography (ME), a multidimensional high frame-rate strain estimation technique using RF-based speckle-tracking, has been shown to stage progressive ischemia in canines and humans [1, 2]. Electromechanical Wave Imaging (EWI) identifies electromechanical activation of the heart through strain changes induced by the electromechanical wave propagation through the heart [3]. In this study, the combination of ME-based metric Time to Peak Maximum Principal Strain (T2P Emax) and EWI-based metric Systolic Activation Time (SAT) are utilized to investigate how to accurately and specifically characterize MI.
**Aims:** Aims: In this study, we stage MI remodeling in a canine chronic infarction model by estimating and imaging the T2P Emax and the SAT over five weeks post-MI.

**Methods:** Infarction was induced in the left anterior descending artery (LAD) of two mongrel canines (male, weight: 22.8±1.4 kg) via complete ligation and were survived for 5 weeks. Closed-chest acquisitions of channel data were acquired of the left ventricle (LV) apex (closest to ligation site) prior to and within 24 hours after ligation surgery with a P4-2 phased array (ATL/Philips, Andover, MA, USA) probe (20-mm 64-element aperture, 2.5 MHz, 0.32-mm pitch) and a research ultrasound system (Vantage, Verasonics, Redmond, WA). The ME acquisitions were performed using Delay-and-Sum beamforming and a compounding sequence with 15 transmits, 60° angular aperture, 15° tilt, 300Hz frame rate and 14-mm depth. EWI employed a single diverging wave at 2000Hz. Emax was estimated by first identifying systole, then estimating displacements using 1-D normalized cross-correlation in a 2-D search (4.6 mm window, 80% overlap) [4]. Cumulative Emax were estimated, and the time after systolic onset of maximum Emax was chosen for T2P Emax. EWI isochrones were generated by estimating displacement using a 1-D cross-correlation (6.2 mm window, 90% overlap) [3] to calculate interframe axial strain. A Lagrangian Least-Squares strain estimator was used to estimate strains from displacements [5]. After onset of the QRS wave, the SAT was identified at the points when the resulting axial strain curve first crossed zero-strain.

**Results:** In Fig. 1A when compared to baseline, both the SAT and T2P Emax maps show localized differences post-LAD ligation. A localized region of SAT delay can be seen in the LAD portion of the LV apex week 1-5. T2P Emax shows a slight global delay at week 1, localized early T2P Emax at the LAD in weeks 2-4, then a large global delay at week 5. SAT in the LAD (Fig. 1B-i) is delayed when compared to the LCX and RCA territories in weeks 1-5, and T2P Emax in the LAD (Fig. 1B-ii) precedes the LCX and RCA weeks 2-4, until all three territories become delayed at week 5 post-MI. Fig 1C-i shows a significant SAT delay between LAD and RCA (101.2ms-52.82ms, p<0.001), while Fig 1C-ii shows a significantly early T2P Emax between the LAD and RCA (127.3ms-147.8ms, p<0.001).

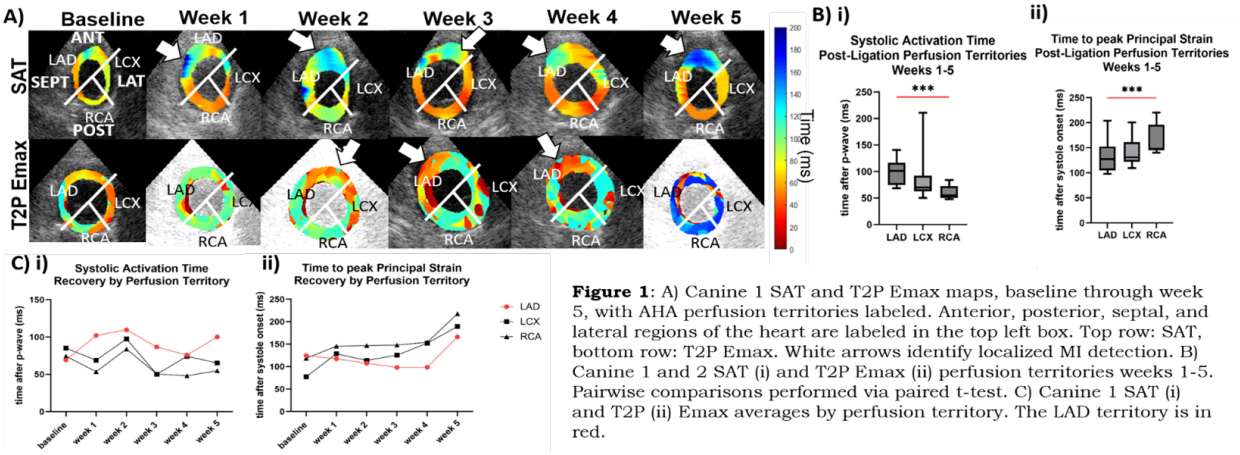


**Figure 1**: A) Canine 1 SAT and T2P Emax maps, baseline through week 5, with AHA perfusion territories labeled. Anterior, posterior, septal, and lateral regions of the heart are labeled in the top left box. Top row: SAT, bottom row: T2P Emax. White arrows identify localized MI detection. B) Canine 1 and 2 SAT (i) and T2P Emax (ii) perfusion territories weeks 1-5. Pairwise comparisons performed via paired t-test. C) Canine 1 SAT (i) and T2P (ii) Emax averages by perfusion territory. The LAD territory is in red.

**Conclusions:** The time to peak strain and systolic activation were hereby shown to localize MI to the left coronary branch (LAD and LCX). T2P Emax, however, was not as sensitive in depicting MI remodeling, while SAT can localize infarction during recovery.
**Acknowledgments:** This study was supported by the National Institutes of Health (R01 EB006042 and R01 HL140646).
**References:**
[1] J. Grondin et. al., UMB, 2017. [2] V. Sayseng et. al., UMB, 2020. [3] J. Provost et. al., Phys. Med. Bio., 2011. [4] T. Y. T. Ling et. al., IEEE IUS, 2022 [5] F. Kallel and J. Ophir, Ultrason. Imag., 1997

# PASSIVE AND ACTIVE ELASTOGRAPHY BY WAVE EQUATION INVERSION

*Thomas Gallot*[1,*], *Camille Chaillous*[1], *Aron Kahrs*[1]

[1]Instituto de Física, Facultad de Ciencias, Universidad de la República, Montevideo, Uruguay.

**Background:** Passive elastography, or noise-correlation elastography refers to the construction of elasticity maps in soft solids based on the measurement of a shear wave-field without control of the wave sources [1]. This method has demonstrated its relevance in situations where coherent shear wave tracking is unfeasible due to the interference of scattered waves from tissue irregularities, waves generated by muscle activity, heartbeats, or external vibrations [2]. Another remarkable aspect of the passive method is how well it works with acquisition systems that operate at low frame rates [3]. The underlying physics of noise correlation requires an interpretation based on a Time Reversal (TR) interpretation of the method [4]. Under the conditions of a reverberant and/or multi-diffuse wave-field, TR is an efficient way to focus waves in a target point. Passive methods, also called noise correlation, have shown that it is possible to numerically calculate a refocusing without controlling the sources.

**Aims:** Demonstrate the equivalence between noise-correlation and TR for elasticity mapping by comparing images derived from Active and Passive refocusing.

**Methods:** Six surface transducers are placed on an agar-gelatin phantom's surface. The impulse responses are captured across a 65x31mm region of interest using ultrasonic speckle tracking. These wave-fields are utilized to (1) calculate passive refocusing and (2) determine active R refocusing. We introduce a wave equation inversion method to extract the shear wave speed from both active and passive refocusing.

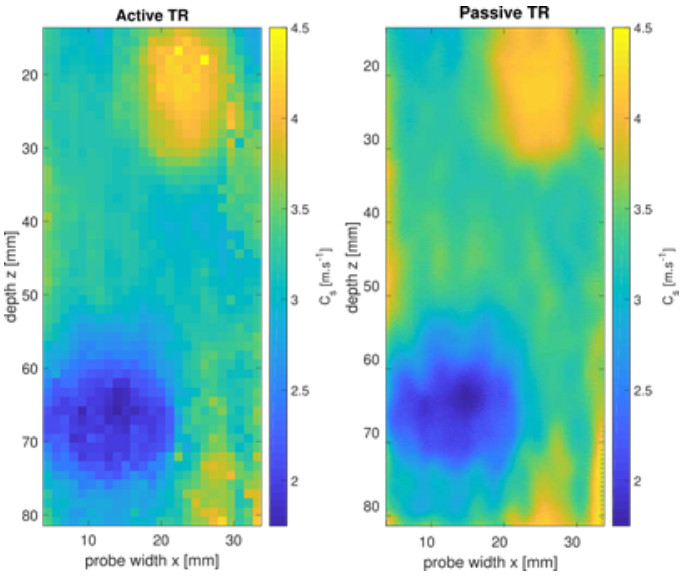


*Figure 1 : Active and passive refocusing wave-fields lead to highly comparable shear wave-speed maps. The resolution gap highlights a challenge of the active method, which demands an extended acquisition time.*

**Results:** The robustness of the spatial and time reciprocity yields to very similar results for the active and passive case (see Figure 1). We describe the differences and explain their origins.

**Conclusions:** A Time Reversal experimental configuration enables the focusing of waves at any desired point within a soft solid. Moreover, the refocusing field can be digitally calculated through noise correlation. A wave equation inversion reveals consistency between active and passive shear wave speed imaging.

**Acknowledgments:** Grupo CSIC 2022 "Ciencias Planetarias y geofísica"

**References:**

[1] Gallot T, et. al. Passive elastography: shear-wave tomography from physiological-noise correlation in soft tissues. IEEE Trans Ultrason Ferroelectr Freq Control (2011) 58:1122–6. doi:10.1109/TUFFC.2011.1920

[2] Brum et.al. Shear Wave Elastography Based on Noise Correlation and Time Reversal, Frontiers in Physics 2021.

[3] Catheline et.al. Tomography from diffuse waves: passive shear wave imaging using low frame rate scanners. Appl Phys Lett (2013) 103:014101. doi:10.1063/1.4812515

[4] A. Derode, et al. "How to estimate the Green's function of a heterogeneous medium between two passive sensors? Application to acoustic wave," Appl. Phys. Lett., vol. 83, no. 15, pp. 3054–3056, 2003.

# IN VIVO AND IN VITRO 3D QUANTIFICATION OF NATURAL WAVE VELOCITY IN THE HUMAN HEART

*J Hanrard*[1,*], *O Pedreira*[1], *T Meki*[1], *J Reydet*[1], *M Tanter*[1], *E Messas*[2], *C Papadacci*[1], *M Pernot*[1]

[1]Physics for Medicine, Paris, Ile-de-France, France; 2Hôpital Européen Georges-Pompidou, Paris, Ile-de-France, France

**Background:** Assessing the velocity of mechanical waves in the myocardium induced by natural events such as valve closures is of major interest for the diagnosis of cardiac disease. The current velocity estimation relies on 2D ultrafast imaging with a cardiac phased-array probe [1]. However, recent studies using 3D imaging have shown that the propagation of mechanical waves in the myocardium is complex and cannot be assumed as a 2D propagation [2]. 3D ultrafast imaging requires complex and costly systems with a matrix transducer composed of thousands of elements which limits the clinical translation.
**Aims:** We propose a 3D ultrafast imaging approach based on a 128 element probe suitable with conventional research systems and we developed a robust assessment method to quantify the velocity of natural waves in 3D.

**Methods:** A 2.5MHz matrix transducer (Vermon, France) composed of 128 elements was designed and connected to a vantage system (Verasonics, USA) to perform 3D transthoracic ultrafast imaging with diverging wave emissions in a volume of 63cm3. Beamforming, axial tissue velocity and acceleration estimations were performed in the 3D volume. Time windows of 40ms containing respectively the mitral valve closure (MVC) and the aortic valve closure (AVC) were selected based on the ECG and acceleration curve. Time of flight of the mechanical waves were computed and an inversion algorithm of the 3D wave propagation was solved numerically to quantify the 3D velocity components. The approach was validated experimentally in a human heart phantom where a mechanical wave of 60Hz was generated using a vibrator. Acquisitions were also performed using a 2D cardiac phased array probe (SSI, France) to compare our method. We demonstrated the clinical feasibility in 4 healthy volunteers.

**Results:** The 3D velocity components Cx, Cy and Cz were successfully measured in the phantom. A velocity of 2.24 +/- 0.09 m/s was estimated versus 2.15 +/- 0.07 m/s measured using the 2D cardiac phased array when set in the propagation direction. In vivo, the mean of the velocities of the MVC and AVC estimated for the 4 volunteers are respectively 3.37 m/s (STD =1.39) and 3.65 m/s (STD = 0.42). We also observed a significant difference in the propagation directions of both waves (angular difference of 16.7° +/- 4.2°).

**Conclusions:** We have shown that our method enables the 3D assessment of the velocity of natural waves induced by the AVC and MVC by 3D ultrafast imaging with a low channel count clinical device.
**Acknowledgments:** This study was supported by Ecole de l'Inserm-Pfizer Innovation (EIPI).

**References:**

[1] Petrescu A, Voigt J U, "Velocities of naturally occurring myocardial shear waves increase with age and in cardiac amyloidosis", JACC: Cardiovascular Imaging, 12(12), 2389-2398, 2019.
[2] Papadacci C, Pernot M, "4D ultrafast ultrasound imaging of naturally occuring shear waves in the human heart", IEEE Transactions on Medical Imaging, 39(12), 4436-4444, 2020.

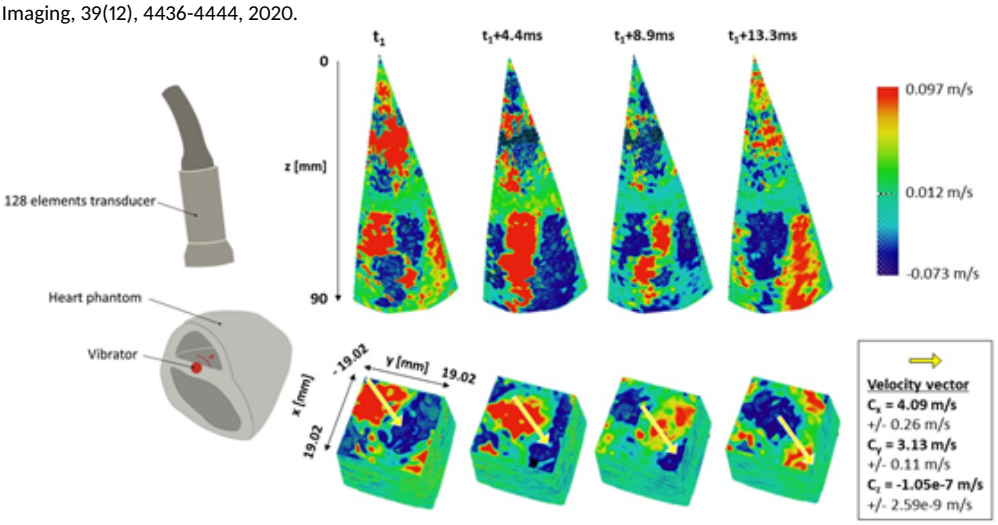

# HOW TO EXTRACT SHEAR WAVE SPEED AND ATTENUATION FROM A DIFFUSE WAVE FIELD?

*B. Giammarinaro*[1,*], *G. Laloy-Borgna*[1], *J. Aichele*[2], *S. Grégoire*[1], *J. Zhu* [1], *S. Catheline* [1]

[1]LabTAU, INSERM, Centre Léon Bérard, Université Claude Bernard Lyon 1, F-69003, LYON, France;
[2]Department of Earth Sciences, Institute of Geophysics, Swiss Federal Institute of Technology, Zürich, Switzerland

**Background:** Estimating the elasticity and the viscosity is a major concern for diagnosis. These parameters represent important biomarkers for tumor detection. Standard approaches are based on active generation of shear waves, either by external source or acoustic radiation force. However, the human body is full of natural waves. These waves propagate in every direction as diffuse wave fields which can be used for elasticity estimation using passive elastography algorithms [1]. These techniques are based on the assumption of far-field sources for a purely elastic medium, neglecting the effect and thus the possibility to directly estimate the attenuation. However, the feasibility of retrieving the attenuation has been demonstrated in seismology with noise correlation techniques on diffuse wave field generated by volumetric distribution of sources, distribution of sources directly present in the medium to characterize [2].

**Aims:** Our objective is therefore to adapt a first method of characterization of the viscoelastic parameters in soft solids using noise correlation techniques, or passive elastography.

**Methods:** The study uses configuration to mimic diffuse fields generated with volumetric source distribution. The first corresponds to experiments using bi-layered Agar gel phantoms containing iron oxide magnetic particles stimulated using a transient magnetic field. Shear waves are generated in the whole volume. They are detected using high framerate ultrasound scanner Vantage 256 (Verasonics, Kirkland, USA). Imaging sequences use plane wave compounding to reach a framerate of 2000fps. Shear waves displacement are then estimated using Loupas phase-based motion estimators. Results are then compared with numerical simulations mimicking the experiments using k-Wave, a toolbox functioning with Matlab 2022a.

**Results:** Characterization approaches using spatial correlation have been applied in gel phantom and numerical experiments, allowing to discriminate the viscoelastic parameters of each layer.

**Conclusions:** To conclude, we propose a method which could allow estimating viscoelastic parameters using ambient noise. A first application concerns the experimental configuration which could be adapted to create an imaging device. Moreover, assumptions have to be refined with more studies about the necessary conditions, each one being also considered in case of in vivo applications with natural waves.

**Acknowledgments:** With financial support from ITMO Cancer of Aviesan within the framework of the 2021-2030 Cancer Control Strategy, on funds administered by Inserm.

**References:**

[1] S. Catheline, R. Souchon, M. Rupin, J. Brum, A. H. Dinh, et J.-Y. Chapelon, « Tomography from diffuse waves: Passive shear wave imaging using low frame rate scanners », Appl. Phys. Lett., vol. 103, no 1, 2013, doi: 10.1063/1.4812515.
[2] G. A. Prieto, J. F. Lawrence, et G. C. Beroza, « Anelastic Earth structure from the coherency of the ambient seismic field », J Geophy Res, vol. 114, no B07303, 2009, doi: 10.1029/2008JB006067.

# NOISE CORRELATION INSPIRED METHOD : AN APPROACH FOR MULTIMODAL IMAGING ELASTOGRAPHY

*N. Dufour*[1,*], *M. Legrand*[1], *E. Martins Seromenho*[1], *JL. Gennisson*[2], *S. Chatelin*[1], *A. Nahas*[1]

[1]University of Strasbourg, CNRS, Inserm, ICube, UMR 7357, Strasbourg, France; [2]BioMaps, University Paris-Saclay, CEA, CNRS UMR 9011, INSERM UMR 1281, Orsay, France.

**Background:** Mechanical properties of a biological tissue, such as the stiffness, can be affected by numerous diseases. Physicians usually perform palpation to detect those changes and establish their diagnosis. This method can quickly meet its limits as the assessment is only qualitative and not possible on all tissue. Elastography was developed to overcome those limitations and proved its clinical usefulness with MRI and US imaging methods. Since the introduction of elastography to OCT, those methods have been adapted to optical setups. Here, we focus on shear wave elastography (SWE), that is based on the generation, encoding and interpretation of shear wave propagation in a tissue to investigate the tissue stiffness.
**Aims:** In classical elastography, an external excitation of the tissue is necessary to propagate shear waves. Different types of excitation can be used. In the case of harmonic excitation, the stiffness can be estimated using Local Frequency Estimation. Alternatively, the tissue can be excited by radiation force creating a pulse and the shear wave celerity is assessed using Time Of Flight. It also is possible to perform SWE without any external excitation source by the use of noise correlation elastography. Inspired by seismology, this method allows to retrieve the tissue stiffness from a diffuse wave field [1]. We propose here a high-resolution and robust-to-noise method for reconstruction from any type of shear wave propagation : the noise correlation inspired (NCi) method.
**Methods:** Considering a noise field in an isotropic medium, the correlation between a point and its neighbors results in a refocalisation spot, as shown in Figure 1.c. From this refocalisation spot, the local mean wavelength is extracted and by the way the local shear wave celerity and stiffness. The refocalisation spot in an anisotropic medium (fibrous tissues such as muscular ones) reflects the mechanical anisotropic mechanical behavior. Initially developed for isotropic media, noise correlation has been validated to measure in-plane mechanical anisotropy [2]. Inspired from these results for anisotropic medium, the method has been generalized to partially coherent mechanical wave field, such as harmonic wave and pulse. As shown in Figure 1, the wave propagation can also be refocused and therefore the wavelength measured. Datas were acquired using commercial MRI and US systems.

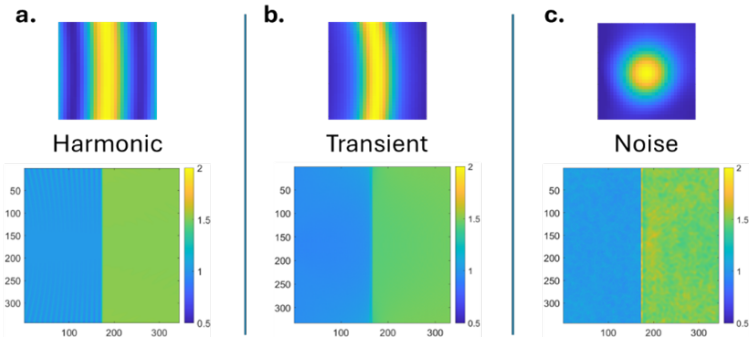


Figure 1: Results on simulations and example of refocused spot for different source type. a., b. and c. respectfully corresponds to harmonic, transient and noise field.

**Results:** The method was tested on 2D finite difference simulations made of 350 by 350 pixels over 500 frames for different excitation type as shown in Fig.1. Simulated celerities are 1 m.s-1 on the left side and 1.5 m.s-1 on the right side. On Fig.1, the simulated values were retrieved with a low error : 1.02 m.s-1, 1.03 m.s-1 and 1.03 m.s-1 for the left side and 1.51 m.s-1, 1.49 m.s-1 and 1.49 m.s-1 for the right side. These results validates the NCi method. Very promising results were obtained on simulations with added noise at a SNR of 0.1.
**Conclusions:** NCi method was validated on simulations for different excitation types, with or without noise. Experimental acquisitions are currently made in order to test the method on commercial devices. First results are promising and will be presented.

**References:**

[1] S. Catheline, et al., Phys. Rev. Lett., 2008, doi: 10.1103/PhysRevLett.100.064301.
[2] A. Marmin, et al., Biomed. Opt. Express, 2024, doi: 10.1364/BOE.516166.

# NON LINEAR STORAGE MODULUS QUANTIFICATION WITH MR ELASTOGRAPHY: FROM IN VITRO TO IN VIVO

*G Pagé[1,2,*], P Garteiser[3], BE Van Beers[3], JL Gennisson[2]*

[1]Université Paris Saclay, CNRS, CEA, NeuroSpin/BAOBAB, Gif-sur-Yvette, France; [2]Université Paris Saclay, CNRS, Inserm, BioMaps, Orsay, France; 2Laboratory of Imaging Biomarkers, [3]Center for Research on Inflammation, Université Paris Cité, UMR 1149 Inserm, Paris, France

**Background:** Assessing simple mechanical parameters, such as shear, storage and loss moduli with ultrasound (US) or magnetic resonance (MR) elastography, has been shown to be useful for diagnosing various fibro-inflammatory diseases and cancer [1, 2]. However, evaluating nonlinear elasticity may improve tumor characterization [3, 4]. In US-elastography, the acoustoelasticity approach enables to determine the nonlinear coefficient of the shear modulus (A) [5]. A first approach shows the feasibility of the method in clinical MR-elastography [6].
**Aims:** The purpose of this study is to develop a preclinical method for assessing the nonlinear coefficient with MR-elastography and show its interest in cancer investigation.

**Methods:** According to the acoustoelasticity theory, the experiment involves measuring the storage modulus of a medium subjected to a uniaxial stress from a shear wave propagating in a specific direction. Under these conditions, we applied the equations developed by Gennisson et al. [5] to estimate the nonlinear coefficient in three configurations of shear wave displacement. We performed MRI in two homogeneous phantoms containing 1% and 1.5% agar concentrations (AGAR_1 and AGAR_2) and in seven mice with patient-derived cholangiocarcinomas implanted in the right flank. We developed a specific compression setup to uniaxially compress a phantom or small animal inside the MRI tunnel. MRI of the phantoms and mice was performed in a 7T MRI scanner (Pharmascan, Bruker, Ettlingen, Germany). MR-elastography was obtained using 300 Hz mechanical vibrations synchronized with a modified spin-echo sequence. T2-weighted MRI was performed with the same spatial resolution as MR-elastography. The morphological T2-weighted images and the functional MR-elastography images were acquired without compression and were repeated after compression steps of 0.5 mm. To obtain storage modulus maps according to the equations developed in [5], a spatio-temporal filter was applied along the direction selected according to the configuration chosen. Phantom deformation ($\epsilon$) maps were calculated by performing 3D affine registration on the T2 images. Stress ($\sigma$) was calculated with the Hooke law, as $\sigma = 3G'\epsilon$. The slope between the storage modulus for each propagation axis and the applied stress was estimated and the nonlinear coefficient A was computed. The results of MR-elastography linear and nonlinear coefficient in mice were compared to those of collagen fraction and entropy (a marker of collagen distribution irregularity), obtained on picrosirius red stained histological tumor slices [7].

**Results:** The dependence of the storage moduli to uniaxial stress in agar phantoms are shown in Fig. 1. Similar nonlinear coefficients were obtained, independently of the chosen configuration (Fig 1.c). In contrast to A, G' was significantly correlated to collagen density (G': r = 0.85, p = 0.02; A: r = 0.23, p = 0.61). However, a significative correlation was observed between A and the entropy (G': r = 0.43, p = 0.33; A: r = 0.84, p = 0.02), suggesting that nonlinear coefficient may help characterizing tissue structure.
**Conclusions:** The results of our study show the feasibility of measuring in vitro and in vivo nonlinear storage modulus with MR-elastography and the interest of the technique to characterize tumor tissue.
**Acknowledgments:** This work was partly funded by France Life Imaging, projet Quantum (grant ANR-11-INBS-0006).
**References:**
[1]. Deffieux T. et al. J. Hepatology (2015). [2] Pagé G. et al. Frontiers in Phys (2022). [3] Kim et al. Acta Radiologica (2015). [4] Bernal M. et al. IEEE Trans Ultrason Ferroelectr Freq 2015). [5] Gennisson J.L. et al. JASA (2007). [6] Pagé G. et al. PMB (2023). [7]. Li et al. Zormpas-Petridis et al. Cancer Reseach (2019)

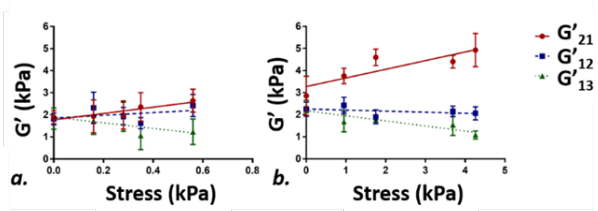


c.

| Phantom | $G'_0$ (kPa) | $A_{12}$ (kPa) | $A_{21}$ (kPa) | $A_{13}$ (kPa) | $A_{Mean}$ (kPa) |
|---|---|---|---|---|---|
| AGAR_1 | 1.8 ± 0.1 | -34.0 | -34.8 | -25.3 | -31.3 ± 5.3 |
| AGAR_2 | 2.5 ± 0.3 | -13.7 | -23.7 | -17.1 | -17.1 ± 5.1 |

*Fig. 1. Storage modulus (G') according to applied uniaxial stress for each propagation in AGAR phantom AGAR_1 (a.) and AGAR_2(b.). Slope is obtained by linear regression. Table c. shows G' without compression and nonlinear coefficient in each configuration.*

# AN OPTICAL RHEOMETRY USING SHEAR WAVE EXCITATION THROUGH NON-SPHERICAL BUBBLE COLLAPSE

*S Ghasemian*[1,2], *Y Fan*[1,2,*], *F Reuter*[1], *C D Ohl*[1,2]

[1]Institute of Physics, Otto-von-Guericke Universität, Magdeburg, Saxony-Anhalt, Germany; [2]Research Campus STIMULATE, Otto-von-Guericke Universität, Magdeburg, Saxony-Anhalt, Germany.

**Background:** Hydrogels are one of the most common tissue phantom materials, but the characterization of elastic modulus of hydrogels at high strain-rates is an experimental challenge, as their mechanical properties could be inhomogeneous and strain-rate dependent [1]. While the ultrasound elastography is very well developed, the hydrogels for physical research need to be optical transparent, which causes seeding with acoustic scatterers to become problematic. During our studies of non-spherical cavitation bubble dynamics in gels we noticed that the cavitation itself is a strong shear source [2].
**Aims:** Developing a shear wave based rheometry in hydrogels that utilizes single cavitation bubbles.
**Methods:** A cavitation bubble is generated in gelatin hydrogel through optical breakdown using a pulsed laser (Litron Nano T-250-10; wavelength 1064 nm; pulse duration FWHM 7 ns) focused with a long working distance microscope close to a solid boundary. The bubble dynamics is recorded with a high-speed camera (Shimadzu XPV-X2) operated at 1 million fps equipped with a macro lens (LAOWA f2.8) with its magnification set to 10$\mu$m per pixel. Gelatin is prepared from powdered gelatin (Gelatin 250 bloom, Yasin Gelatin Co. Ltd.). Narrowband illumination is provided by a continuous green laser (Shaan'xi Richeng Ltd, DPSS Green Dot Laser Module, wavelength 532nm). The gelatin gel becomes doubly refractive under stress. Thus, to visualize the material stresses during the cavitation bubble dynamics, the sample is contained within a circular polariscope. It is built from two linear polarizers with their polarization direction oriented under 90° to each other and two $\lambda/4$ waveplates with their fast axis also under 90° to each other. The intensity of the light exiting the second linear polarizer is a function of the retardation $\delta$, which is directly proportional to the differences in the principal stresses, and the incident light intensity. The shear wave is observed with a high-speed camera at moderate framing rates of 50,000 frame/s (Photron AX-Mini 200).
**Results:** The dynamics of a single bubble in proximity to a rigid boundary is presented in Fig.1 (a). Fig.1(b) presents a typical photoelasticity measurement for a laser induced cavitation bubble at unchanged experimental conditions from Fig.1(a). The shear wave is excited during the violent deformation of the hydrogel by the cavitation bubble. Shear wave propagation over a longer time period is presented in Fig. 2, which corresponds to the red marked area in Fig.1 (b). The speed of the shear wave is 3.4m/s.
**Conclusions:** Non-spherical cavitation bubble dynamics can excite shear waves. By observing the shear wave with the circular polariscope, the local elastic modulus can be measured spatially and temporally resolved.
**Acknowledgments:** We acknowledge funding from the German Federal Ministry of Education and Research (Research Campus STIMULATE No. 13GW0473A) and the German Science Foundation DFG (ME 1645/12-1).

**References:**

[1] J. B. Estrada, C. Barajas, D. L. Henann, E. Johnsen, and C. Franck, "High strain-rate soft material characterization via inertial cavitation," Journal of the Mechanics and Physics of Solids 112, 291–317 (2018).
[2] Ghasemian S I, Reuter F, Fan Y, et al. Shear wave generation from non-spherical bubble collapse in a tissue phantom[J]. Soft Matter, 2023, 19(48): 9405-9412.

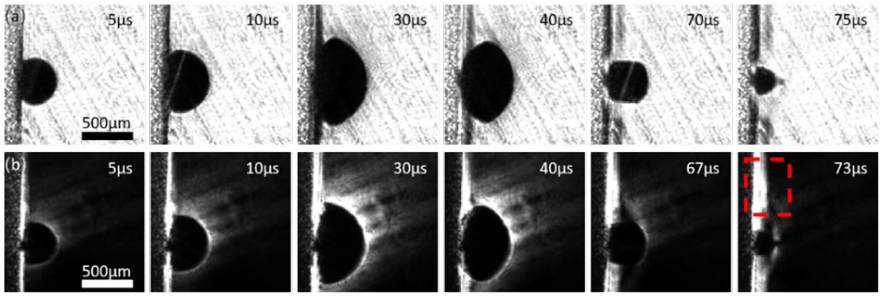


Figure 1 (a) Selected shadowgraphy frames (a) and photoelastic frames (b) of the dynamics of a laser induced cavitation bubble nucleated in gelatin gel recorded at 1,000,000 fps.

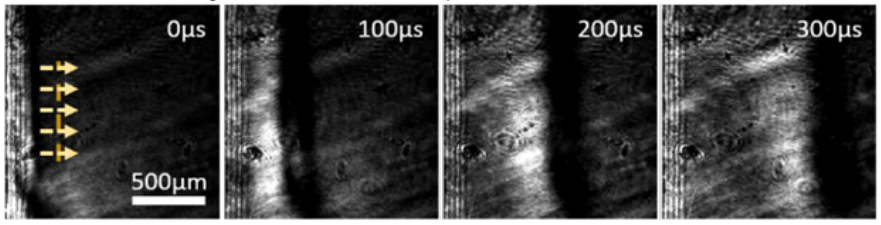


Figure 2 (a) Shear wave propagation visualized by high-speed circular polariscope for gelatin gel.

# IN VIVO STUDY OF THE IMPACT OF ULTRASONIC INERTIAL CAVITATION ON THE STIFFNESS OF PANCREATIC TUMORS IN MURINE MODEL

*A Rohfritsch*[1,*], *M Lafond*[1], *A Drainville*[1], *B Giammarinaro*[1], *G Bibaki*[2], *S Urro*[2], *G Renault*[2], *B Beye*[2], *F Prat*[2], *S Catheline*[1], *C Lafon*[1]

[1]LabTAU, INSERM, Centre Léon Berard, Université Lyon 1, Univ Lyon, F-69003, LYON, FRANCE; [2]Life Imaging Facility, University of Paris, PIV Platform, Institut Cochin, Paris, FRANCE

**Background:** Pancreatic ductal adenocarcinoma (PDAC) is one of the fastest-growing cancers that is likely to become the second cause of death by cancer in the world by 2030. Among emerging therapeutic strategies, ultrasound induced inertial cavitation (IC) is a promising tool to help treating patients with unresectable tumor. However, physical impact of IC on tumor remains unclear.
**Aims:** Here, we study orthotopic murine models of pancreatic cancer and measure elasticity, before and after applying IC on the whole tumor volume, using passive elastography.
**Methods:** The device used to generate and maintain cavitation is composed of two focused confocal transducers (center frequency, 1.1 MHz). An ultrasonic imaging probe is used to visualize cavitation clouds during the treatment and a second probe to perform passive elastography before and after the treatment. Elasticity maps and average tumor elasticity changes are reported.
**Results:** Eighteen mice have been treated. Before IC treatment, no correlation is seen between tumor stiffness and tumor volume. However, we report significant modifications of tumor stiffness after IC treatment, that strongly depends on tumor volume. A significant softening is observed for the group with larger tumor volume (> 800mm$^3$, n=9, see Figure (A-B) below). On the other side, the smaller tumors (< 800mm3, n=9, Figure C-D), are stiffer after IC treatment ($p<0.05$).
**Conclusions:** Our study shows for the first time that IC impact on tumor stiffness depends on tumor volume. This strong result has to be linked with the quantification of the development of collagen fibers network inside the extra-cellular matrix. Altogether, these results will help understanding IC impact on tumor micro-environment and bring new major elements of thought for a better predictability of stiffness changes induced by IC.

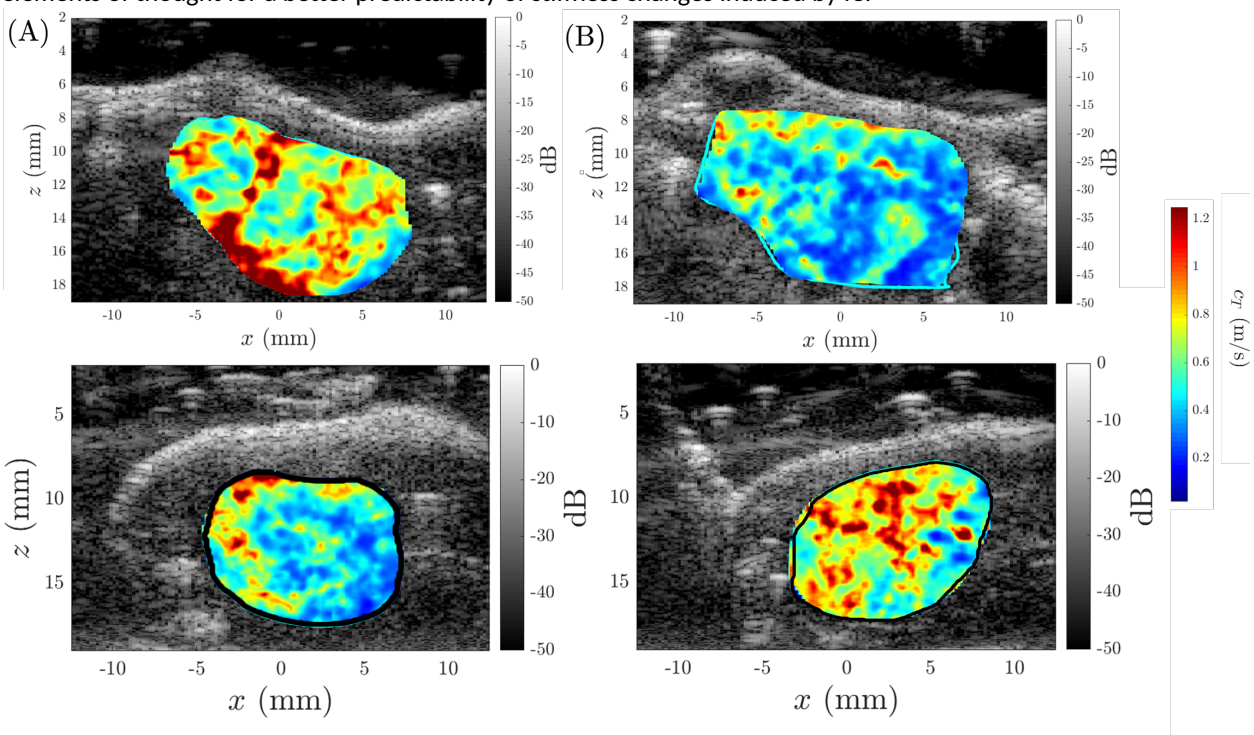


*Figure : Shear wave speed maps inside two pancreatic tumors, (A, C) before and (B, D) after inertial cavitation (IC) treatment. Tumor volume is 965 mm$^3$ at the day of treatment for (A, B) and 501mm3 at the day of treatment for (C, D).*

# NONLINEAR ELASTIC PARAMETER RESPONSIBLE FOR SHEAR SHOCK FORMATION IN BRAIN

*Bharat B Tripathi*

University of Galway, School of Mathematical & Statistical Sciences, University Road, Galway, H91TK33 IRELAND

**Background:** Recent observations of shear shock waves in ex vivo porcine brain [1] suggest that shock formation deep inside the brain could be the primary mechanism behind many types of traumatic brain injury, especially diffuse axonal injury. These observations were performed with a custom high-frame rate ultrasound imaging (≈6200 frames/sec) [1, 2] of planar propagation of linearly polarized shear waves.
**Aims:** Current biomechanical models of TBI do not include this recently observed shock wave physics. To model and predict the shear shock wave formation in the brain, the nonlinear elastic parameter, $\beta$, has to be estimated.
**Methods:** Here, $\beta$ is estimated using ultrasound-based measurements of brain motion [1] and recently developed theoretical/numerical models capable of simulating the nonlinear propagation of linearly polarized shear waves in relaxing soft solids [3, 4]. This deterministic solver [3] was coupled with the Metropolis Markov chain Monte Carlo simulation algorithm to generate the probability density function for the nonlinear parameter $\beta$ in brain.
**Results:** The magnitude of the third-harmonic component of the particle velocity as a function of distance was taken as the optimization variable, with all other physical parameters as constants. With an attenuation power law of: $0.06\omega^{1}.05$, where $\omega$ is the angular frequency, and the reference shear speed is 2.10 m/s at 75 Hz, the estimate, $\beta$ = 44.24±8.23 was obtained.
**Conclusions:** This $\beta$estimate can model realistic shear shock wave physics in simulations that can be used in the analysis of injury and the design of protective equipment.

**References:**
[1] D. Espindola, S. Lee, and G. Pinton. Shear shock waves observed in the brain. Physical Review Applied, 8(4):044024, 2017.
[2] G. Pinton, J. L. Gennisson, M. Tanter, and F. Coulouvrat. Adaptive motion estimation of shear shock waves in soft solids and tissue with ultrasound. IEEE Transactions on Ultrasonics, Ferroelectrics, and Frequency Control, 61(9):1489–1503, 2014.
[3] B. B. Tripathi, D. Esp´ındola, and G. F. Pinton. Piecewise Parabolic Method for Propagation of Shear Shock Waves in Relaxing Soft Solids: One Dimensional Case. Int. J. Num. Meth. Bio. Med. Eng., 35(5):e3187, March 2019.
[4] B. B. Tripathi, D. Esp´ındola, and G. F. Pinton. Modeling and Simulations of Two-Dimensional Propagation of Shear Shock Waves in Relaxing Soft Solids. J. Comput. Phys., 395:205–222, October 2019

# BUBBLE-INDUCED SHEAR WAVE IN A SINGLE CELL

*G Laloy-Borgna, G Regnault, S Grégoire, C Inserra, S Catheline*

LabTAU, INSERM, Centre Léon Bérard, Université Claude Bernard Lyon 1, F-69003, LYON, France

**Background, Motivation and Objective:**
Single-cell microelastography has been demonstrated recently in oocyte using a microscope (x100) and an ultrafast camera. Elastic waves were generated using vibrating micro-pipettes in contact with the wall cell. From thousands of images captured at hundreds of kHz, the elastic wave field was estimated and then used through passive elastography algorithms to construct a velocity map. These maps are crucial to better understand the mechanical behavior of cells.

**Methods:**
In this work, two important novelties are reported: first the novel approach concerns a megakaryocyte cell, around four times smaller than oocyte cells and second, the method is contactless. Based on bubble-oscillations in the neighborhood of a megakaryocyte cell, the induced elastic waves in the range of 15kHz, are free of any rigid boundaries as opposed to micropipette use.

**Results and Discussion:**
Elastic wave propagation is observed and allows as in figure 1, to give a velocity map in relation to elasticity. The limit of mechanical characterization is thus pushed back in object as tiny as 20$\mu$m. Microelastography thus becomes a useful quantitative technique in the field of common cell mechanics. The bubble vibration is controlled with ultrasound (30kHz) and Faraday's mode at half the driving frequency are carefully studied.

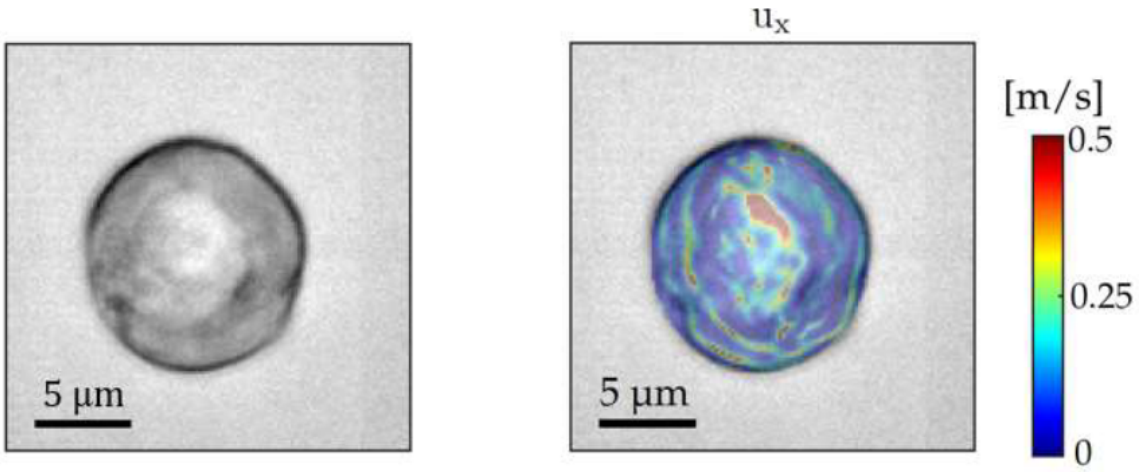


*Fig.1 Optical image of a megakaryocyte cell. Elastic wave velocity resulting from bubble-induced shear wave. The vertical component $u_x$ is used for the reconstruction map.*

# DEVELOPMENT OF HIGH FREQUENCY ULTRASOUND SHEAR WAVE ELASTOGRAPHY FOR PRECLINICAL LIVER INVESTIGATION: A PILOT STUDY ON OGT MODEL.

*G Renault*[1], *L Chichilla*[2], *P Monbernard*[1], *L Massengo*[1], *F Benhamed*[1], *M Regnier*[1], *C Postic*[1], *A. Novell*[2], *JL Gennisson*[2,*]

[1]Université Paris-Cité, CNRS, Inserm, Institut Cochin, Paris, France; [2]Université Paris-Saclay, CNRS, Inserm, BioMaps, Orsay, France.

**Background:** Measurement of stiffness in preclinical models is a key parameter to study tumor stoma development of liver pathologies, but in ultrasound (US) is still limited to dedicated clinical or research programmable scanners. Both systems do provide such information, but make it necessary to use a high-resolution US scanner for conventional preclinical measurements and then switch to a dedicated machine for elasticity measurement with poorer image resolution or specific methodological developments. Such limitations impair the use of shear wave elastography (SWE) imaging in preclinical studies when follow-up of large animal cohorts is needed.

**Aims:** Here we proposed an integrated solution combining conventional high-resolution imaging modes together with SWE imaging mode.

**Methods:** *In vivo* experiments were carried out on a genetic mouse model of spontaneous liver fibrosis induced by constitutive hepatocyte-specific deletion of the gene coding for O-GlcNAc transferase (OGTLKO), or its littermate as control. The study was approved by the ethical board of our institution. This model shows a progressive fibrosis initiated as early as 4 weeks with a maximum extent at 7-8 weeks, as documented by immunohistology. SWE non-invasive follow-up was performed during this time course and end point histologic analysis was performed to correlate with SWE findings. For SWE assessments, experiments were conducted on an ultrafast high frequency ultrasound scanner (VevoF2, Fujifilm Visualsonics) driving a high frequency ultrasound transducer array (UHF29x). The sequences were modified trough the VADA option available on the VevoF2. The sequence was composed of two steps [1]: 1/ A pushing beam that generate shear waves, a focusing beam at 16 MHz, 1000 cycles consecutively at three different depth (6, 8 and 10 mm). 2/ An ultrafast plane wave compounded imaging sequence with 5 angles (-5°, -3°, 0, 3°, 5°), providing a movie of 40 frames of the propagating shear waves with 1 kHz repetition frequency. After beamforming of raw data and time of flight computation on the shear wave movie, a shear modulus map of the liver was quantified. Measurements were confronted to those obtained using a reference SWE ultrasound imaging device considered as a gold standard (Aixplorer, Supersonic Imagine) driving a comparable central frequency transducer array (SHL20-6).

**Results:** Our results show that OGTLKO mice present, as expected, a progressive increase in liver stiffness from weeks 4 to weeks 7 (Aixplorer: from 2.32±0.71 kPa to 3.39±1.33 kPa and, VevoF2: from 2.24±0.87 kPa to 2.77±0.88 kPa (mean over all mice)). It also shows a variable stiffness increase from one mouse to another, reflecting the biological variability associated to the model. Confrontation of the shear modulus quantified with both devices shows a very good correlation (Pearson 0.94, p=5.8e-14). Confrontation with qPCR analysis of genes involved in inflammation and fibrosis confirmed increased levels in OGT KO mice. High resolution US images showed modifications of the liver structure with early detection and progressive development of regenerative nodules.

**Conclusions:** These results show that SWE measurement of stiffness can be integrated seamlessly in routine examination of mouse models of liver pathology together with high-resolution B mode images in a single preclinical ultrafast US device. This extends the range of measurable parameters in pre-clinical routine allowing non-invasive follow-up of large cohorts of mouse models of liver pathology.

**Acknowledgments:** Authors thanks gratefully the Visualsonics R&D team for their expert assistance

**References:**
[1] Bercoff et al., IEEE-UFFC (2004)

# AN ORIGINAL PIEZOELECTRIC ACTUATOR DESIGN WITH DEDICATED SEQUENCES FOR MOUSE MULTI-ORGAN MAGNETIC RESONANCE ELASTOGRAPHY (MRE) AT 7T

*Aude Loumeaud*[1,2,*], *Chrystelle Po*[1], *Benoît Wach*[1], *Sabine F Bensamoun*[2], *Gwenaël Pagé*[3], *Sabrina Doblas*[3], *Philippe Garteiser*[3], *Denis Grenier*[4], *Kevin Tse Ve Koon*[4], *Olivier Beuf*[4], *Pilar Sango-Solanas*[4], *Simon Chatelin*[1]

[1]University of Strasbourg, CNRS, Inserm, ICube UMR7357, 67000 Strasbourg, FRANCE; [2]Université de technologie de Compiègne, CNRS, BMBI, UMR 7338, 60203 Compiègne, FRANCE; [3]Center for Research on Inflammation, UMR Inserm 1149, Université Paris-Cité, ERL CNRS 8252, 75018 Paris, FRANCE; [4]INSA Lyon, Université Lyon 1, CNRS, Inserm, CREATIS UMR 5220, U1294, 69621 Villeurbanne, FRANCE

**Background:** MRE allows to non-invasively assess the in vivo mechanical response of soft tissues using 3 elements [1]: (A) Excitation: generation of shear waves; (B) Imaging: MRI encoding of the displacement; (C) Reconstruction: estimation of mechanical properties. Small animal MRE poses specific technical issues and only few teams have developed such a device using different approaches (electromechanical [2], piezoelectric [3] and electromagnetic [4]), mostly with a transmission bar synchronized with dedicated sequences (spin-echo SE [3] or gradient-echo [5]).
**Aims:** We propose an original solution for mouse 7T MRE based on a piezoelectric actuator with a small footprint enabling multiorgan MRE-assessment and associated with 2 sequences: an echo-planar imaging EPI and a turbo SE for rapidity and artefact robustness, respectively.

| | $f_0$ [Hz] | TR [ms] | TE [ms] | FOV [mm$^2$] | Matrix |
|---|---|---|---|---|---|
| EPI (gel) | 200-400 | 1000 | 36.64 | 30x30 | 64x64 |
| Turbo SE (gel) | 200-1000 | 1000 | 7.75-10.7 | 23x23 | 140x140 |
| Turbo SE (muscle) | 600-1200 | 1000 | 7.3-14 | 20x20 | 133x133 |

**Table 1.** Parameters for the MRE sequences (Bruker 7T MRI)

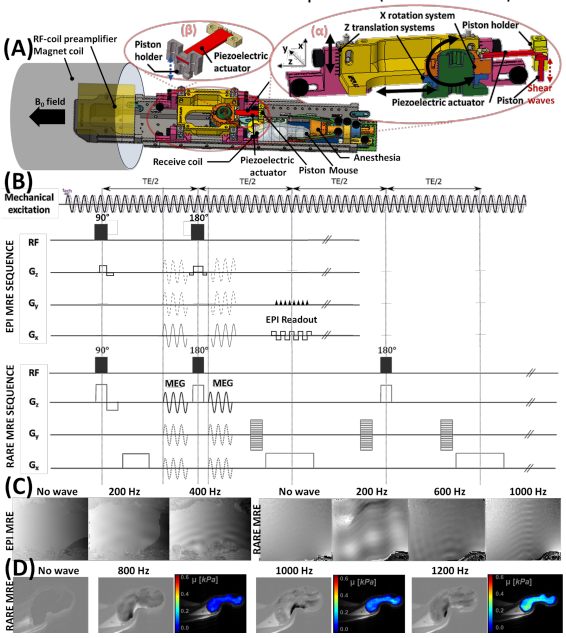


Fig 1. (A) Vibration setup: a piezoelectric bender adjustable by a 3D-printed positioning system ($\alpha$) with a piston ($\beta$). (B) Chronogram for the EPI and Turbo SE MRE sequences. Phase images in (C) phantom and (D) in vivo skeletal muscle elastograms using classical Local Frequency Estimator algorithm.

**Methods:** The vibration setup consists in 3 subassemblies (Fig 1A): a multilayer piezoelectric plate bender actuator powered by an amplified sinusoidal signal to generate the vibrations. Prior to acquisitions, bench tests were carried out to determine the frequency, amplitude and thermal properties of the actuator; a 3D-printed support ($\alpha$) to link the actuator to the animal bed, adaptable for a large set of organs; a piston ($\beta$) transmits actuator motions through a 3D printed system. A cross-coil configuration with a transmit volume coil and a 10mm surface coil was used. Motion Encoding Gradients were added between excitation and signal acquisition in 2 different MRI sequences: a single shot SE EPI sequence for fast acquisitions and a Turbo SE sequence for high resolution image and robustness to motion (Fig 1B). In the latter case, the generator was triggered at each TR to achieve steady-state wave propagation. Then, a phase-unwrapping algorithm was used on MRI phase images [6].

**Results:** Fig 1C-D shows phase images obtained on a 4% gelatin phantom and in vivo murine lower limb skeletal muscles, respectively. Resolutions of $\approx$500$\mu$m are achieved using the EPI sequence with acquisition times below 1s, allowing the study of kinetic evolutions. At the cost of acquisition time ($\approx$2min), the Turbo SE sequence enables better spatial resolution (150$\mu$m) and imaging organs prone to animal motion.

**Conclusions:** Thanks to this compact device with associated MRE sequences, emphasizing either speed or robustness to artefacts, we propose a powerful biomechanical tool adaptable to study many organs on mouse models.
**Acknowledgments:** This work was supported by France Life Imaging (ANR-11-INBS-0006), LabEx PRIMES (ANR-11-LABX-0063), ITI HealthTech (IdEx ANR-10-IDEX-0002, ANR-20-SFRI-0012).

**References:**

[1] Muthupillai et al Science 1995; [2] Tang et al JMRI 2022; [3] Clayton et al PMB 2011; [4] Riek et al NeuroImage Clin 2012; [5] Riek K et al J Biomech 2011; [6] Zhao et al Meas Sc & Tech 2018

# HIGH-FREQUENCY ELASTIC WAVE STIMULATION AND IMAGING OF WAVE DISPLACEMENTS IN MOUSE MACROPHAGES

*Hari S. Nair*[1,2,*], *Sajad Ghazavi*[1,2], *Guillaume Flé*[1,2], *Boris Chayer*[1], *Elijah E. W. Van Houten*[3], *Patrick Laplante*[4], *Jean-François Cailhier*[4,5], *Guy Cloutier*[1,2,6]

[1]Laboratory of Biorheology and Medical Ultrasonics, University of Montreal Hospital Research Center, Montreal, QC, Canada; [2]Institute of Biomedical Engineering, University of Montreal, Montreal, QC, Canada; [3]Department of Mechanical Engineering, University of Sherbrooke, Sherbrooke, QC, Canada; [4]University of Montreal Hospital Research Center, Montreal, QC, Canada; [5]Department of Medicine, University of Montreal, Montreal, QC, Canada; [6]Department of Radiology, Radio-Oncology and Nuclear Medicine, University of Montreal, Montreal,QC, Canada

**Background:** Macrophages are essential immune system cells that engulf foreign particles and debris. Understanding their mechanical properties in that process could offer new therapeutic targeting strategies. In our prior art, we have non-invasively assessed the mechanical properties of mouse oocytes ($\approx$ 80 $\mu$m diameter) with an actuation frequency close to 15 kHz [1], [2]. We observed wave fields with wavelengths close to the diameter of the oocytes [2]. In Laloy-Borgna et al., authors calculated a high-frequency cutoff limit of around 20 kHz for shear wave propagation in soft tissues with a viscosity approximately equal to the elasticity, and showed shear wave propagation up to 1 mm in phantoms [3]. Macrophages have a size of approximately 20 $\mu$m and may thus require a higher actuation frequency than oocytes for shear modulus reconstruction.
**Aims:** To develop a device and approach for inducing and tracking high-frequency ($\geq$ 20 kHz) elastic waves within individual macrophages, enabling the characterization of mechanical properties at the subcellular level.

**Methods:** The experimental setup utilizes a vibrating micropipette attached to a piezoelectric stack to generate vibrations at 10 to 60 kHz, significantly surpassing the previously reported maximum of 20 kHz [3]. The vibrations are then induced to RAW 264.7 mouse macrophages. The wave tracking is done by a high-speed camera (Photron Fastcam SA-Z) at 180000 fps or higher, thereby respecting the Nyquist-Shannon criteria. The Lagrangian speckle model estimator (LSME) algorithm estimates the displacement fields [4]. A window size of 20 × 20 pixel$^2$ with a 90% overlap was used for the calculation.

**Results:** Elastic waves at frequencies up to 40 kHz could be successfully induced and tracked within macrophages (Fig. a-d). Shorter wave length per cell size ratios were obtained at increasing frequencies, allowing for a more granular analysis of mechanical properties. Waves could propagate throughout the entire structure of the macrophages ($\approx$20 $\mu$m).
**Conclusions:** The ability to induce and track high-frequency waves within macrophages represents a significant advancement in the field of cellular optical micro-elastography (OME). By overcoming the upper-frequency limitations previously reported, our research opens new avenues for studying cellular mechanics at a sub-cellular level. Higher frequency waves will allow for detecting subtle mechanical variations within cells, which could be critical for understanding cellular behavior in different physiological and pathological conditions.

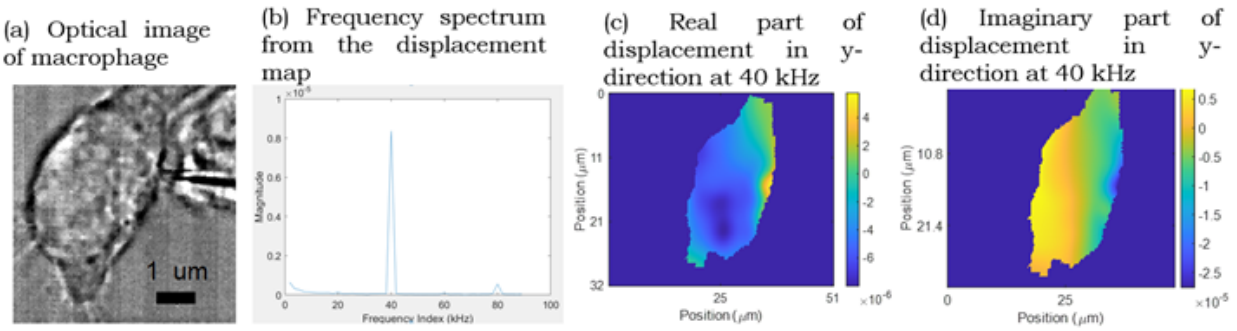


**Acknowledgments:** Scholarship from the TransMedTech Institute of Montreal; grant from the Canadian Institutes of Health Research (#497451-MPI-ADWY-22963).

**References:**

[1] Grasland-Mongrain, P., et al. 2018, Proc Natl Acad Sci USA, 115(5):861–6.
[2] Flé, G., et al. 2023, Proc Natl Acad Sci USA, 120(21), p.e2213836120.
[3] Laloy-Borgna, G. et al. 2021, Appl Phys Lett, 118(11).
[4] Poree, J. et al. 2015, IEEE Trans Med Imaging, 34(12).

# IMAGING THE ELECTROMECHANICAL PROPERTIES OF THE MOUSE BRAIN DURING TRANSCRANIAL ELECTRICAL STIMULATION: NUMERICAL SIMULATIONS

*G Flé*[1,*], *E Van Houten*[2], *G Gilbert*[3], *G Cloutier*[4]

[1]University Hospital Erlangen, Radiology Department, Erlangen, GERMANY; [2]University of Sherbrooke, Mechanical Engineering Department, Sherbrooke, Québec, CANADA; [3]MR Clinical Science, Philips Healthcare Canada, Mississauga, Ontario, CANADA; [4]Laboratory of Biorheology and Medical Ultrasonics, University of Montreal Hospital Research Center, Montréal, Québec, CANADA.

**Background:** Recent investigations into the biomechanics of the brain have unveiled alteration in tissue stiffness triggered by external stimuli. For instance, visual stimulation effects can be measured in elasticity images of the cortex generated by functional magnetic resonance elastography (MRE) [1]. Such a mechanical characterization method combined with non-invasive brain stimulation (NIBS), a technique that seeks to selectively modulate particular parts of the brain using weak electrical currents, has the potential to influence research on various neurological disorders [2].

**Aims:** In this in silico study, we aimed to elucidate individual and interdependent aspects related to a synchronized biomechanical imaging and non-invasive brain stimulation methodology [3]. Magnetic resonance electrical impedance tomography (MREIT) was incorporated to the pipeline, providing a promising way of evaluating NIBS-induced electrical current patterns in the brain while leveraging MRE and transcranial alternating current stimulation (tACS) experimental settings.

**Methods:** A mouse head model (Fig. 1.a) was assembled using open-access atlases to include five anatomical structures: skin/subcutaneous tissue, skull, cerebrospinal fluid (CSF), brain white and grey matters. MRE, tACS, and MREIT experiments were simulated using Comsol Multiphysics (Comsol Inc. Stockholm, Sweden) with Matlab Livelink (Matlab R2019b, The Mathworks, Massachusetts, United States). Synthetic MRE and MREIT data were processed using the subzone non-linear inversion and harmonic Bz algorithm, respectively, to reconstruct images of the distributed complex shear modulus and electrical conductivity [4,5].

**Results:** Lorentz body forces arising from simultaneous MRE and tACS elicited elastic waves of negligible amplitude compared with the extrinsic actuation levels reported in the literature (displacement component $u$ in Figs. 1.b and 1.c), which allowed accurate reconstructions of the complex shear modulus $\mu$ (Figs. 1.d and 1.e). Qualitative maps of the electrical conductivity $\sigma$ retrieved by MREIT accurately delineated anatomical regions of the brain model (Fig. 1.f) and could be used to recover reasonably accurate distributions of tACS-induced currents.

**Conclusions:** This multi-physics approach has potential for translation to human brain imaging and may provide more possibilities for the characterization of brain function together than in isolation.

**Acknowledgments:** This work was partially funded by the Natural Sciences and Engineering Research Council of Canada (#2022-03729 and Discovery #06660). We acknowledge the support by the Deutsche Forschungsgemeinschaft (DFG, German Research Foundation) project number 460333672–CRC 1540 Exploring Brain Mechanics (subproject Y).

**References:**

[1] Forouhandehpour R, Bernier M et al. Cerebral stiffness changes during visual stimulation: differential physiological mechanisms characterized by opposing mechanical effects. Neuroimage: Rep, 1:100014, 2021.
[2] Patz S, Fovargue D et al. Imaging localized neuronal activity at fast time scales through biomechanics. Sci Adv, 5:eaav3816, 2019.
[3] Flé G, Van Houten E et al. Simulation of a synchronized methodology for MR-based electromechanical property imaging during transcranial electrical stimulation. Front. Phys., 12:1324659, 2024.
[4] Hiscox L, McGarry M et al. Standard-space atlas of the viscoelastic properties of the human brain. Hum Brain Mapp, 41:5282–300, 2020.
[5] Seo JK and Eung JW, Magnetic resonance electrical impedance tomography (MREIT). SIAM review, 53.1:40-68, 2011.

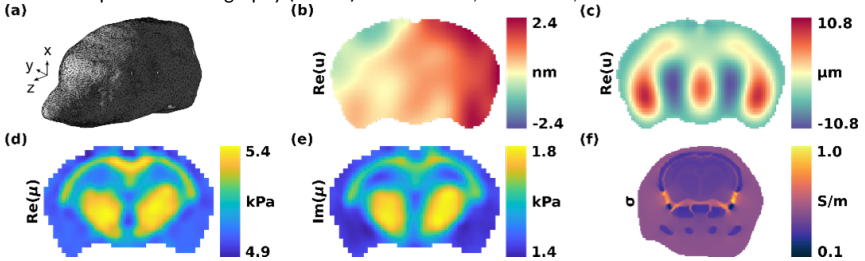


**Figure 1**: Mouse head model mesh **(a)**. Lorentz-force and Dirichlet boundary condition-induced displacements **(b-c)**. Reconstructions of the storage and loss moduli **(d-e)** and electrical conductivity **(f)**.

# FREE-BREATHING IN VIVO MAGNETIC RESONANCE ELASTOGRAPHY OF MOUSE LIVER: PROSPECTIVE VS RETROSPECTIVE SYNCHRONIZATION

*T Bakir Ageron**, *K Tse Ve Koon*, *P Sango-Solanas*, *O Beuf*.

INSA Lyon, Université Lyon 1, CNRS, Inserm, CREATIS UMR 5220, U1294, 69621 Villeurbanne, FRANCE

**Background:** Magnetic Resonance Elastography (MRE) is a recognized non-invasive technique used to measure tissue stiffness, particularly in cases of liver fibrosis[1], [2]. In clinical settings, MRE acquisitions are performed during the expiratory phase of apnea. However, apnea can be challenging for patients, leading to relatively high rates of technical errors thus hindering the development of MRE in clinical practice [3]. Free-breathing techniques [4] have recently been proposed as an alternative to apnea. In the preclinical field, MRE experiments are essential for developing new acquisition methods, such as optimal control MRE [5]. Effective MRE experiments in mice require precise synchronization with their rapid respiratory cycle. Integrating mouse respiration into MRE methods could improve clinical translation and reduce technical failures.

**Aims:** To compare the performance of a retrospective Intragate© (IG) Gradient Echo (IG FLASH MRE) and a prospective (a triggered FLASH MRE) free-breathing in vivo liver MRE acquisition on mouse.

**Methods:** Methods: One healthy female mouse (C57BL/6) was examined following ethical approval and adherence to institutional animal care guidelines. The mouse was anesthetized with 2% isoflurane in an air/oxygen mixture via a nasal cone and its respiratory rate and body temperature were monitored and maintained throughout the experiment. The FLASH MRE sequence is trigger-based, initiating data acquisition in real-time via an external sensor monitoring the animal's breathing cycle. This ensures consistent data acquisition at the desired phase of the respiratory cycle, thereby enhancing image quality and minimizing motion artifacts. The IG FLASH MRE sequence continuously acquires an oversampled k-space and retrospectively sorts the acquired data using the IG navigation signal provided by Bruker. This self-gated sequence results in an increased acquisition time (TA) due to the user-defined oversampling. MRE acquisitions were conducted using a 7T MRI system (Bruker, Germany), with a slice thickness of 1 mm and motion encoding in the slice direction, at frequency acquisitions of 300, 400 and 600Hz, with acquisition parameters detailed in Table 1. For each frequency, 4 equally distributed phase-steps were acquired. Subtraction of phase images and removal of static phase offsets were performed using 2 acquisitions with opposite MEG polarity. Displacement fields were obtained through unwrapping and Fourier transformed to isolate desired frequency information. Directional and spatial filtering techniques were applied for noise reduction. Finally, storage modulus G' maps, representing tissue elasticity, were extracted using the Algebraic Inversion of the Differential Equation (AIDE) algorithm [6].
**Results:** The magnitude, phase images, and elastograms (Figure 1) were analyzed and compared for all frequencies. *Table 1* shows the measured SNR and the mean and standard deviation of G' values in the ROI, placed within the same liver area. The SNR varies slightly with excitation frequency due to differences in TE/TR values, and is possibly also affected by the variability of the mouse's respiratory motions during acquisitions. The G' values were found to be similar regardless of the acquisition technique used.

**Conclusions:** The obtained results confirm the efficacy of our IG FLASH MRE method in assessing liver stiffness at multiple frequencies. Although the mean G' values are very close for both acquisition methods, IG FLASH MRE acquisitions exhibit lower standard deviations, which is an interesting outcome. Furthermore, multi-frequency acquisitions allowed to observe the dispersive behavior of mouse liver. In parallel, employing a retrospective respiratory synchronization acquisition method like IG FLASH MRE ensures dynamic equilibrium of the magnetization. SNR is satisfactory for both methods. The next step involves validating the IG FLASH MRE method by acquiring data from a cohort of mice and conducting test-retest experiments to evaluate the reproducibility of the developed method.

Table 1

| MRE Sequence | $F_{exc}$ (Hz) | TR (ms) | TE (ms) | Flip Angle (°) | Matrix (pix²) | FOV (mm²) | TA | G' (kPa) ± SD | SNR |
|---|---|---|---|---|---|---|---|---|---|
| FLASH | 300 | 120.16 | 5.82 | 22 | 128 x 128 | 35 x 35 | 2'30" | 2.1 ± 0.43 | 58.92 |
| | 400 | 121,01 | 4.99 | 22 | 128 x 128 | 35 x 35 | 2'30" | 2.47 ± 0.62 | 60.71 |
| | 600 | 78,16 | 5.82 | 22 | 128 x 128 | 35 x 35 | 1'35" | 5.06 ± 0.72 | 57.46 |
| IG FLASH | 300 | 85.34 | 4.82 | 22 | 96 x 96 | 35 x 35 | 7'55" | 2.1 ± 0.38 | 83.24 |
| | 400 | 67.01 | 3.99 | 22 | 96 x 96 | 35 x 35 | 6'20" | 2.33 ± 0.4 | 77.15 |
| | 600 | 50.51 | 4.82 | 22 | 96 x 96 | 35 x 35 | 5'05" | 4.95 ± 0.53 | 76.22 |

Figure 1

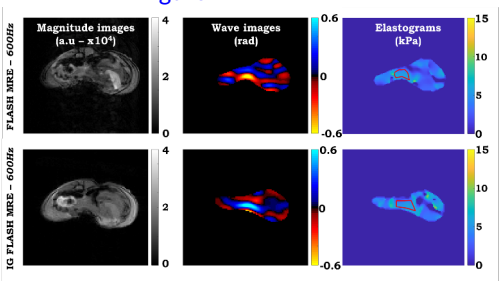


**Acknowledgments:** LABEX PRIMES (ANR 11 LBX 0063), PIONEER (ANR 22 CE19 0023 01), PILOT platform.

**References:**

[1] J. Chen et al., Alhocolism Clin & Exp Res, 2021, [2] S. Hoodeshenas et al., Top. MRI,2018, [3] SL Choi et al., Eur. Radiol, 2020, [4] M. Shahryari et al., MRM, 2021, [5] P. Sango-Solanas et al., Scientific Rep., 2022, [6] Oliphant et al., MRM, 2001

# List of Posters

# PARAMETERIZATION OF MULTI-FREQUENCY NON-LINEAR INVERSION RECONSTRUCTION ON IN VIVO MOUSE LIVER MAGNETIC RESONANCE ELASTOGRAPHY DATA

*P Sango-Solanas*[1,*], *T Bonnafy*[1], *T Bakir Ageron*[1], *O Beuf*[1], *E Van Houten*[2], *K Tse Ve Koon*[1]

[1]INSA Lyon, Université Lyon 1, CNRS, Inserm, CREATIS UMR 5220, U1294, 69621 Villeurbanne, FRANCE; [2]Department of Mechanical Engineering, Université de Sherbrooke, Sherbrooke, Quebec, CANADA.

**Background:** Magnetic resonance elastography (MRE) enables non-invasive quantitative assessment of the mechanical properties of tissues and has been successfully applied on clinical MR scanners for liver fibrosis staging [1]. Its application on preclinical MR scanners is also of interest for researchers with the availability of different animal models where MRE parameters, such as higher mechanical frequencies, have to be adapted with the standout feature being the smaller imaging volume. Multifrequency MRE [2] has been proposed for tissue characterization as a valuable tool enabling detection of tissue alterations occurring below the MR image resolutions through the measurement of the dispersion relationship of the shear storage modulus [3]. However, tackling multifrequency MRE data reconstruction is still an open question; the simplest approach being to apply mono-frequency reconstruction and analyzing the subsequent summation of the individual results. More evolved algorithms considering simultaneously all the individual harmonic data, such as the Non Linear Inversion (NLI) reconstruction method [4], have demonstrated their ability to better characterize the mechanical properties through brain MRE [5].
**Aims:** In this work, we seek to demonstrate the ability of the NLI reconstruction method to characterize in vivo mouse liver viscoelastic parameters.
**Methods:** One healthy female mouse (mean weight 25g) was examined after receiving ethical approval and adhering to institutional animal care guidelines. Multifrequency MRE acquisitions were carried out on a Bruker Biospec 7T MR scanner using a Turbo Spin Echo MRE sequence (turbo factor=4) developed inhouse [6]. Single frequency acquisitions at 400 and 600 Hz were run and 4 equally distributed phase-steps were acquired for each frequency. 2 acquisitions with opposite motion encoding gradient (MEG) polarity were completed, 3 orthogonal MEGs were applied and 5 contiguous slices (1mm) were acquired to obtain 3D wave field images. Complex MR images were extracted and processed to obtain magnitude and unwrapped phase images. Power-law ($\approx \theta f^{\alpha}$) NLI reconstruction minimizes a multi-frequency objective function combining the uniformly weighted displacement error at each measurement frequency using gradient descent algorithms based on the adjoint field. The multi-frequency displacement fields were collectively processed using NLI inversion, yielding $\theta$ and $\alpha$ maps that allow the calculation of shear storage (G') and loss (G") modulus across frequencies. Sensitivity to initialization parameters was evaluated via a convergence criteria so as to determine the optimal parameterization: $\alpha_0 = 0.15, 0.3, 0.4, 0.5, 0.7$, ($G'_0$,$G''_0$ )=(3,1),(5,2). Optimal NLI subzone size was found to be 5mm for the studied frequencies.

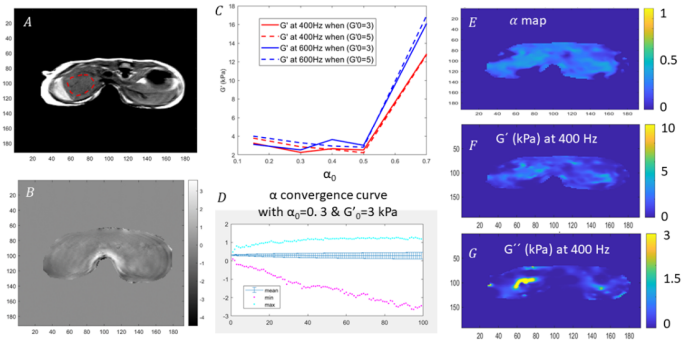


**Results:** MR magnitude (A) and phase (B) images are shown on Figure 1 with the ROI (red). Mean G' values (C) at 400 (red) and 600 Hz (blue) are given for varying $G'_0$ = 3 (solid line) or 5 kPa (dashed line) and $\alpha_0 = 0.15, 0.3, 0.4, 0.5, 0.7$. A good compromise between correct G' values and convergence of $\alpha$ (D) was found at $\alpha_0$= 0.3 and $G'_0$=3 kPa. For this configuration, the obtained $\alpha$ (E), G' (F) and G" (G) maps are shown.

**Conclusions:** This work presents the application of multi-frequency NLI inversion on preclinical mouse liver MRE data obtained in vivo. With the optimal initial parameters, NLI inversion is able to characterize the liver elasticity (G'), yielding to very good homogeneity, and the viscosity (G"). In future work, a cohort of several mice will be studied to evaluate the repeatability of the method.
**Acknowledgments:** LABEX PRIMES (ANR-11-LBX-0063), CNRS (IEA00289-2020). The experimental data is based upon work carried out on the ISO 9001:2015 PILoT facility.
**References:** [1]Hoodeshenas et al. 2018 Top MRI; [2]Asbach et al. 2008 MRM; [3]Jugé et al. 2015 NMR Biomed; [4]Van Houten et al. 1999 MRM; [5]Smith et al. 2022 Brain Multiphysics; [6]Sango-Solanas et al. 2021 NMR Biomed.

# ELASTOGRAPHY TECHNIQUES FOR CHARACTERIZING SOFT GRANULAR MEDIA

*Camila Sedofeito**, *Bruno Melissari*, *Thomas Gallot*

Instituto de Física, Facultad de Ciencias, Universidad de la República, Montevideo, Uruguay

**Background and Aims:** Granular media serve as vital laboratory-scale models for understanding complex natural phenomena like seismic fault dynamics. Wave propagation in granular media provides crucial insights, yet remains challenging due to nonlinear propagation, constitutive equations, wave dispersion, multiple scattering, and path-dependent effects [1]. Ultrasound elasticity imaging, developed extensively for medical applications like liver cirrhosis and breast tumor detection [2][3], has also proven effective in non-medical studies such as observing shock waves in soft solids and studying laboratory earthquakes [4][5]. This technique offers non-destructive means to investigate granular media dynamics following perturbations, revealing phenomena like velocity changes in compressional waves and altered Rayleigh-like wave propagation in dense granular suspensions [6][7]. Unlike traditional elastography focused on solid-like media, this approach explores dynamic and quasi-static processes in unconsolidated soft granular materials.

**Methods:** We perform dynamic and quasi-static elastography techniques to characterize soft granular media. In both approaches, the fundamental principle involves monitoring the material's response to an externally applied force. For dynamic elastography, a sinusoidal wave of varying oscillation frequency from several hertz to some hundreds, propagates through the material in the x-direction (Fig, 1.), inducing bulk waves that are detected using a 128-element L11-4v Philips probe with a central frequency of 7.5MHz. In contrast, the quasi-static method involves applying a vertical force to the material's surface, altering its compaction state. Here, displacement and external stress are measured using a load cell and ultrasound scanner.


*Figure 1: A 128-element ultrasound probe controlled by a Verasonics scanner allows measuring the response of the granular medium. The 1 mm diameter spherical silicon beads are saturated with water. Plane waves are generated with a corrugated plate attached to a vibrating exciter. Frequency ranges from 50Hz to 700 Hz*

**Results:** The study measures shear wave speed and attenuation of various granular media with different properties (size, angularity, and elasticity) as a function of frequency and quasi-static pressure.

**Conclusions:** Adapting elastography methods to soft granular media offers a novel technique for wave characterization in such materials. The depth of measurement is limited to 15 mm due to multiple scattering in grains. This experiment holds potential applications for characterizing grain-like tissues or conducting geophysics laboratory-scale experiments.

**Acknowledgments:**
Grupo CSIC 2022 "Ciencias Planetarias y geofísica"

**References:**

[1] Zhang, Q., at. al.: Nonlinear wave scattering at the interface of granular dimer chains and an elastically supported membrane, International Journal of Solids and Structures, 182, 46–63, doi:https://doi.org/10.1016/j.ijsolstr.2019.08.001, 2020.
[2] Barr et. al. : WFUMB guidelines and recommendations for clinical use of ultrasound elastography: Part 2: breast, Ultrasound in medicine & biology, 41, 1148-1160, doi:https//doi.org./10.1016/j.ultrasmedbio.2015.03.008, 2015.
[3] Ferraioli, G., et al.: WFUMB guidelines and recommendations for clinical use of ultrasound elastography: Part 3: liver, Ultrasound in medicine & biology, 41, 1161–1179, doi:https://doi.org/10.1016/j.ultrasmedbio.2015.03.007, 2015.
[4] Catheline, et. al. : Observation of shock transverse waves in elastic media, Physical review letters, 91, 164 301, doi:https://doi.org/10.1103/PhysRevLett.91. 164301, 2003.
[5] Latour, S.,el.al. Characterization of nucleation during laboratory earthquakes, Geophysical Research Letters, 40, 5064–5069, doi:https://doi.org/10.1002/grl.50974, 2013.
[6] Jia, X., Brunet, T., and Laurent, J.: Elastic weakening of a dense granular pack by acoustic fluidization: Slipping, compaction, and aging, Physical Review E, 84, 020 301, doi:https://doi.org/10.1103/PhysRevE.84.020301, 2011.
[7] Brum, J. et. al. Drastic slowdown of the Rayleigh-like wave in unjammed granular suspensions, Physical Review E, 99, 042 902, doi:https://doi.org/10.1103/PhysRevE.99.042902, 2019.

# IN SILICO VALIDATION OF CARDIAC TIME-HARMONIC ELASTOGRAPHY

*Stefan Klemmer Chandía*[*], *Chiara Manini*, *Anja Hennemuth*, *Marcel Bauer*, *Matthias Ivantsits*, *Lars Walczak*, *Heiko Tzschätzsch*, *Brunhilde Wellge*, *Ingolf Sack*, *Tom Meye*

[1]Charité - Universitätsmedizin Berlin, Corporate Member of Freie Universität Berlin, Humboldt-Universität zu Berlin, and Berlin Institute of Health, Berlin, GERMANY. 1Charité - Universitätsmedizin Berlin, Corporate Member of Freie Universität Berlin, Humboldt-Universität zu Berlin, and Berlin Institute of Health, Berlin, GERMANY; [2]Institute of Computer-Assisted Cardiovascular Medicine, Deutsches Herzzentrum Der Charité (DHZC), Berlin, GERMANY.

**Background:** Ultrasound-based, time-harmonic elastography (THE) utilizes continuous harmonic vibrations in a low frequency range to generate full field-of-view stiffness maps. Cardiac THE (cTHE) is a cost-effective, real-time method for assessing myocardial stiffness [1] but has never been validated in a numerical phantom with ground truth reference values.
**Aims:** To validate cTHE using simulated ultrasound data with known ground truth stiffness values.
**Methods:** cTHE measurements were simulated using Field II [2]. Heart anatomy was obtained from segmented CT reference volumes. The simulations were conducted for three different anatomies and five ground truth stiffness values. As in real cTHE measurements, 400 frames were simulated by displacing tissue using a 2 $\mu$m amplitude, 60, 70 and 80 Hz frequency harmonic wave and adding realistic levels of gaussian noise. The simulated data was processed using the same pipeline as used in vivo [3].
**Results:** Figure 1 shows a comparison between experimental and simulated B-modes and corresponding shear wave speed (SWS) maps. The SWS values estimated by cTHE showed excellent agreement with ground truth, as given by a median absolute error of 0.067 $m.s^{-1}$ [range 0.005 to 0.274 $m.s^{-1}$] and a 0.98 Pearson's correlation coefficient (figure 2).

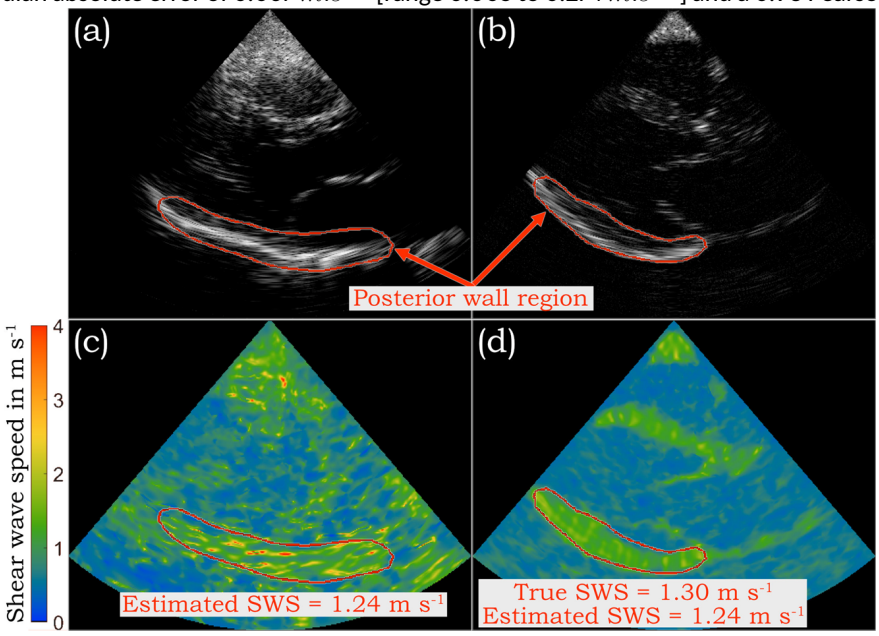


Figure 1: B-modes and SWS maps from (a, c) a healthy volunteer (30 years, male) and (b, d) simulated data.

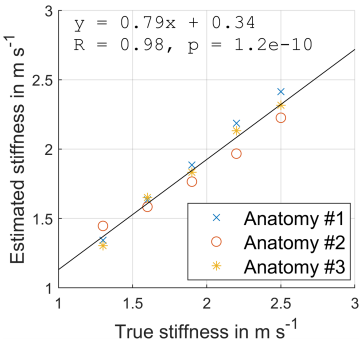


Figure 2: SWS estimation against ground truth stiffness for three anatomies and five stiffness values. A linear fit and its equation are included.

**Conclusions:** cTHE accurately estimated the underlying myocardial stiffness from realistic ultrasound simulations – which mimic real ultrasound images' echogenicity, texture and noise features – despite changes in anatomy and mechanical properties.
**Acknowledgments:** German research foundation FOR5628, CRC1340 and GRK2260.

**References:**

[1] Meyer T, Wellge B, et al. Point-of-care cardiac elastography with external vibration for quantification of diastolic myocardial stiffness. medRxiv. 2024;2024.01.26.24301851.
[2] Jensen JA. Field: A Program for Simulating Ultrasound Systems. Medical & Biological Engineering & Computing. 1997;34(sup. 1):351-3
[3] Tzschätzsch H, Nguyen Trong M, et al. Two-Dimensional Time-Harmonic Elastography of the Human Liver and Spleen. Ultrasound Med Biol. 2016;42(11):2562-71

# SHEAR WAVE PROPAGATION SIMULATION OF LAYERED MEDIUM NEAR LUNG TISSUE BY USING FDTD METHOD.

*M Tabaru*[1,*], *K Shimizu*[1], *N Tano*[1], *R Koda*[1], *Y Yamakoshi*[1,2]

[1]Tokyo Institute of Technology, Yokohama, Kanagawa, Japan; [2]Gunma University, Kiryu, Gunma, Japan.

**Background:**
There is an increasing demand of rapid bedside diagnosis of patients with acute lung disease. There have been reports of lung elasticity measurement using MRI and ultrasound [1, 2]. We are investigating evaluation method of lung properties from shear wave characteristics using tablet echo-based continuous shear wave elastography (C-SWE) [2, 3]. One of the difficulties is that shear wave propagation in lung is not directly observed, since the ultrasound does not penetrate the lung. **Aims:**
To establish the diagnosis indices to distinguish healthy and diseased lungs, we investigate the relationship between the lung conditions (normal or abnormal) and characteristics of shear waves propagating through the chest wall.

**Methods:**
Finite-difference time-domain (FDTD) simulation based on Navier-Stokes equations was employed. Two-layered model consists of chest wall and lung was considered (Fig. (a)). From previous study, we found the goat lungs became stiffer when there was inflammation due to pulmonary fibrosis, and low damping in the lungs was observed [3]. To simulate normal and inflamed lungs, shear wave velocity in lung, Vs_l, was set to 1 and 6 m/s, respectively. Continuous sine wave (78.1 Hz) was input at t = 0 s to generate shear wave. The experimentation with tissue-mimicking phantoms consisted of Konjac and pulp paper was also performed. Konjac and paper were supposed as chest wall and lung, respectively. The damping was changed by changing the number of sheets of paper. We assumed that 5 sheets of paper have larger damping. **Results:**
The simulation results of shear wave amplitude maps were illustrated in Fig. (b). When Vs_l was large (i.e. stiff), reflection at the boundary of chest wall-lung was large. B-mode images and shear wave amplitude maps reconstructed by C-SWE of the experiments are illustrated in Fig. (c). We found that shear wave in the konjac penetrated to the pulp paper in normal model (Fig. (c)). Fig. (d) shows the simulation and experimental results of attenuation characteristics of shear wave along z-direction in chest wall. We found that when the lung became stiffer, attenuation in the chest wall was decreased due to small damping.

**Conclusions:**
The resulted attenuation characteristics in Fig. (d) confirm the results with goat lung experiment [3]. By using the shear wave propagation characteristics such as attenuation in chest wall could be used to diagnosis indices of lung.

**Acknowledgments:**
Part of this work was supported by JSPS KAKENHI Grant Number 22K04134 and the Cooperative Research Project of Research Center for Biomedical Engineering. **References:**
[1] Zhang X, Osborn T, et al. Lung Ultrasound Surface Wave Elastography: A Pilot Clinical Study, IEEE TUFFC, 64, 1298-1304 (2017). [2] Koda R, Taniguchi H, et. al., B-line Elastography Measurement of Lung Parenchymal Elasticity, Jpn J Med Ultrasonics, Ultrason Imaging. 45, 30-41 (2023). [3] Koda R, Taniguchi H, et. al., Lung Elasticity Measurement in a Goat Lung Fibrosis Model Using Tablet Echo-Based C-SWE, Jpn J Med Ultrasonics, Vol. 51, S708 (2023).

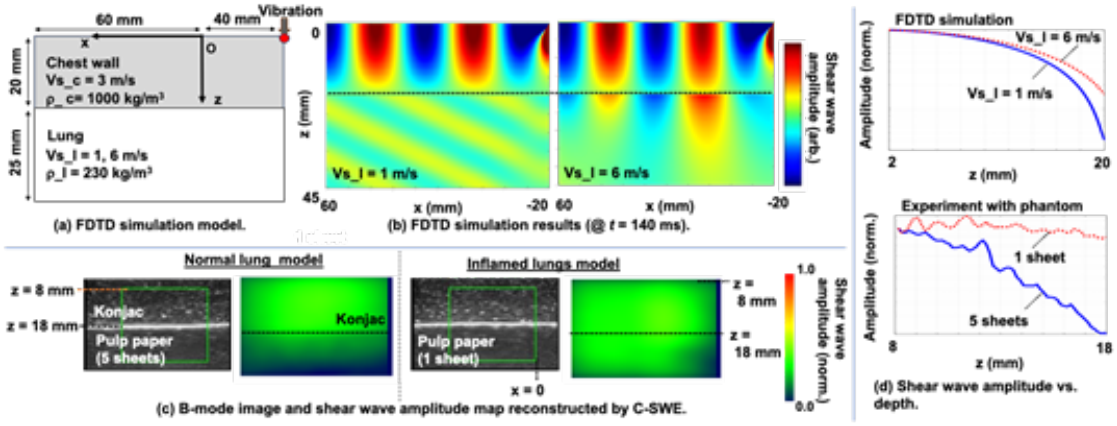

# HIGH-FREQUENCY SHEAR WAVE EVALUATION OF VISCOELASTIC PROPERTIES IN TISSUE-MIMICKING PHANTOMS USING A NOVEL MICRO-ELASTOGRAPHY SYSTEM.

*José Cortés*[1,2,*], *Inas H Faris*[1,2,3], *Jorge Torres*[4], *Antonio Callejas*[1,2,3+], *Guillermo Rus*[1,2,3+]

[1]UltrasonicsLab, Dept of Structural Mechanics, University of Granada, Granada 18001, SPAIN; [2]TEC-12 Group, Instituto de Investigación Biosanitaria, ibs.Granada Granada 18001, SPAIN; [3]Excellence Research Unit "ModelingNature" (MNat), University of Granada, Granada 18001, SPAIN; [4]INSERM LabTAU U1032, Lyon, FRANCE.

[+]Antonio Callejas and Guillermo Rus have contributed equally to this work as leading authors.

**Background:** Mapping living histological mechanics is challenging [1]. Our research addresses this by studying the interplay between chemical and mechanical responses within cells, focusing on mechanotransduction [2]. Understanding tissue elasticity, which varies with context and scale, is crucial as it influences cell structure and responses. Cells adapt to their mechanical microenvironment, affecting division and drug sensitivity [3,4]. By studying viscoelastic behavior at the microscopic level, starting with phantoms, we aim to enhance our understanding of dynamic cellular mechanics and their biological roles.
**Aims:** Our goal is to enhance elastography to the microscopic scale [5], allowing us to characterize the dynamic elastic properties of cells and structures like spheroids (150-500$\mu$m). We aim to increase the current 2-10kHz range of shear wave elastography to 25kHz, achieving a spatial resolution around 100$\mu$m at physiological timescales.
**Methods:** We designed and prototyped the imaging system using prestressed stacked piezoelectric transverse actuators. The system tracks shear dynamic stress fields and quantitatively characterizes viscoelasticity maps of tumor cells and their microenvironment using a high-speed camera (2M fps Photron SAZ 32G) attached to a microscope with a halogen light source. This advancement offers unprecedented spatial resolution and insights at physiological timescales, making it a significant step forward in the field of elastography.
**Results:** In our study, polyacrylamide samples with distributed particles and varying concentrations were measured to assess their elasticity and viscosity. Using our advanced microelastography system, we obtained viscoelastic values for all samples across a frequency range of 5 to 25kHz (Figure 1). These measurements provided a detailed understanding of the samples' mechanical properties, demonstrating the system's capability to analyze viscoelastic behavior at the microscopic level.
**Conclusions:** Our advanced microelastography system effectively measured and analyzed viscoelastic behavior at the microscopic level, capturing detailed viscoelastic values for polyacrylamide samples across a 5 to 25kHz range. This significant advancement in spatial resolution and physiological relevance enhances our ability to characterize the dynamic elastic properties of cells and multicellular structures. Future applications will focus on live biological tissues, providing deeper insights into cellular mechanics and disease mechanisms.newline **Acknowledgments:** Ministerio de Ciencia e Innovación grant numbers PID2020-115372RB-I00, PYC20 RE 072 UGR; Junta de Andalucía - Consejería de Universidad, Investigación e Innovación- proyecto (P21_00182); Listen2Future funding by 101096884 in HORIZON-KDT-JU-2021-2-RIA and by PCI2022-135048-2 by Ministerio de Ciencia e Innovación; Proyectos Intramurales IBS.Granada INTRAIBS-2022-05; MCIN/AEI 10.13039/501100011 033 grant number PRE2021-096978 (Co-funded by European Social Fund "Investing in your future"); Ministerio de Universidades Ayudas para la recualifcación del sistema universitario español, MS2022-96 (Co funded by European Union Next GenerationEU/PRTR).

**References:** [1] Burgess JK, Mauad T, Tjin G, Karlsson JC, Westergren-Thorsson G. The extracellular matrix – the under-recognized element in lung disease? J Pathol. 2016;240:397–409. [2] Plodinec M, Loparic M, Monnier CA, Obermann EC, Zanetti-Dallenbach R, Oertle P, et al. The nanomechanical signature of breast cancer. Nat Nanotechnol. 2012;7:757–65. [3] Rus G, Faris IH, Torres J, Callejas A, Melchor J. Why Are Viscosity and Nonlinearity Bound to Make an Impact in Clinical Elastographic Diagnosis? Sensors. 2020;20:2379. [4] Garteiser P, Doblas S, Daire JL, Wagner M, Leitao H, Vilgrain V, et al. MR elastography of liver tumours: value of viscoelastic properties for tumour characterisation. Eur Radiol. 2012;22:2169–77. [5] Torres, J., Callejas, A., Gomez, A., & Rus, G. (2023). Optical micro-elastography with magnetic excitation for high frequency rheological characterization of soft media. Ultrasonics, 132, 107021.

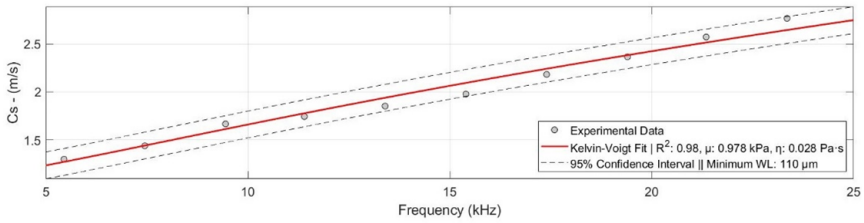


Figure 1: Kelvin model fitting for a 15% polyacrylamide gel across a frequency range of 5 to 25 kHz, 110$\mu$m of $\lambda$.

# TORSIONAL WAVE BIOREACTOR TO EVALUATE EFFECT ON MELANOMA CANCER CELL

*Manuel Hurtado*[1,5,*], *Carmen Griñán-Lisón*[2,4,5], *Gema Jiménez*[2,4,5], *Elena Lopez.*[2,4,5], *Daniel Martínez-Moreno*[2,4,5], *Antonio M. Callejas*[1,4,5], *Juan A. Marchal*[2,4,5], *Juan M. Melchor*[3,4,5], *Guillermo Rus*[1,4,5]

[1]UGR Department of Structural Mechanics, University of Granada, Politécnico de Fuentenueva Granada E-18071, Spain. manuelhurtado@go.ugr.es; [2]UGR Biopathology and Regenerative Medicine Institute (IBIMER), Biomedical Research Centre, University of Granada, Granada E-18100, Spain; [3]UGR Department of Statistics and Operations Research, University of Granada, E-18071 Granada, Spain; [4]Excellence Research Unit "Modeling Nature" (MNat), University of Granada, Granada, Spain; [5]Biosanitary Research Institute of Granada (ibs.GRANADA), University Hospitals of Granada-University of Granada, Granada, Spain

**Aims:** In this study we have designed and manufactured a bioreactor that allows to study, for the first time, the effect of torsional shear mechanical waves on a population of melanoma CSCs (MEL-1) and differentiated cells over tumor and non-tumor cells as a potential alternative cancer treatment. There is no previous information on the scientific literature explaining the use of torsional waves in the treatment of cancer. The stimulation is produced by these elastic shear waves that propagate through soft tissue radially and in depth with a curved geometry. Malignant melanoma is the most aggressive skin cancer with poor prognosis; contributes to 90% the mortality of skin cancers. The main problem of melanoma therapies is the lack of effectiveness treatments, due to the presence of the cancer stem cells (CSCs), cells responsible for tumor initiation, metastasis and cancer recurrence. Cancer Stem cells (CSCs) are a small subpopulation of cells present in tumors and they are considered as tumor initiating cells (TICs). They also are capable of maintaining the heterogeneity. Tumor growth is related to diverse changes in biomechanical structure of microenvironment such as matrix stiffness, growth-induced solid stresses, high fluid pressure and increased interstitial flow. All those changes are controlled by mechanical forces that contribute and promote to tumorigenesis and tumor cell invasion (1)(2)(3).
**Methods:** Torsional waves, with different configurations were employed in diverse types of tumor cells, aggregates of differentiated tumor cells, and healthy cells (fibroblasts). Incorporated motors in this device were tailored in such a way that exerting contact pressure was optimiezed modifying the motor height to ensure proper rotation. Each well-plate was carefully filled with a mixture of alginate hidrogel. Those ones were stimulated with different frequencies and amplitudes: from 10 Hz to 1000 Hz and from 2 volt to 10 volt. Control samples were same conditions but without motor movement.
**Results ans Conclusions:** A bioreactor has been developed that allows the application of novel torsion waves. These waves have been shown to affect differently depending on the cell type. In a first experiment, torsion waves decreased the proliferation of tumor cells during the first 72 hours; with the 10 Hz resulted in the most attenuated CSCs proliferation. On the other hand, the 1000 Hz frequency also affected isolated differentiated cells. For healthy cells, such as fibroblasts, the tendency was mostly to grow. Next, we increased the stimulation time up to 7 days with 10 Hz, focusing on CSCs and monolayer cultures, again, torsional waves decreased the proliferation of tumor cells (Figure 1). Our results of this pilot study allow us to observe the effect of torsional waves with various frequencies on CSCs. In conclusion, torsion waves could have the potential to constitute a new non-invasive treatment against melanoma that can be applied in clinic in monotherapy or with existing ones as a combined treatment.

**Acknowledgments:** Junta de Andalucía - Consejería de Universidad, Investigación e Innovación - Proyecto (P21_00182). PCI2022-135048-2, PID2020-115372RB-I00.

**References:**

1. Shieh AC. Biomechanical Forces Shape the Tumor Microenvironment. Ann Biomed Eng [Internet]. 2011 May.
2. Suresh S. Biomechanics and biophysics of cancer cells. Acta Biomater [Internet]. 2007 Jul.
3. House M, Kaplan DL, Socrate S. Relationships Between Mechanical Properties and Extracellular Matrix Constituents of the Cervical Stroma During Pregnancy. Vol. 33, Seminars in Perinatology. 2009. p. 300–7.

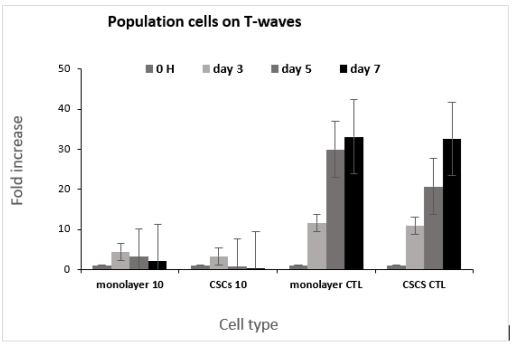


Figure 1: Proliferation assay in cancer stem cells and control for 7 days.

# 2D ULTRASOUND ELASTICITY IMAGING OF ABDOMINAL AORTIC ANEURYSMS USING DEEP NEURAL NETWORKS

*U Tuladhar*, R Simon, M Richards*

Rochester Institute of Technology, Rochester, NY, USA.

**Background:** Abdominal aortic aneurysm (AAA) is a critical cardiovascular condition characterized by the localized dilation of the abdominal aorta, which can lead to life-threatening consequences if left untreated. Biomechanical characterization of (AAA) patient vessels may improve clinical assessment of the risk rupture, a life threatening event. Ultrasound (US) elasticity imaging is a technique that enables non-invasive quantification of mechanical properties or states from image sequences of deforming tissue. It often requires solving the elastic inverse problem to identify the modulus distribution from a measured displacement field.
**Aims:** We propose using a Deep Learning (DL) framework to reconstruct the spatial distribution of the shear modulus of the aortic cross-sections from the axial and lateral components of an US measured displacement field.

**Methods:** *Finite Element Simulation.* 2D, nearly incompressible plane strain finite element (FE) model was used to generate the directional displacement fields, ux(x,y) and uy(x,y). The inputs to the FE model were the FE mesh of irregularly spaced nodes in quadrilateral elements, the modulus distribution discretized at the nodal locations, and the boundary conditions (Figure 1). The modulus of the background material was fixed and a known pressure was applied to the vessel surface.

*Deep Learning.* A U-net [1] based regression architecture for image-to-image translation was used to learn the mapping from the 2D displacement field to the modulus distribution (Figure 2). The mean square error (MSE) was chosen as the loss function, $MSE = \sum_{i=1}^{N}(E_i^t - E_i^p)^2$ , where N is the number of pixels, $E^t$ is the true modulus and $E^p$ is the predicted modulus. Furthermore, this model was evaluated using both the MSE and the Mean Absolute Percentage Error (MAPE) metric, $MAPE = \sum_{i=1}^{N} |(E_i^t - E_i^p)/(E_i^t)|$.

*3D Simulated and Phantom Experimental Data.* A central transverse slice of displacement data from 3D FE simulation using COMSOL with known aortic modulus variation was used. These displacements were used to create US images of the deforming aorta, utilizing a point spread function approximating a curvilinear transducer. Additionally, aortic-mimicking US phantoms with varying material properties were created and imaged using a 5 MHz curvilinear US transducer [2]. Displacements within these images were tracked using a registration of the radiofrequency image sequences combined with a regularization technique.
**Results:** For simulated test data, we had 500 test images for which the mean MSE was 0.392±0.825 and the mean MAPE was 0.172±0.090. An example with MSE 0.002 and MAPE 0.91 is shown in Figure 3. On experimental phantom data, the expected modulus of proximal end was 40 kPa [2] and the obtained modulus of proximal end was in the range of 40-50 kPa as shown in Figure 4.
**Conclusions:** We demonstrate, using FE simulated data, the development and preliminary evaluation of a DL approach capable of predicting the shear modulus from both simulated and experimental US elastography data. Formatting, a,b,c,d in pics, not depth and lateral, say x and y direction…

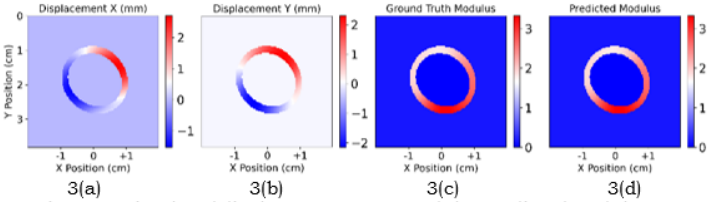


3(a) 3(b) 3(c) 3(d)

Figure 3. Simulated displacements, true and the predicted modulus

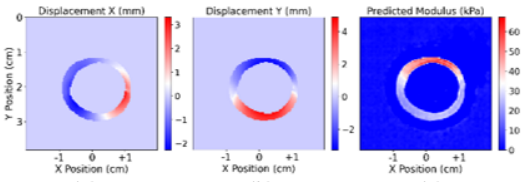


4(a) 4(b) 4(c)

Figure 4. Phantom displacements and prediction

**References:**
[1] Ronneberger, O., Fischer, P., and Brox, T., "U-net: Convolutional networks for biomedical image segmentation," in [International Conference on Medical image computing and computer-assisted intervention], 234–241, Springer (2015).
[2] Mix, Doran S., et al. "Detecting regional stiffness changes in aortic aneurysmal geometries using pressure-normalized strain." Ultrasound in medicine & biology 43.10 (2017): 2372-2394.

# SHEAR WAVE ATTENUATION IN MUSCLE MODELED AS TRANSVERSELY ISOTROPIC TISSUE

*A Camargo*[1], *E Budelli*[2], *J-L Gennisson*[3,*], *T Frappart*[4], *CA Negreira*[1], *N Benech*[1], *J Brum*[1]

[1]Laboratorio de Acústica Ultrasonora, Instituto de Física, Facultad de Ciencias, Universidad de la República, Montevideo, URUGUAY; [2]Instituto de Química, Facultad de Ingeniería, Universidad de la República, Montevideo, URUGUAY; [3]Laboratoire d'Imaginerie Biomedicale Multimodale (BioMaps), Université Paris Saclay, Paris, FRANCE; [4]Supersonic Imaging, Aix en Provence, FRANCE.

**Background:** Noninvasive evaluation of muscle viscosity could provide an important biomarker. Currently, commercial ultrasound systems only offer shear elasticity estimation based on shear wave velocity (SWV) measurement, assuming a purely elastic, transversely isotropic tissue (TIT). However, to fully characterize the rheological behavior of muscle it is crucial to estimate shear wave attenuation (SWA). Most elastography techniques generate shear waves using ultrasound's acoustic radiation force. As a result, shear waves are not planar, requiring a diffraction correction for accurate SWA estimation. While a cylindrical correction was proposed for isotropic tissue [1], to our knowledge no diffraction correction for SWA in TIT has been reported.
**Aims:** The aim of this work is to introduce a diffraction correction for SWA in TIT by analytically solving the wave equation for an infinite line source. The diffraction correction was then validated through numerical simulation and ex-vivo experiments in meat. Finally, a proof of concept was carried out in the biceps brachii of a healthy volunteer under different levels of isometric contraction.

**Methods:** Numerical simulations based on a Green's function algorithm (anisotropic and viscoelastic) [2] were carried out to validate the analytical diffraction correction. Moreover, two experiments were performed using different methods to generate shear waves: (i) a vibrating plate (transient elastography-TE experiment) and (ii) the ultrasound's acoustic radiation force (SSI experiment). For the TE experiment, the plate vibrates perpendicular to the fiber orientation, resulting in the generation of plane shear waves with propagation directions either parallel or perpendicular to the fibers. A 128 element, 7 MHz probe (model L11-4v) driven by a Verasonics Vantage System was used to track the shear wave. For the SSI experiment an Aixplorer System (Supersonic Imagine, France) was used to generate and track shear waves. Both experiments were performed on the same beef sample of the "peceto" type obtained from a local butcher. For the in-vivo experiment the SSI technique was used. The experiment was carried out on the biceps brachii of one volunteer. The transducer was placed in the parallel and perpendicular configuration (i.e. shear wave propagation parallel or perpendicular to fibers, respectively), with the muscle at rest and under isometric contraction at 90° holding different loads of 0 (forearm), 1.0 and 2.0 kg.

**Results:** The analytical solution of the wave equation in TIT reveals an amplitude decay with distance (x) following a power-law behavior of $x^{-0.5}$. Simulation results indicate that the analytical correction is valid from a distance 1/k from the source, being k the shear wavenumber. SWV measurements in the meat results in a SWV anisotropy factor of 1.12. In the meat sample, SWAs of 0.16 $\pm$ 0.06 Np/mm, 0.15 $\pm$ 0.03 Np/mm, and 0.141 $\pm$ 0.08 Np/mm, 0.143 $\pm$ 0.1 Np/mm were obtained for the TE and SSI experiments corrected by diffraction in the parallel and perpendicular directions, respectively. A very good agreement was found between both experiments. The in-vivo results for the perpendicular configuration show an increase in the attenuation coefficient between rest and the 2 kg contraction conditions with mean values of 0.31 $\pm$ 0.1 Np/mm and 0.51 $\pm$ 0.2 Np/mm, respectively. For the parallel configuration the attenuation coefficient decreased from 0.193 $\pm$ 0.05 Np/mm at rest to 0.114 $\pm$ 0.03 Np/mm for the 1 kg contraction. For this configuration it was not possible to properly measure SWA at 2 kg.

**Conclusions:** In this work a diffraction correction for SWA in TIT was proposed and validated through numerical simulation and ex-vivo experiments. In vivo results are promising for full rheological characterization of skeletal muscle. Future works we will focus on improving the protocol to estimate SWA in both directions during isometric contraction,
**Acknowledgments:** This work was funded by grant FMV_1_2019_1_155527 - ANII, Uruguay.
**References:** [1] Budelli Phys.Med.Biol. 2017, [2] Chatelin Phys.Med.Biol. 2015.

# Useful Information

**Talks** will be held at the **Lyon Est medical school** (8 Av. Rockefeller, 69003 Lyon). It is situated on the first floor of the central courtyard and has independent access from the rest of the building (through stairs located at the ground floor, main entrance of PRBB).

## How to get to the ITEC 2024?

There are several ways to get to the Lyon Est medical school:

By metro: There are 4 metros in Lyon, but the one that will get you to the Lyon Est medical school is metro D, and you need to stop at Grange Blanche. If you don't have direct access to metro D, there are several connections.

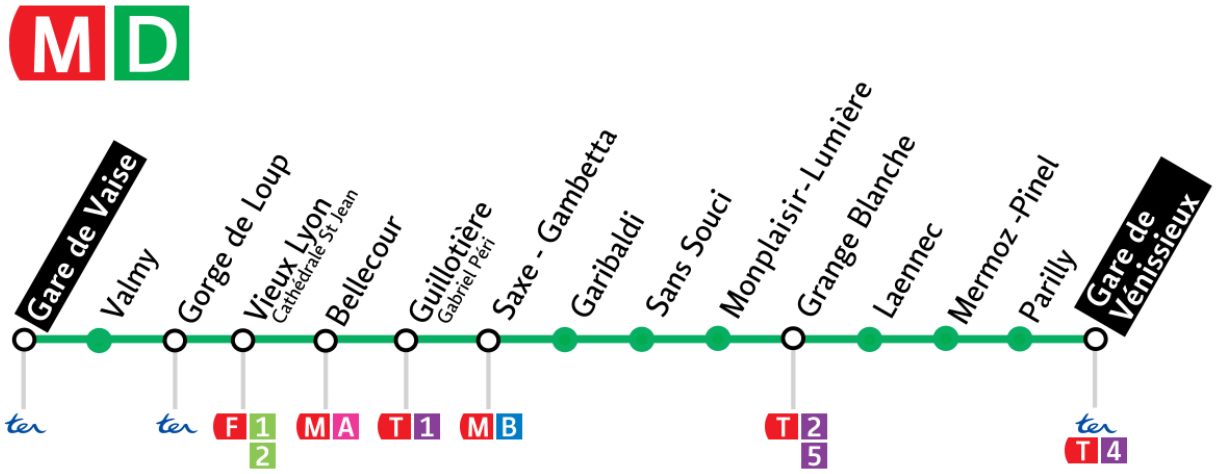


By tramway: Lyon Est medical school is served by 2 tramways, the T2 and the T5. For both streetcars, get off at the Grange blanche stop.

By bus: Lyon Est medical school is served by a large number of buses (34, C13, C16 and C26).

You may be lost with all this information. To remedy this, we recommend you install the TCL app, available on IOS and Android.

Map of the surroundings

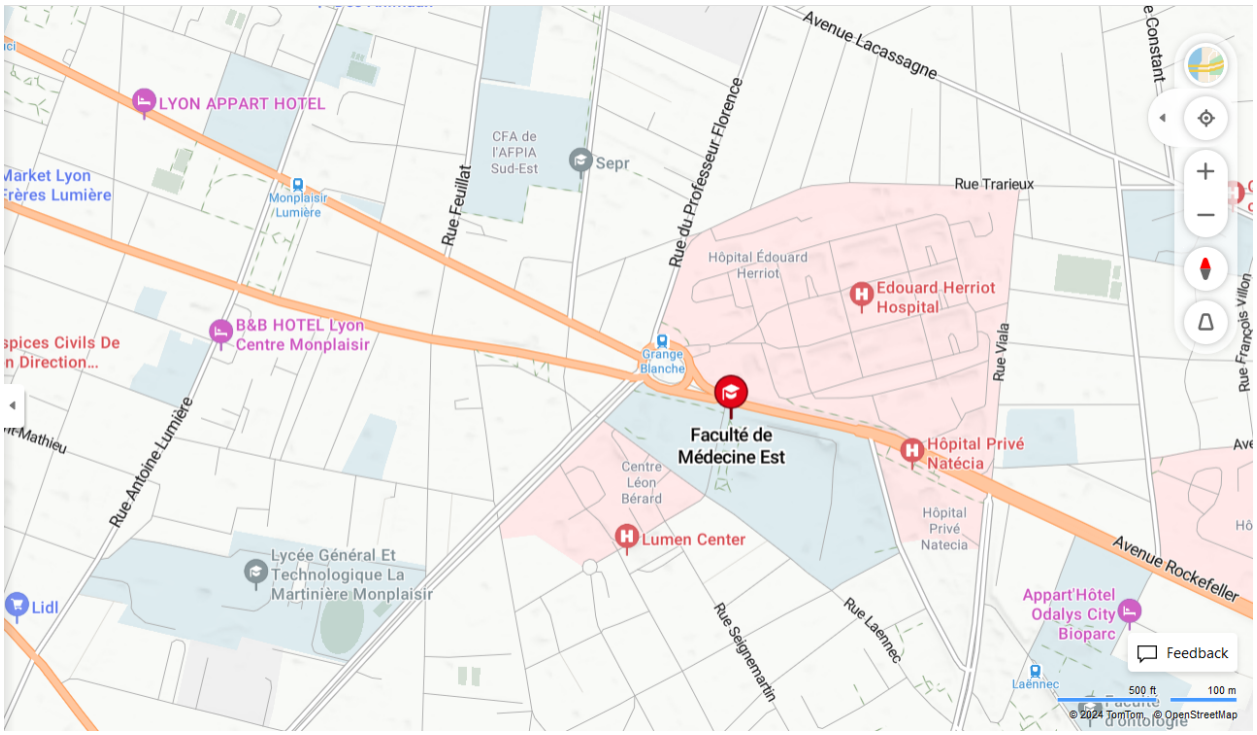

# Partner Institutions and Sponsors

SUPERSONIC imagine™

https://www.supersonicimagine.fr/

SuperSonic Imagine®, a pioneering company in the field of ultrasound imaging, offering advanced solutions to improve patient care across various medical specialties.

Created in 2005 in Aix en Provence, SuperSonic Imagine® was born from a collaboration with the Institut Langevin in Paris. This collaboration led to the introduction to the innovative technology – Real-time ShearWave® Elastography.

At SuperSonic Imagine®, we strive to protect, heal and nurture healthier lives in the relentless pursuit of a healthier world. Our mission is to continuously enhance our ultrasound platform to provide invaluable resources to our customers and make a difference in patients' lives.

FUJIFILM VISUALSONICS

FUJIFILM VisualSonics specifically focuses on developing ultrasound technology that has been scaled to much higher frequencies than commonly found in many of the conventional ultrasound systems on the market today. As a result, our ultrasound platform provides images at resolutions that far exceed any other system available on the market; as fine as 30 micrometers, clearly differentiating our company from our competitors.

© DelphineCastel / ONLYLYON Tourisme & Congrès

# International Tissue Elasticity Conference™

## *October 21-23, 2024*

## Lyon, France

LabTAU - Unité de recherche U1032

LABTAU
LABORATOIRE THÉRAPIE ET APPLICATIONS ULTRASONORES

Inserm

CENTRE LÉON BÉRARD

Lyon 1